NOLTR 67-22

WIDEBAND ELECTRICAL CHARACTERISTICS OF SMALL-DIAMETER INSTRUMENTATION CABLES IN SEAWATER

26 JUNE 1967

NOL

UNITED STATES NAVAL ORDNANCE LABORATORY, WHITE OAK, MARYLAND

NOLTR 67-22

Distribution of this document is unlimited.

WIDEBAND ELECTRICAL CHARACTERISTICS OF SMALL-DIAMETER INSTRUMENTATION CABLES IN SEAWATER

Prepared by:
James E. Cottrell, Jr.

ABSTRACT: Certain oceanographic applications exist where it is desired to transmit data over an electrical cable from sea depths of ten to twenty thousand feet. Mechanical handling-packaging and streaming considerations limit cable diameter, yet impose severe strength requirements. In addition, the amount of information to be transmitted dictates a large bandwidth requirement.

The propagation characteristics of several possible cables are analyzed theoretically, considering the effects of seawater. Accurate values of attenuation and characteristic impedance have been determined by IBM 7090 computations and are presented graphically over the frequency range from ten cycles to one megacycle. The coaxial line has the least attenuation of any configuration; for low frequencies the sea-return type is found best, but above about 250 kilocycles a metallic return offers smaller loss. Small-diameter cables ($\leq$ 0.1") can have losses as high as 4 to 9 db per thousand feet.

The inclusion of steel in cables for strength was studied for its effects on electrical characteristics. The primary result is an increase in conductor resistance. Measurements made on samples of two steel-bearing lines agreed well with predicted values. A novel configuration having a steel braid over a copper shield was designed and appears to offer the best electrical-mechanical tradeoff.

All cables showed wide parameter variations with frequency, therefore the suitability of a representative cable for transmission of digital signals is briefly investigated. Insofar as receiving amplifier and cable noises allow, a method of countering waveform degradation by proper cable equalization is shown.

U. S. NAVAL ORDNANCE LABORATORY
WHITE OAK, MARYLAND

NOLTR 67-22 26 June 1967

Wideband Electrical Characteristics of Small-diameter Instrumentation Cables in Seawater

This report discusses the most important of the electromagnetic properties of small coaxial transmission lines, both dry and in the presence of seawater, and presents methods for calculation of their effects. Underlying the approach taken have been the following objectives: (1) a general feel for the expected magnitude of electrical parameters, (2) prediction of the relative effect of changes in dimensions or materials, and (3) determination of suitability for data transmission at frequencies up to 1 megahertz.

This report was originally prepared by the author as a master's thesis. For the most part the study is theoretical, although supported by experiment where possible. The work was peformed under BUWEPS Task No. RUDC-3B-000/212-1/S046-00-00. It will be of interest to those concerned with data transmission over subminiature cables, especially in the presence of seawater.

E. F. SCHREITER
Captain, USN
Commander

E. H. Beach

E. H. BEACH
By direction

CONTENTS

TABLES

ILLUSTRATIONS

ILLUSTRATIONS (Continued)

I. INTRODUCTION

In certain oceanographic research applications at great depths, it is desirable that the cable from which the deeply submerged instruments are suspended also be used as a communications channel over which data can be transmitted to a surface vessel. Conversely, it may also be said that the wire(s) used for data transmission should also function as a strength member. In either case, if the length or strength requirements are high, or the volume of information to be transmitted large, or both, the electrical and mechanical cable requirements are likely to conflict. This is especially true for deep submergence applications when the allowable size of the cable is limited, as, e.g., to minimize cable underwater streaming. If the cables have an overall outer diameter of a few tens to a few hundreds of a thousandth of an inch, and lengths of ten to twenty thousand feet, these conflicts and the trade-offs to be effected bear close scrutiny.

The work presented here is the result of investigations of the foregoing factors which were conducted to determine the comparative merits of some possible transmission line configurations, the propagation characteristics to be expected in some representative sizes, and the quantitative effects of including ferromagnetic material

(i.e., steel) for strength purposes. A further aim was to obtain some idea of the transmission channel effective bandwidth (or maximum permissible signalling speed - whichever approach one prefers) obtainable with a reasonable amount of error and terminal equipment complexity.

By way of introduction, and for reference purposes, a brief review of some pertinent facts about transmission lines is presented below and in Appendix A. These topics are discussed at length in any standard work on the subject [21,25,27]*, and only the essentials are given here. In all that follows, unless otherwise specified, the rationalized MKS system of units is employed; the basic assumptions made are that the sea is an infinite homogeneous medium, and that the cables are of infinite length (or long enough compared to their diameter to be considered so).

Only coaxial cables are considered in this investigation because Curtis, Green, and Leibe have thoroughly investigated this configuration, along with several other possibilities, and have shown that this type has the least attenuation of any studied. The relative merits of the several types as reported by them [2, p. 282] are tabulated

---

*Numbers in brackets denote references listed in the selected bibliography.

for reference below. The coaxial configuration was taken as a standard.

Type of Cable	Relative Attenuation
Coaxial	1.0
Shielded Pair: Round Conductors and Oval Shield (approximate)	1.3
Shielded Pair: Round Conductors and Circular Shield	1.5
Double Coaxial Circuit	2.0

A uniform transmission line may be considered for convenience to be made up of a cascaded series of identical network sections of the form of Figure 1-1, each representing a portion of the line. The larger the number of sections, and the shorter the length represented by each section, the better does this lumped-parameter model approximate the real line. Thus, the line is characterized completely by four parameters, as shown in Figure 1-1, namely:

R, the series resistance in ohms per meter

G, the shunt conductance in mhos per meter

L, the series inductance in henries per meter

C, the shunt capacitance in farads per meter

These quantities are entirely determined by the geometry of the line and the materials of which it is made, as will be shown.

With regard to signal propagation, the properties of any line may be described [21;27;31, Chp. 20] in terms of two quantities, both of which are complex in their most general form. These are (1) the characteristic impedance, Z_o, and (2) the propagation constant, γ:

$$Z_o = R_o + jX_o = |Z_o| \angle \theta$$
$$\gamma = \alpha + j\beta \qquad (1\text{-}1)$$

In the above equations, R_o and X_o are the characteristic resistance and reactance of the line, respectively; α is the attenuation constant, a measure of loss on the line; β is the phase constant, describing the phase shift a signal undergoes in traversing the line. Since Z_o and γ are together sufficient to describe the line, as were the group R, G, L, and C introduced above, it is to be expected that the two sets of parameters are related. From Appendix A, the pertinent equations are:

$$Z_o = \sqrt{\frac{R + j\omega L}{G + j\omega C}} \qquad \text{(a)}$$
$$\qquad (1\text{-}2)$$
$$\gamma = \sqrt{(R + j\omega L)(G + j\omega C)} \qquad \text{(b)}$$

If R, G, L, and C are expressed in the units shown above, then Z_o, R_o, and X_o all have the dimensions of ohms; α is expressed in nepers per meter, and β in radians per meter.

A glance at equations (1-2) shows that Z_o and γ are functions of frequency, first because of the appearance of the factor ω, and second, because R, L, G, and C are themselves functions of frequency. Both Z_o and γ may vary widely with frequency; thus description of the line's properties for large bandwidths is not generally a simple thing.

Of the four quantities R, L. G, and C, the shunt parameters G and C, which are determined largely by the dielectric, are found to be independent of frequency (or nearly so) up to very high frequencies. For the purposes of this discussion, they may be considered constants. It is the series parameters R and L, depending upon material, size, and placement of the conductors, which are responsible for the major part of the variation in Z_o and γ. These variations of R and L with frequency are the result of the well known phenomenon of skin effect. In the frequency range of interest, which is 10 cps to 1 megacycle, the amount of variation is considerable, thus complicating the description and employment of the lines.

Reference to handbooks or books on transmission lines will reveal simple formulas for characteristic impedances of various configurations, as well as for the attenuation and phase constants α and β. Sometimes, if the reference author is careful, he will state that the formulas are only valid

for high frequencies, or for "lossless" lines. Sometimes other formulas are given for very low frequencies. What is usually missing is a statement as to what such simple expressions really represent, i.e., limiting cases of much more general (and unfortunately far more complicated) expressions which are obtained from the solutions of Maxwell's equations over the line. Equations (1-2) are perfectly general, and true at any frequency; substitution into them of the proper expressions for R. L. G. and C yields the desired quantities Z_o and γ. The complications arise in the expressions for R and L, which will be shown to be made up largely of Bessel functions. When their arguments are large, these Bessel functions may be replaced by simpler functions to which they are asymptotic; then Z_o and γ reduce to their well known simple expressions. The arguments become large at high frequency, or for large-diameter coaxial structures. But for the size of cable under investigation here, and for the specified frequency range, the luxury of asymptotic approximations will have to be foregone except in special cases.

The first step, then, will be to examine the simplest type of line, the sea-return type. From there, we may proceed logically to more complicated configurations.

II. THE SEA-RETURN LINE

The sea-return line, in which an insulated wire is immersed in the ocean, is the simplest form of coaxial line to build. In such a line, the wire itself is the center conductor. The insulation surrounding it serves as the dielectric layer, and the surrounding ocean, extending nominally to infinity, forms the outer conductor. Such lines were the earliest form of transoceanic communications cables laid, and some of them are still in use today. The propagation characteristics were studied around 1921 by J. R. Carson and J. J. Gilbert [1], who seem to have been the first to realize that the "sea-return" impedance is not negligible. The form of most of the results presented in that paper, while general and extensive, is not readily adapted to computation of specific examples, especially of the relatively simpler samples treated here. Greater ease of practical application may be had from one of the later papers which treat the subject [33,34,36].* Von Aulock's work for example, is especially convenient.

---

*It might be noted in passing that the equations developed in reference [34], because of the assumption made in their derivation (p. 16), do not apply throughout the present frequency range of interest; they are the high frequency approximations to the more general expressions used here, and yield attenuation values which are too small at low frequencies. (See equations (B-15) and (B-16), Appendix B. See also [24, p. 214].) This limitation is not stated in the reference.

A cross-sectional diagram of the sea-return line is shown in Figure 2-1. Calculation of the characteristics will begin with the shunt parameters, G and C, and then take up the series parameters. In disposing of this case, several points will be settled which will apply to the rest of the cases as well. The first of these concerns conductance, G. Unless otherwise noted, the dielectric material postulated for all lines treated herein is high-density polyethylene, for which the value of conductivity σ is taken [33, p. 36] as 10^{-13} mho/meter. Then, for coaxial structures, the conductance per unit length (meter) is given by the expression, [24, p. 332].

$$G = \frac{2\pi\sigma}{\ln (b/a)} \qquad (2\text{-}1)$$

where

G = conductance in mhos/unit length (meter, in RMKS units)

σ = conductivity in mhos/meter

b = outer radius of dielectric in meters

a = inner radius of dielectric in meters

Calculations show that the value of G due to leakage of the dielectric will be of the order of 10^{-12} to 10^{-13} mho/meter for the small-diameter lines considered here.

There are also other dielectric losses at higher frequencies, which are usually described by the imaginary part of a complex dielectric constant, or a "loss angle"

(or its tangent), or a dissipation factor δ, all of which are really different ways of describing the same thing. For low dissipation factors, dielectric loss may be expressed as an equivalent conductance [27, p. 161f].

$$G' = (\omega C)(\delta)$$

where

G' = equivalent conductance per unit length due to dielectric loss, mhos/meter

δ = dissipation factor

C = capacitance in farads/unit length

ω = 2π x frequency

Then in general, the line admittance per unit length Y is given by

$$Y = G + G' + j\omega C$$

Calculations show that capacitance per foot in these small-diameter lines will be of the order of 10^{-10} farads. Since, even at 10 cycles, G is smaller than C by more than two orders of magnitude (a disparity that becomes more marked with increasing frequency), loss due to conductance of the dielectric may be neglected. Then, considering only high-frequency losses, which increase as the first power of frequency, $Y = G' + j\omega C$. But the dissipation factor of high-density polyethylene is given by MIL-P-22748 as 5×10^{-4}

in the frequency range 1 KC - 1 MC. Thus,

$$Y = \delta\omega C + j\omega C$$

$$= \omega C(5 \times 10^{-4} + j)$$

Thus it is reasonable to assume that for our purposes, in all that follows

$$Y = j\omega C$$

The remaining shunt parameter, C is independent of frequency up to very high frequencies. For coaxial structures, the expression for it is entirely analogous to that for G, and may be also obtained from any standard text on electromagnetic theory. It is [24, p. 332]

$$C = \frac{2\pi\epsilon}{\ln(b/a)} \qquad (2\text{-}2)$$

where

C = capacitance in farads/unit length (meter, in RMKS units)

ϵ = dielectric constant of the insulation, $= \epsilon_o\epsilon_r$

b = outer radius of the dielectric in meters

a = inner radius of the dielectric in meters

For high-density polyethylene $\epsilon_r = 2.38$; ϵ_o is the permittivity of free space, $1/(36\pi \times 10^9)$. As indicated in Figure 2-1, the center conductor is stranded, rather than a smooth single conductor. If $b \gg a$, reference [18], p. 69 shows that a suitable value for a is the radius of the circumscribed circle, i.e., 1.5 times the strand radius in the

case of 7-strand conductors. As it turns out, the same value gives tolerable results even when b is only a few times as great as a. ("Tolerable" may be defined here as within 4.5% for b/a = 3, 7% for b/a = 2, or 12-13% for b/a = 1.5. The error is less for cables of more than seven strands.) This "calipered" radius (half the "calipered" or maximum strand-bundle diameter) is the value used in all capacitance calculations here.

The resistance and inductive reactance of the cable arises from a variety of sources. Resistance is present in both the center conductor and the return path through the seawater. They will be treated separately. The inductance normally thought of as the inductance of a coaxial configuration, and the value most often given in reference works, is the high-frequency or external inductance, that is, the inductance between conductors. For the coaxial configuration, it is easily found to be [20, p. 167]

$$L = \frac{\mu}{2\pi} \ln(b/a) \qquad (2\text{-}3)$$

where

L = inductance in henries/unit length (meter, in RMKS units)

μ = permeability of the space between conductors, = $\mu_0\mu_r$

b = inner radius of outer conductor in meters

a = outer radius of inner conductor in meters

The relative permeability μ_r of most dielectrics, including polyethylene, is unity; μ_0 is the permeability of free space, $4\pi \times 10^{-7}$.

In addition to the external inductance, each conductor has some self-inductance of its own, due to partial flux linkages with the current within the conductors. This inductance is known as the internal inductance; it is a function of frequency, is intimately bound up with the phenomenon of skin effect, and is not so easily described.

Normally, the external inductance predominates in a transmission line, because the inter-conductor spacing is reasonably large with respect to the dimensions of the conductors. Equation (2-3) shows that for a coaxial line, inductance will increase with the ratio b/a. Since only the current-carrying portion of a conductor's cross-sectional area contributes to the internal inductance, this inductance will be small at high frequencies where skin-effect forces current to the periphery of the conductors; it will usually be negligible with respect to the external inductance. If the outer conductor is thin, as is often the case with coaxial lines, its internal inductance may be negligible at any frequency. But at low frequencies the internal inductance of the center conductor is not entirely negligible, being up to several percent of the external inductance for conductor spacings normally found in practical coaxial cables. In a

sea-return line, large cross-sections of the ocean are involved in the return path, especially at low frequencies. Under these conditions, the internal inductance of the outer conductor can be several times the external inductance, and thus the controlling parameter.

The behavior of a solid, round straight wire with frequency is well understood. For direct currents, the resistance is the reciprocal product of cross-sectional area and material conductivity, times the length of the wire. On a unit length basis

$$R_{dc} = \frac{1}{\pi b^2 \sigma} \qquad (2\text{-}4)$$

where

R_{dc} = dc resistance, ohms/ unit length

b = radius of the wire, meters

σ = conductivity of the material, mhos/meter

The internal inductance of a solid, round wire with uniform current distribution is found to be [23; 27, p. 159]

$$L_{dc} = \frac{\mu}{8\pi} \qquad (2\text{-}5)$$

where

L_{dc} = "dc" inductance in henries/unit length

μ = permeability of the material

The subscript "dc" is applied to this inductance because the

condition of uniform current distribution implies zero frequency.

The ac resistance and reactance of round wires, accounting for skin effect, have been computed by many authors [1,8,19,27]. Rigorous expressions may be obtained as special cases of equations developed in Chapter IV, or may be taken directly from [24], p. 213 with due allowance for differences in notation. They are:

for the resistance,

$$R = R_{dc} \frac{u}{2} \frac{(\text{ber } u)(\text{bei}' u) - (\text{bei } u)(\text{ber}' u)}{(\text{ber}' u)^2 + (\text{bei}' u)^2} \qquad (2\text{-}6)$$

and for the inductance,

$$L = L_{dc} \frac{u}{2} \frac{(\text{ber } u)(\text{ber}' u) + (\text{bei } u)(\text{bei}' u)}{(\text{ber}' u)^2 + (\text{bei}' u)^2} \qquad (2\text{-}7)$$

where

R = ac resistance in ohms/unit length

L = ac inductance in henries/unit length

$u = b\sqrt{\omega\mu\sigma}$

ω = radian frequency

and the other quantities have been defined immediately above. The ber and bei functions and their derivatives, ber' and bei', sometimes collectively called Thomson functions, are related to the real and imaginary parts of Bessel functions of the first kind with complex arguments. They

are discussed in most books covering Bessel functions. Reference [22], in addition to a thorough treatment, gives numerical tables and lists of identities for both the first and second kinds (p. 168ff). A brief treatment is also given in Appendix B. The dimensionless parameter u, which appears here as the argument of the Thomson functions, is a quantity related to "skin effect". Skin depth, δ, is the distance from the surface of a conductor at which the current has decreased to 1/e (1/2.71828...) of its surface value. Since this value is often taken as a measure of the current penetration into a conductor, it is of interest to list here the relation between u and δ for convenience of reference. Skin depth is given by [24; 25, p. 147] the formula

$$\delta = 1/\sqrt{\pi f \mu \sigma} \quad , \tag{2-8}$$

from which

$$u = b\sqrt{2}\,/\delta \tag{2-9}$$

where b is the conductor radius.

Again, as with capacitance, the question of stranding is raised. The above formulas are based on a solid, round wire, to which, strictly speaking, a stranded conductor is only an approximation. The effects of stranding are difficult to handle analytically. In addition to accounting for

interstices within the conductor and the complicated current distributions arising from skin effects, there are second-order effects, such as the twist of the strands. Since each of the outer six strands is wound around the center strand, they actually form small solenoids. The resulting slight increase in inductance is, of course, a function of the degree of twist (i.e., the pitch), and will offset the loss of inductance due to the interstices to some extent. In general, it has been found [4; 14, p. 39] that, for a wire of seven uninsulated equal-sized strands in intimate contact, the ac behavior is essentially the same as that of a solid round conductor having the same conducting cross-section. Thus, if the strand radius is r, the radius of the circumscribing circle is $b = 3r$, and the radius of the equivalent solid conductor is b',

$$\pi b'^2 = 7\pi r^2 = 7\pi (b/3)^2$$

or

$$b' = \frac{\sqrt{7}}{3} b \qquad (2\text{-}10)$$

This adjustment of the radius is made for stranded conductors in all that follows.

Expressions must also be found for resistance and inductance of the seawater return. The procedure begins with the electric and magnetic fields of an infinite

straight wire in seawater, which may be derived from the material of Appendix C and which have been computed by several authors. Of several equivalent forms, those derived by Von Aulock [33, p. 13] are, in terms of effective-value phasors and at a distance x from the wire:

$$\check{E} = \frac{j\omega\mu\check{I}}{2\pi} (\ker u_x + j \operatorname{kei} u_x) \qquad (2\text{-}11)$$

$$\check{H} = \frac{\check{I}u_x}{2\pi x} (\ker' u_x + j \operatorname{kei}' u_x) \qquad (2\text{-}12)$$

where

$\check{E}$ = longitudinal electric field along the cable (Z-direction in cylindrical coordinates)

$\check{H}$ = tangential magnetic field around the cable (φ-direction in cylindrical coordinates)

$\check{I}$ = current in the wire

$u_x = x\sqrt{\omega\mu\sigma}$

and the supercarat denotes the effective-value phasor representation, e.g., $E(x,t) = \mathcal{R}_e \sqrt{2}\, \check{E}\, e^{j\omega t}$.* The permeability, μ, of seawater is essentially that of free space, μ_o [33, p. 15]; the value of conductivity assumed in the work presented here is 3.3 mhos/meter. See Appendix D for the reasons presented. The ker, kei, ker', and kei' functions arise from modified Bessel functions of the second kind, and are analogous to the previously introduced Thomson functions

*The notation $\mathcal{R}_e$ is read as "the real part of"

(ber, etc.) of the first kind. They are also discussed in Appendix B.

The mean power dissipated in the sea per unit length is $\mathcal{R}_e \{\check{E}(\check{I})^*\}$ or $|\check{E}|^2/R$; in field form the expression is

$$P = \sigma \int_b^\infty \check{E} \cdot (\check{E})^* \quad 2\pi r \, x \, dx \tag{2-13}$$

where

P = mean power dissipated in the sea in watts/unit length

σ = conductivity of seawater, mhos/meter

$\check{E}$ = longitudinal electric field (eq. (2-11))

b = radius of the wire (including insulation)

and the asterisk denotes the complex conjugate. This mean power P is also equal, of course, to $|\check{I}|^2 R$, where $|\check{I}|$ is the RMS or effective value of the current in the wire and R is the total resistance of the sea-return path. Then,

$$R = \frac{\omega\mu}{2\pi} \int_{b\sqrt{\omega\mu\sigma}}^\infty \left[(\text{ker } u_x)^2 + (\text{kei } u_x)^2\right] u_x \, du_x \tag{2-14}$$

In the seawater, the lower limit of integration will be quite small for the wire sizes and frequencies of interest, as shown in Appendix E; it may conveniently be taken here as zero. The only disquieting thought is the fact that the ker function becomes infinite at the origin. Nevertheless, it is possible to show (e.g., using the approximations of Appendix B) that the limit of the integral in (2-14) approaches zero as the argument approaches zero. Armed with this fact,

the integral may be looked up [22, p. 172] and evaluated to yield

$$R = \frac{\omega\mu}{8} \tag{2-15}$$

where

R = resistance of the sea-return path, ohms/unit length

μ = permeability of seawater

ω = radian frequency

Note that, as a first approximation, this resistance is independent both of the wire diameter and the conductivity of the sea.

The internal inductance of the sea is computed from the average energy stored in the magnetic field:

$$U = \frac{1}{2}\int_V \mathrm{Re}\{\check{B} \cdot \check{H}^*\}\,dV \tag{2-16}$$

$$= \frac{\mu}{2}\int_V \check{H} \cdot \check{H}^*\,dV$$

where U = energy in joules/meter^3

$\check{B}$ = magnetic induction in webers/meter^2

$\check{H}$ = magnetic force in amperes/meter

V = volume in cubic meters

Equation (2-16) is a general formula, true anywhere. In this case, the volume is a unit length of the seawater return. From circuit concepts, the stored mean energy is also equal to $\frac{1}{4} L\,\overline{I(t)^2} = \frac{1}{2} L|\check{I}|^2$, then

$$L|\check{I}|^2 = \mu \int_b^\infty \check{H}\cdot\check{H}^* \, 2\pi x \, dx \qquad (2\text{-}17)$$

Inserting equation (2-12) into (2-17),

$$L = \frac{\mu}{2\pi} \int_{b\sqrt{\omega\mu\sigma}}^\infty \left[(\mathrm{ker}' \, u_x)^2 + (\mathrm{kei}' \, u_x)^2\right] u_x \, du_x \qquad (2\text{-}18)$$

This integral may also be found in reference [22], p. 172, but in general it does not assume such a simple form as equation (2-15). However, the Thomson functions can be approximated well by the first few terms of their series expansions if their arguments are small enough (see Appendix B). If, the large-argument approximations [22, pp. 179-180] are used, it is found that the integral in (2-18) approaches the form $-\frac{\pi}{\sqrt{2}} \, e^{-u_x\sqrt{2}}$ and hence approaches zero as the argument becomes infinite. The actual evaluation of (2-18) is straightforward but tedious; one convenient form is:

$$L = \frac{\mu}{2\pi} \ln \frac{2}{1.781 \, u_x} \quad , \quad u_x \ll 1 \qquad (2\text{-}19)$$

where

L = internal inductance of the sea-return path henries/unit length

μ = permeability of seawater

u_x = $b\sqrt{\omega\mu\sigma}$

b = inner radius of the sea-return path

σ = conductivity of seawater

ω = radian frequency

At the upper frequency of interest, which is one megacycle here, $\sqrt{\omega\mu\sigma} \approx 5.1$; furthermore only small-diameter cables are being considered, for which $b \leq 10^{-3}$ meter. Therefore, the approximation of (2-19) is justified.

Because of the immense amount of labor involved in computation of the exact expressions involving the Thomson functions, considerable attention has been given to simplifications. Appendix B gives some low- and high-frequency approximations to the expressions obtained in this section. Some others, worked out by Schelkunoff, will be met with in a later section. In the numerical results presented here, the approximations have usually been used where applicable.

Now that expressions have been obtained for all quantities in all regions, the propagation characteristics can be computed from equations (1-2), in which it must be borne in mind that R, G, L, and C are <u>total</u> quantities per unit length. G has been disposed of as negligible, and C has only the one term, given by equation (2-2). For the series parameters,

$$R = R_{wire} + R_{sea}$$
$$L = L_{wire} + L_{sea} + L_{ext} \qquad (2\text{-}20)$$

where

R_{wire} = ac resistance of the center conductor (eq. (2-6))

R_{sea} = ac resistance of the sea-return path (eq. (2-15))

L_{wire} = internal inductance of the center conductor (eq. 2-7))

L_{sea} = internal inductance of the sea-return path (Eq. (2-19))

L_{ext} = external inductance between coaxial conductors (eq. 2-3))

and all quantities are, of course, per unit length. Then equations (1-2) become

$$Z_o = \sqrt{\frac{Z}{Y}} = \sqrt{\frac{R + j\omega L}{j\omega C}} \qquad (2\text{-}21)$$

for the characteristic impedance, and for the propagation constant

$$\gamma = \sqrt{ZY} = \sqrt{(R + j\omega L)(j\omega C)} = \sqrt{-\omega^2 LC + j\omega RC} \qquad (2\text{-}22)$$

The second form of equation (2-22) shows that it may be a dangerous assumption to neglect the inductance of a line entirely and assume that one is dealing with an RC line (i.e., one having resistance and capacitance only). This is especially true at the higher frequencies, above the audio range. Such an assumption may very well turn out to be valid, but it ought not to be casually made, especially in the case of sea-return lines with their large internal inductances in the return path.

Equations (2-21) and (2-22) have been computed over the range of 10 cps to 1 megacycle for several sizes of wire and insulation. The choice of dimensions is admittedly somewhat arbitrary, being made as it is partly to relate it to other work, and partly as a matter of convenience in design of instrumentation; the details are not germane to the discussion here, which is concerned mainly with comparative results. Dimensions are listed in Table 2-1. Curves of characteristic impedance are shown in Figure 2-2, and of attenuation in Figure 2-3.

A further word about attenuation and the form in which the results are presented may be in order at this point. Equation (A-11), Appendix A shows that, for a line terminated in its characteristic impedance,

$$\overset{\times}{V}_s = \overset{\times}{V}_g e^{-\gamma s} = \overset{\times}{V}_g e^{-\alpha s} e^{-j\beta s} \quad , Z_o = Z_L \qquad (2\text{-}23)$$

where

$\overset{\times}{V}_s$ = voltage at distance s from the source

$\overset{\times}{V}_g$ = source (generator) voltage

$\gamma = \alpha + j\beta$ = propagation constant of the line

s = distance from the source along the line

and the overcross denotes a peak phasor, e.g., $V(s,t) = \mathcal{R}_e(\overset{\times}{V} e^{j\omega t})$. Then the insertion loss is given by

$$\text{Loss} = \alpha s \text{ nepers} \qquad (2\text{-}24)$$

Since the matched loss is the loss that is characteristic of the line itself, it is the only interesting quantity here. The mismatch losses (if any) due to the terminations can be kept separate and worried about at some other time.

Specifically, for a line of length ℓ, insertion loss $= \alpha\ell$, where $\alpha = \mathcal{R}_e(\gamma)$. It is this insertion loss that is presented as "attenuation" in the graphs herein. For convenience, line length was taken as 4 kilometers. In all that follows, unless otherwise specified, it may be assumed that $\ell = 4{,}000$ meters.

III. THE METALLIC-RETURN COAXIAL LINE

Regardless of the configuration of conductors which will be employed, the first question to be answered concerns the return path -- should it be seawater, or would a customary coaxial configuration using a metallic outer conductor be preferable? Qualitatively, the two greatest advantages of the seawater-return are simplicity and relatively large inductance at moderate frequencies. This is due in large measure to the internal inductance of the return, which is large because the effective cross-sectional area is large. But $\frac{d\delta}{df}$ is inversely proportional to $\sqrt{\sigma}$, where δ is skin depth, defined in (2-8), and σ is conductivity; hence skin effects are more pronounced in seawater than they would be in copper. Thus, over the rather wide range of frequency under consideration, R and L (and hence Z_o and γ) will vary more than in a conventional cable.

In a metallic-return, resistance will be greater and inductance less at low frequencies, but at high frequencies the opposite will be true. Hence, it is of considerable interest to compare the examples of the previous configuration with conventional coaxial cables of the same dimensions.

Consider the coaxial line whose cross-section is shown in Figure 3-1; it is the insulated wire of the previous

section, to which has been added an outer copper conductor consisting of an appropriate number of strands of round metallic wire. Each strand is bare and is in contact with its neighbors throughout its length. For purposes of computing its impedance, the return will be considered to be a tubular conductor of inner radius a, outer radius b, and thickness $d = b - a$. Calculations of this configuration will parallel those of the previous section, except that the internal inductance and resistance of the seawater return will be deleted, and the internal inductance and resistance of a tubular conductor substituted. For the time being, this coaxial cable is assumed to be on land, so that the sea exerts no effect on it.

The general expression for the impedance (often called "surface impedance" because of its manner of computation) of a tubular conductor in which all the conduction current flowing in the tube returns, i.e., completes the circuit path, via a route lying inside the tube, will be shown later to be a special case of the equations of Chapter 4. Alternatively, we may use directly any one of several equivalent expressions [8, p. 557; 22, p. 149; 24, p. 219], whose derivations may be found in the references cited. One convenient form is

$$Z = \frac{\Gamma}{2\pi\sigma a} \frac{I_0(\Gamma a)K_1(\Gamma b) + K_0(\Gamma a)I_1(\Gamma b)}{I_1(\Gamma b)K_1(\Gamma a) - K_1(\Gamma b)I_1(\Gamma a)} \qquad (3\text{-}1)$$

where

Z = $R + j\omega L$ = impedance of the tubular conductor per unit length, accounting for skin effect

a = inner radius of tube

b = outer radius of tube

Γ = $\sqrt{j\omega\mu\sigma}$

σ = conductor material conductivity

μ = conductor material permeability

ω = radian frequency

I_0, I_1 = modified Bessel functions of the first kind, of orders zero and one respectively (see Appendix B)

K_0, K_1 = modified Bessel functions of the second kind, of orders zero and one (see Appendix B)

If a new parameter, v, is defined such that $v = \sqrt{\omega\mu\sigma}$, then

$$\Gamma = v\sqrt{j} = \frac{v}{\sqrt{2}}(1 + j) \qquad (3\text{-}2)$$

and equation (3-1) becomes, by use of the relationships listed in Appendix B,

$$Z = \frac{\Gamma(1 + j)}{2\pi\sigma a\sqrt{2}} \frac{A - B}{C - D} = \frac{jv}{2\pi\sigma a} \frac{A - B}{C - D} \qquad (3\text{-}3)$$

where

A = (ber va + j bei va)(ker' vb + j kei' vb)

B = (ker va + j kei va)(ber' vb + j bei' vb)

C = (ber' vb + j bei' vb)(ker' va + j kei' va)

$$D = (\text{ker}' vb + j\,\text{kei}' vb)(\text{ber}' va + j\,\text{bei}' va)$$

$$v = \sqrt{\omega\mu\sigma}$$

As mentioned in the previous section, the exact expressions for the impedance of a solid wire may be taken directly from [3], p. 213. The same reference (p. 219) gives an exact expression for the impedance of a tubular conductor. A little reflection will show that the difference between that expression, which contains Hankel functions, and equation (3-1) is only in the choice of function to be used as a second solution to Bessel's equation during the derivation. This is largely a matter of personal taste, for Hankel functions are tabulated, too [17]. They have their infinite series forms and their asymptotic approximations, just as do the Thomson functions. However, only the latter are used here.

When Z is computed from equation (3-3), the real part yields the a.c. resistance, and the imaginary part the internal reactance, of a tubular conductor at any frequency. Unfortunately, Z does not simplify greatly upon expansion and collection of terms. The ber, bei, ker, and kei functions, their four derivatives, and the two arguments involved yield 12 quantities which will appear in the function, of the 16 possible.

Multiplication of numerator and denominator of the fraction by the complex conjugate of the denominator leads to terms which are each the product of four of these quantities. A disheartening percentage of the possible combinations will appear; the denominator, for instance, is the sum of 16 terms. If the exact expression must be used in computing Z, the last form given is probably the most convenient.

High- and low-frequency approximations to the modified Bessel functions may be used for frequencies such that the arguments are " $\gg 1$" and " $\ll 1$" respectively. While these qualifications are often seen in tables, collections of formulas, derivations, and the like, the question of exactly how much less or greater frequently goes begging. If a double inequality sign is interpreted as requiring a difference in size at least an order of magnitude, then the approximations may be used for frequencies where

$$v_a \gtrsim 10$$

$$v_b \lesssim 0.1$$

For the dimensions and materials which will be under consideration in this section the frequencies are, unfortunately, about 540 kc and 41 cycles, respectively. This is half the frequency range considered, and the half in which most of the interesting things are happening, at that.

The exact expression may still be avoided in the specific case under consideration. Schelkunoff, in a paper of basic and far-reaching importance [8, p. 557f] states that, if the thickness of the tube is not more than 25 percent of the tube's high-frequency (i.e., inner) radius, use of the high-frequency approximations at low-frequencies yields errors of less than 1%. Since the dimensions met with here will conform to this restriction, advantage is taken of the opportunity to use the high-frequency or so-called "thin-wall" approximations.

These approximations are given by the following expressions, as will be brought out in Chapter IV:

$$R = R_{dc}\left[\frac{u_1}{2}\,\frac{\sinh u_1 + \sin u_1}{\cosh u_1 + \cos u_1} - \frac{d}{8a}\left(1 + \frac{3a}{b}\right)\right] \qquad \text{(a)}$$

$$\omega L = R_{dc}\left[\frac{u_1}{2}\,\frac{\sinh u_1 - \sin u_1}{\cosh u_1 - \cos u_1}\right] \qquad \text{(b)}$$

(3-4)

where

R = resistance of tubular conductor, ohms/unit length

L = internal inductance of tubular conductors, henries/unit length

a = inner radius of tube, meters

b = outer radius of tube, meters

d = thickness of tube = b - a

u_1 = $dv\sqrt{2}$

γ = $\sqrt{\omega\mu\sigma}$ (evaluated within the conducting material of the tube)

R_{dc} = dc resistance of the tubular conductor, ohms/unit length = $\frac{1}{2\pi\sigma da}$

Equations (3-4) are not quite those given by Schelkunoff. If the second term in brackets of (3-4a) is deleted, the expressions for R and L are the plane-conductor (i.e., large-radius) approximations given by Ramo and Whinnery and others [24, p. 219]. The additional term is the first-order correction for curvature (it applies to the resistance only), and is incorrect as presented in [8]. This has been pointed out in reference [5], p. 838, which lists the correct values (p. 869) as well as the second-order correction terms. It might be noted in passing that if the frequency is very high, further simplifications of the formulas are possible; they will not be given here, but may be found in references [8] or [33], if desired. With respect to Schelkunoff's paper [8], careful interpretation allows us to tie down the vaguely specific term "very high": Schelkunoff's equations (84) may be used in place of equations (3-4) of this paper to within 1% accuracy, if the arguments of the Bessel functions in equation (3-1) are greater than about 6. If the arguments are greater than 50, the first terms alone may be used. (Most of the error is in the resistance; the inductance is little affected.)

The dc resistance of the tube may be computed from the thin-wall approximation:

$$R_{dc} = \frac{1}{2\pi\sigma bd} \tag{3-5}$$

where

R_{dc} = dc resistance, ohms/unit length

b = inner radius of the tube, meters

d = thickness of the tube, meters

σ = conductivity of the material, mhos/meter

However, because of the geometry of the outer conductor, the dc resistance may be computed exactly with ease; it is the resistance of an appropriate number of circular strands in parallel. In a sample calculation where the value was computed exactly as $5.03 \times 10^{-2}\,\Omega$/meter, the resistance given by equation (3-5) is only $4.24 \times 10^{-2}\,\Omega$/meter. Such a discrepancy is to be expected, for in assuming a field pattern based on a cylindrical conductor one tacitly assumes the existence of much more conductor than is actually present. This could be compensated for, at zero frequency at least, by adjusting one or more dimensions to some equivalent value. A safer procedure seems to be to adjust the conductivity of the material, for a variety of reasons. First, while the coaxial ring of conductors closely approximates a cylinder, it is exactly the return conductor of a "cage" transmission line. This configuration is discussed by King [19]; the expressions for the internal impedances of the coaxial- and cage-line conductors are derived and compared, and adjustment of conductivity is mentioned as a technique. Second,

the equations for skin-effect resistance and reactance of a tubular conductor, or the graphs of these functions [8, p. 561; 24, p. 220] ; show at a glance that they are functions of the dc values. Given that the fields are circularly symmetrical, their behavior with frequency depends on the tube and the constants of the material; thus it seems reasonable that a configuration of very similar geometry and the same dimensions and materials will exhibit similar behavior.

With these thoughts in mind, an adjusted conductivity may be defined:

$$\sigma_a = \frac{nr^2}{2bd}\,\sigma \qquad (3\text{-}6)$$

where

σ_a = adjusted conductivity, mhos/meter

σ = conductivity of the material, mhos/meter

n = number of strands in the tube

b = radius of the inscribed circle tangent to the ring of strands

r = radius of the strands

d = thickness of the tube of strands

As applied to the configuration of Figure 3-1, a further simplification could be effected by recognizing that d = 2r. This will not always be the case, however, as will become evident later on, and it seems better to leave equation (3-6) as it is.

Then, the d.c. resistance may be computed from

$$R_{dc} = \frac{1}{2\pi\sigma_a bd} \text{ ohms/unit length} \qquad (3\text{-}7)$$

The ratio σ_a/σ will, of course, vary as dimensions and spacings vary.

The manner in which the coaxial configurations considered here were arrived at has already been discussed. Table 3-1 lists the pertinent dimensions of the examples computed. Attenuation and characteristic impedance curves are presented in Figures 3-2 and 3-3. Conditions and assumptions are the same as for the calculations of the previous section.

IV. THE METALLIC-RETURN COAXIAL LINE, IMMERSED

Since the purpose of the cables discussed here is oceanographic instrumentation, they will necessarily be immersed in the sea. If the cable is bare, so that the return is in intimate contact with seawater throughout its length, it cannot be assumed that the return current will be confined to the copper at all frequencies. As a matter of fact, the assumption may not be valid even with a jacket, because of the ever-present possibility of breaks, cracks, or pin holes which may compromise its water-integrity. If there are sufficient of these such that the metallic return is shorted to the sea at intervals which are small compared to a wave-length of the longitudinal current at the highest frequency of interest, the behavior will be essentially that of an unjacketed line. (At the maximum frequency considered here, which is one megacycle, λ_{min} = 300 meters in air, or about 195 meters for a polyethylene dielectric.)

The method of attack is based on the analysis of a laminated conductor, i.e., a conductor consisting of concentric layers in contact. This analysis was originally carried out in [8], and extended in [33]. The results are quite general and lead to many interesting points, as will become evident later in this section.

As in the previous section, use is made of most of the work on the sea-return line, the principal difference being in the calculation of the a.c. resistance and internal reactance of the outer conductor. This time, however, the outer conductor consists of two laminations, an inner copper one and an outer one of infinite thickness (the sea). But, before proceeding, it is desirable to digress long enough to summarize the method of analysis of a laminated conductor, because of its extensive implications.

At the outset, let us make a point of stating explicitly what has been implicit in all the discussion of propagation characteristics, transmission over the line, and so forth. In the steady-state, as soon as frequency is mentioned, or an ω committed to paper, we are speaking of periodic time functions. Specifically, in all that has gone before and all that is to follow, rotating phasor representations of all field quantities and currents have their time dependence given as $e^{j\omega t}$. It is customary in the literature not to carry along this factor for reasons of conciseness of notation, but to understand its presence at the proper places. Because this is a mnemonically dangerous practice, it seems better to use phasor notation. This is the reason for the overmarks (carat and cross) previously introduced. Hence

$$\frac{\partial^n}{\partial t^n} = (j\omega)^n \qquad (4\text{-}1)$$

The problem of transmission of currents over the structure of coaxial conductors consists in finding a particular periodic time solution of Maxwell's equations which satisfies the boundary conditions: continuity of tangential electric and magnetic forces at the surfaces of the conductors. To begin, Maxwell's equations are written within the conductor, making use of (4-1). From these equations, electric field intensities may be eliminated to obtain a differential equation for the magnetic field intensity. The procedure is undertaken in Appendix C and in most books on electromagnetic theory; article 6.03 of reference [24] is one example. In cylindrical coordinates, which are best suited to the coaxial structure, the resulting equation is, from (C-21), Appendix C,

$$\frac{d}{dr}\left[\frac{1}{r}\frac{d}{dr}(r\overset{\times}{H})\right] = \Gamma^2\overset{\times}{H} \qquad (4\text{-}2)$$

where

r = radial distance from the axis of the conductor

$\overset{\times}{H}$ = tangential magnetic field

$\Gamma = \sqrt{j\omega\mu\sigma}$

and the overcross denotes the peak phasor value. In the derivation of this equation, the assumption is almost always made that displacement current within the conductor is negligible with respect to conduction current. If so, then

(4-2) stands as it is. Otherwise, the above approximation for Γ cannot be used to replace the exact value of the propagation constant, which is seen from (C-7) to be $\sqrt{j\omega\mu\sigma - \omega^2\epsilon\mu}$. Here then is the criterion by which one may decide whether displacement current effects can be ignored. If they can, it must be true that

$$\frac{\omega^2\epsilon\mu}{\omega\mu\sigma} = \frac{\omega\epsilon}{\sigma} \ll 1 \qquad (4\text{-}3)$$

In any metallic conductor σ is sufficiently large that equation (4-3) holds for any frequency likely to be met with in practice. However, we had better check the inequality in seawater. At the highest frequency of interest here, one megacycle, $\omega\epsilon/\sigma = 10^{-5}$, which is definitely much less than unity. But it is seen that, as frequency mounts, seawater will begin to look less like a conductor and more like a dielectric. Ramo and Whinnery [24, p.277] give a value of around 9 megacycles as the frequency at which displacement current has increased to one hundredth of the conduction current. In any case, however, (4-2) and Γ are sufficiently accurate for the purposes of this investigation.

Equation (4-2) is a form of Bessel's equation, the solution of which is, from Appendix B with $n = 1$ and $x = \Gamma r$ in (B-6),

$$\overset{x}{H} = AI_1(\Gamma r) + BK_1(\Gamma r) \qquad (4\text{-}4)$$

where A and B are constants to be determined. The modified Bessel functions I_1 and K_1 have been met with previously. Now equation (4-4) may be substituted back into Maxwell's equations (specifically, into (C-5b), Appendix C). After use of some identities relating the modified Bessel functions, there results a similar expression for the longitudinal electric field:

$$\overset{\times}{E} = (\Gamma/\sigma)\left[AI_0(\Gamma r) - BK_0(\Gamma r)\right] \qquad (4\text{-}5)$$

where A and B are the same constants appearing in (4-4). Some labor is involved in the calculations.

The two expressions (4-4) and (4-5) can be applied to any conductor configuration in cylindrical coordinates. Let it apply specifically to a tubular conductor, Figure 4-1, which has an inner radius a and an outer radius b. In the most general case, the current in the tubular conductor may return to the source through two paths, one within the tube and the other lying outside. Let the total current in the conductor be $I_a + I_b$, and let the portion I_a be the return current which flows inside the tube, the remainder I_b flowing outside. Then the constants A and B in equations (4-4) and (4-5) may be evaluated by applying Ampere's Law at the inner and outer surfaces of the tube, where the magnetic field intensity is known:

$$\overset{\times}{H}(a) = -\frac{\overset{\times}{I}_a}{2\pi a}, \quad r = a \qquad (4\text{-}6)$$

$$\overset{\times}{H}(b) = \frac{\overset{\times}{I}_b}{2\pi b}, \quad r = b \qquad (4\text{-}7)$$

The minus sign appears in (4-6) because current is taken as flowing in the positive direction within the tube. If (4-5) is written at the surfaces of the tube (r = a and r = b), and (4-6) and (4-7) are substituted in these expressions, simple manipulation yields the values of A and B. Collection of terms then yields equations which have the form

$$\left.\begin{aligned} \overset{\times}{E}(a) &= Z_a \overset{\times}{I}_a + Z_t \overset{\times}{I}_b \quad (a) \\ \overset{\times}{E}(b) &= Z_t \overset{\times}{I}_a + Z_b \overset{\times}{I}_b \quad (b) \end{aligned}\right\} \qquad (4\text{-}8)$$

where

$\overset{\times}{E}(a)$ = longitudinal electric field at the inner surface of the tubular conductor

$\overset{\times}{E}(b)$ = corresponding quantity at the outer surface

$\overset{\times}{I}_a$ = portion of current flowing in the conductor which returns to the generator by a path lying in the hole within the tube

$\overset{\times}{I}_b$ = corresponding quantity returning over a path outside the tube

Z_a = "Surface impedance" for internal return current

Z_b = "Surface impedance" for external return current

Z_t = "Transfer impedance" (The development of this expression again requires the use of modified Bessel function identities.)

It is now obvious where the name "Surface impedance" comes from. Together these last three quantities define the resistance and reactance of a tubular conductor at any frequency.

The expressions for these impedances, developed in the manner just described, are:

$$Z_a = \frac{\Gamma}{2\pi\sigma a} \frac{I_0(\Gamma a)\, K_1(\Gamma b) + K_0(\Gamma a)\, I_1(\Gamma b)}{I_1(\Gamma b)\, K_1(\Gamma a) - K_1(\Gamma b)\, I_1(\Gamma a)} \quad \text{(a)}$$

$$Z_b = \frac{\Gamma}{2\pi\sigma b} \frac{I_0(\Gamma b)\, K_1(\Gamma a) + K_0(\Gamma b)\, I_1(\Gamma a)}{I_1(\Gamma b)\, K_1(\Gamma a) - K_1(\Gamma b)\, I_1(\Gamma a)} \quad \text{(b)} \qquad (4\text{-}9)$$

$$Z_t = \frac{1}{2\pi\sigma ab} \frac{1}{I_1(\Gamma b)\, K_1(\Gamma a) - K_1(\Gamma b)\, I_1(\Gamma a)} \quad \text{(c)}$$

where

$\Gamma = \sqrt{j\omega\mu\sigma}$

a = inner radius of the tubular conductor, meters

b = outer radius of same, meters

Z_a, Z_b, Z_t = impedances of previously defined, ohms per unit length

As was done in Chapter 3, equations (4-9) may be put in a form somewhat more convenient for computation with the aid of a few identities from Appendix B and patience in algebraic manipulation. The results are

$$Z_a = \frac{jv}{2\pi\sigma a}\,\frac{A - B}{C - D} \quad \text{(a)}$$

$$Z_b = \frac{jv}{2\pi\sigma b}\,\frac{E - F}{C - D} \quad \text{(b)} \qquad (4\text{-}10)$$

$$Z_t = \frac{jv}{2\pi\sigma ab}\,\frac{1}{C - D} \quad \text{(c)}$$

where

$$\begin{aligned} A &= (\text{ber } va + j\ \text{bei } va)(\text{ker}' vb + j\ \text{kei}' vb) \\ B &= (\text{ker } va + j\ \text{kei } va)(\text{ber}' vb + j\ \text{bei}' vb) \\ C &= (\text{ber}' vb + j\ \text{bei}' vb)(\text{ker}' va + j\ \text{kei}' va) \\ D &= (\text{ker}' vb + j\ \text{kei}' vb)(\text{ber}' va + j\ \text{bei}' va) \\ E &= (\text{ber } vb + j\ \text{bei } vb)(\text{ker}' va + j\ \text{kei}' va) \\ F &= (\text{ker } vb + j\ \text{kei } vb)(\text{ber}' va + j\ \text{bei}' va) \\ v &= \sqrt{\omega\mu\sigma} \end{aligned} \qquad (4\text{-}11)$$

Just as in the case of the dry coaxial line considered earlier, there are approximations to the expressions (4-10) - (4-11) which, while not simple, afford a considerable improvement in ease of calculation. The restrictions and qualifications on their use, which were mentioned in the previous chapter, apply to them all. Specifically, it is the relative thinness of the laminations that permits the use here of asymptotic expressions for the modified Bessel functions. Then separating the resulting quantities into real and imaginary parts gives

$$R_a = \frac{1}{2\pi\sigma da}\left[\frac{u_1}{2}\,\frac{\sinh u_1 + \sin u_1}{\cosh u_1 - \cos u_1} - \frac{d}{8a}\left(1 + \frac{3a}{b}\right)\right] \quad \text{(a)}$$

$$\omega L_a = \frac{1}{2\pi\sigma da}\left[\frac{u_1}{2}\,\frac{\sinh u_1 - \sin u_1}{\cosh u_1 - \cos u_1}\right] \quad \text{(b)}$$

$$R_b = \frac{1}{2\pi\sigma db}\left[\frac{u_1}{2}\,\frac{\sinh u_1 - \sin u_1}{\cosh u_1 - \cos u_1} + \frac{d}{8b}\left(1 + \frac{3a}{b}\right)\right] \quad \text{(c)}$$

$$\omega L_b = \frac{1}{2\pi\sigma db}\left[\frac{u_1}{2}\,\frac{\sinh u_1 - \sin u_1}{\cosh u_1 - \cos u_1}\right] \quad \text{(d)}$$

$$R_t = \frac{u_1}{2\pi\sigma d\sqrt{ab}}\left[\frac{\sinh\frac{u_1}{2}\cos\frac{u_1}{2} + \cosh\frac{u_1}{2}\sin\frac{u_1}{2}}{\cosh u_1 - \cos u_1}\right] \quad \text{(e)}$$

$$\omega L_t = \frac{u_1}{2\pi\sigma d\sqrt{ab}}\left[\frac{\sinh\frac{u_1}{2}\cos\frac{u_1}{2} - \cosh\frac{u_1}{2}\sin\frac{u_1}{2}}{\cosh u_1 - \cos u_1}\right] \quad \text{(f)}$$

(4-12)

where

R = resistance, ohms per unit length

L = inductance, henries per unit length

a = inner radius of tubular conductor, meters

b = corresponding outer radius

d = thickness of tube = b - a

$u_1 = vd\sqrt{2} = d\sqrt{2\omega\mu\sigma}$

σ = conductivity of conductor material, mhos/meter

μ = permeability of conductor material

subscript a = designator referring to return current flowing within the tube (internal return current)

subscript b = corresponding designator for external return current

subscript t = designator for transfer quantities

ω = radian frequency

A reminder is made again about the first-order correction terms to the surface resistances, as discussed following equation (3-4).

By now it has probably been noted that equations (3-1) and (4-9a) are identical, as are (3-3) and (4-10a), and finally (3-4a & b) and (4-12a & b) respectively. This is only to be expected, for a glance at equations (4-8) shows that if the external return current I_b is zero, we have just the case of an ordinary coaxial line; it is seen to be a special case of the more general case treated here.* In computing R_a and L_a in the previous chapter, the factor outside the square brackets was called R_{dc}. There seems to be little profit in continuing the notation

*A second glance shows that, for $I_b = 0$, the field is not necessarily confined to the space between the conductors; it has a value at the outer surface of the conductor which depends on the current in the conductor and the transfer impedance. Of course, as the layer becomes thicker and/or the frequency increases, this field becomes weaker, but it is a mistake to say that none exists. As a matter of fact, for thin-wall structures where the ratio of radii is not greater than 4/3, the external field due to internal currents is still about one-tenth of its dc value when $u_1 = 10$.

in the present case, for the factor differs for each of the impedances in (4-12). It is worth noting, however, that in every case it corresponds to a dc resistance per unit length which is calculated using the inner radius of the lamination (for internal return current as in the dry line), the outer radius (for external return current), or the geometric mean radius (for the transfer parameters). In calculating these resistances, it will again be necessary to adjust the conductivity, as was done for the R_{dc} term, in any cases in which one must account for the fact that a conductor made up of smaller strands is not really a smooth tube. An adjusted conductivity will be used in the factors corresponding to R_{dc} in the expressions for surface resistances and reactances, but not in the arguments u and v.

Up to this point the discussion has centered on the properties of a single tubular conductor. Since any layer of a laminated conductor is just a tubular conductor, all that remains is to match up the fields at the boundaries between layers, in terms of the current in each layer, and the properties of the laminated conductor are thereby determined. The procedure is carried out in Appendix F. The result is a pair of recursion formulas which, as applied to an outer conductor, take the form

$$z_{am} = Z_{am} - \frac{Z_{tm}^2}{Z_{bm} + z_{a,m-1}}$$

$$z_{tm} = \frac{Z_{tm}\, z_{t,m-1}}{Z_{bm} + z_{a,m-1}} \qquad (4\text{-}13)$$

where

z_{am} = surface impedance, for internal return current, of the first m laminations (starting with the outermost lamination as No. 1 and counting inward), ohms per unit length

z_{tm} = corresponding transfer impedance, ohms per unit length

Z_{am}, Z_{bm}, Z_{tm} = surface and transfer impedances of the m^{th} lamination, ohms per unit length

As applied to a laminated outer conductor, only the quantity z_{am} is required, for there will be no conduction current returning outside the complete structure by hypothesis. By definition of z_{am} and z_{tm}, it is obvious that

$$z_{a1} = Z_{a1}$$

and

$$z_{t1} = Z_{t1} \qquad (4\text{-}14)$$

Thus, for any conductor having k laminations in all, it is just the quantity z_{ak}, as determined by (4-13) and (4-14), which is sought; this gives the ac resistance and internal reactance of the conductor at any frequency. The quantity z_{tk} is also available if desired.

In the present case, the outermost lamination is the sea, the internal impedance of which may be computed from (4-9c). For the seawater lamination $b = \infty$; if the limit of (4-9c) is taken as $b \to \infty$, it is seen that $Z_{t1} = 0$. Reference to (4-13) then shows that if $Z_{t1} = 0$, all z_{tm} will also be zero. Such a result is intellectually very satisfying, for the transfer impedance z_{tk} is a measure of the field outside a tubular structure due to current flowing inside it, and it is difficult to see how to get outside such a structure if it has an infinite radius.

Before leaving these theoretical considerations for calculation of some specific cases, it is worthwhile to digress yet a little further and savor once more equations (4-9), the expressions for surface and transfer impedances of a tubular conductor. It has already been stated that these expressions are quite general, and so they are; for they apply equally well to tubular conductors whose inner radius is zero, or whose outer radius is infinite. Consider (4-9b), the surface impedance for external return current; for the former case it may be rewritten in the form

$$Z_{b}\Big|_{a=o} = \lim_{a\to o}\left[\frac{\Gamma}{2\pi\sigma b}\,\frac{I_o(\Gamma b) + K_o(\Gamma b)\,\dfrac{I_1(\Gamma a)}{K_1(\Gamma a)}}{I_1(\Gamma b) - K_1(\Gamma b)\,\dfrac{I_1(\Gamma a)}{K_1(\Gamma a)}}\right] \qquad (4\text{-}15)$$

Now, $\lim_{a\to o} I_1(\Gamma a) = 0$, and $\lim_{a\to o} K_1(\Gamma a) = \infty$, leaving the well-known [22, p. 140; 24, p. 212; 27, p. 153] expression for the

impedance of a solid round wire:

$$Z_{wire} = \frac{\Gamma}{2\pi\sigma b} \frac{I_0(\Gamma b)}{I_1(\Gamma b)} \qquad (4\text{-}16)$$

where

b = radius of the wire

$\Gamma = \sqrt{j\omega\mu\sigma}$

After rewriting (4-16) in terms of Thomson functions (Appendix B) and performing some minor manipulations, there results the form

$$Z_{wire} = \frac{jv}{2\pi\sigma b} \frac{\text{ber } vb + j \text{ bei } vb}{\text{ber}' vb + j \text{ bei}' vb} \qquad (4\text{-}17)$$

where

b = radius of wire

$v = \sqrt{\omega\mu\sigma}$

If the denominator of (4-17) is rationalized and terms of the fraction collected, it is found that the real part of the resulting expression is just equation (2-6), and the imaginary part is ω times equation (2-7), which is only to be expected.

A similar procedure can be undertaken for a tubular conductor whose outer radius is infinite; this should yield the expressions for the impedance of a sea-return. Equation (4-9a), the expression for surface impedance with internal

return current, is rewritten in this case as:

$$Z_a\Big|_{b=\infty} = \lim_{b\to\infty}\left[\frac{\Gamma}{2\pi\sigma a}\,\frac{I_0(\Gamma a)\,\dfrac{K_1(\Gamma b)}{I_1(\Gamma b)} + K_0(\Gamma a)}{K_1(\Gamma a) - I_1(\Gamma a)\,\dfrac{K_1(\Gamma b)}{I_1(\Gamma b)}}\right] \qquad (4\text{-}18)$$

This time, $\lim_{b\to\infty} K_1(\Gamma b) = 0$, and $\lim_{b\to\infty} I_1(\Gamma b) = \infty$, and the result is an expression quite analogous to (4-16):

$$Z_{sea} = \frac{\Gamma}{2\pi\sigma a}\,\frac{K_0(\Gamma a)}{K_1(\Gamma a)} \qquad (4\text{-}19)$$

where

$\Gamma = \sqrt{j\omega\mu\sigma}$

a = inner radius of the infinitely thick hollow tube (radius of the "hole" in the sea)

In terms of the Thomson functions, (4-19) becomes

$$Z_{sea} = \frac{-jv}{2\pi\sigma a}\,\frac{\ker va + j\,kei\,va}{ker'\,va + j\,kei'\,va} \qquad (4\text{-}20)$$

where

$v = \sqrt{\omega\mu\sigma}$

If the same procedure of rationalization of the denominator, multiplication, and collection of terms is undertaken, it can be shown that the real and imaginary parts of the resulting expression correspond to results previously obtained. The Thomson functions of the second kind are unwieldy and the algebra is therefore not so straightforward, but the

procedure is carried through for the real part in Appendix E to illustrate the procedure.

The dimensions of the cables calculated in this chapter are listed in Table 3-1 of the previous chapter, since the cables themselves are identical and only the surrounding sea has been added. The internal impedance of the center wire, the capacitance, and the external inductance have all been calculated in the second chapter. Internal impedance of the sea was also calculated there; the resistance term, which is independent of radius, can still be used but the reactance will have to be redetermined because the copper outer conductor has now added thickness to the cable. Impedance of the copper layer was determined in the third chapter. The results of this chapter show how to combine the effects of the separate laminations. Then calculations of attenuation and characteristic impedance proceed as before. Results are presented graphically in Figures 4-2 and 4-3.

V. LINES WITH STEEL

A. General

Up to this point the theory as presented has been general enough to accommodate materials of any kind, but all the lines considered have contained only materials whose permeability was essentially that of free space. Since one of the stated goals of this investigation is a cable with a breaking strength higher than that obtainable using only copper or other non-ferrous materials, it is obvious that any acceptable design will be based largely on the question, not of whether steel will be included, but of where steel will be included. As far as the mechanical requirements are concerned, it is sufficient just to have the necessary strength members present, but their placement within the cable can make a big difference in the electrical characteristics.

Qualitatively it is not hard to predict what the effects of the steel will be: resistance will be higher, first because of the lower conductivity of steel, and second because, as equation (2-8) shows, skin effects will be more pronounced than in copper at any given frequency. On the other hand, internal inductance and hence total inductance will also increase, which is always desirable for the propagation characteristics of the line. In addition,

the rate of change of skin depth, $\frac{d\delta}{df}$, will be smaller since it varies inversely as $\sqrt{\mu}$. It is expected, however, that the disadvantages will outweigh the advantages. This expectation is the motivation for the practice followed in this section of additionally computing each sample cable as if it were nonmagnetic, in order to give a basis for direct comparison. Since the signals to which the line is to be exposed will be small in the present application, the assumption will be made whenever steel is encountered that μ_r is a constant, and that hysteresis effects are small enough to be negligible compared to other losses.

B. Steel-Core Line

The first cable sample to be investigated is the simplest configuration using steel: it is an ordinary coaxial configuration, in which each of the seven strands making up the center conductor is now of carbon steel of very high tensile strength instead of copper. The outer conductor is a ring of copper strands, as in previous cables. A cross-section of the sample would look quite like that shown in Figure 3-1, except that the center and outer conductors are of different material.

The configuration is not difficult to compute; all that is required is to use the appropriate value of μ_r in the equations already developed in Chapters 3 and 4.

The results, both for the actual line and the corresponding all-copper case are shown graphically in Figures 5-1 and 5-2. As is only to be expected, this line, while strong, has a relatively high attenuation which becomes especially objectionable at the higher frequencies. Breaking strength of the sample was about 170 pounds.

C. Bimetal-Braided Line

The design of the next cable sample is based on the premise that the center conductor is a bad place for the strength members, at least in a cable with such strength, diameter, and bandwidth requirements as are stipulated here. If the steel is moved to the outer conductor, the same cross-sectional area will displace proportionally less copper, and the steel is likely to do less damage to the propagation characteristics. In this sample, the center conductor is again composed of seven copper strands; the novelty of the configuration lies in its outer conductor which represents at the least, an unusual capability in cable manufacturing. This outer conductor is a woven braid (having one strand per carrier) in which each strand is a bimetal conductor similar to the steel-cored, copper-coated

conductors known generally by the trade names "Copperweld" and "Copperply." The braid is laid on at a very shallow angle (almost parallel to the axis of the cable); the exact figure was not furnished by the manufacturer, but appears from inspection to be about 2½ degrees. A cross-sectional diagram of the sample is shown in Figure 5-3.

Nothing that has been presented so far will enable us to handle an outer conductor of such complexity, for the fields are almost impossible to describe exactly, and not at all worth the effort for any practical purpose. The logical answer is to try to arrive at some sort of "equivalent circuit" which is more easily calculated and will give satisfactory results, at least over a limited frequency range. A considerable amount of work has been done by various investigators in characterizing braided conductors. Among the unclassified papers on the subject, reference [38] is a good example. Most of these, however, are limited to frequencies well above the range considered here, where most present-day applications for cables exist, where losses are greater, and where it is especially necessary (and at the same time more difficult) to be able to predict and compute the electrical behavior of the conductor. Fortunately, the problem ought not to be so severe in this case, because the frequency is lower. But at this point it will be necessary to digress

long enough to provide some sort of rationale for the assumptions which are made later in calculating the propagation characteristics of this cable. The digression forms the major portion of this section.

If the outer conductor of a coaxial cable is braided, and if each of the strands making up the braid is a bimetallic wire consisting of an iron core over which a layer of copper is plated or welded, then the cable geometry becomes extremely complex. Not only are all the strands of the braid no longer parallel to one another, but they rise and dive over and under one another in their passage along and around the cable. As indicated previously, it would be almost impossible to obtain an exact expression for the fields as a function of current distribution in the braid. The cable sizes and frequencies dealt with here are such that internal inductance of the outer conductor cannot always be ignored with respect to external inductance, but it would be better to do so, or to make an outright unsupported guess, than to attempt an exact solution under the circumstances.

There is one feature of the braid, however, that points the way to a possible method of attack: its periodicity. By this is meant that the lay of the strands of the braid is periodic in space, or alternately, that if we choose properly

we can cut a small volume from the braid, within which the placement of the strands is the same as in any other identical small volume. A convenient approximate representation is shown in Figure 5-4. Then it may be possible to arrive at some set of average values which will characterize the braid sufficiently well for making comparative estimates of various cables. The basic method used here is adapted from Sakurai [7], who used a similar procedure in connection with his investigations of artificial dielectrics.

The key idea is the concept of "macroscopic" or average dielectric constant, permeability, conductivity, etc. Assume the structure of the material under investigation to be periodic along all axes of the coordinate system, and that the periods are all small with respect to the wavelength of any electromagnetic waves present. Finally, assume that permeability, conductivity, dielectric constant, etc., are constant.

Since the primary interest is in the average permeability, the following procedure will be carried out in terms of the magnetic field intensity, although the results are equally valid, and the procedure is exactly the same, for the average dielectric constant and the electric field.

Assume a small long cylinder of circular cross-section, perpendicular to the plane of the paper and situated somewhere in an area Δ A. The area will be taken as a rectangle

of width a and height b with axes parallel to the coordinate axes. (Such a restriction avoids unnecessary complication and is convenient, but there is no loss of generality since the analysis holds for any coordinate system, including non-orthogonal ones). If the analysis is undertaken for unit length of a very long cylinder, the three-dimensional problem of [7] reduces to a two-dimensional one. Periodic volume ΔV becomes periodic area ΔA, etc. Let the cylinder have permeability μ_1, and the remainder of the area ΔA have permeability μ_o. ΔA is the "period" of the macroscopic configuration of which the small cylinder is a part. Let there be a uniform static field H_o which lies in the plane of the paper parallel to the X-axis. All dimensions are small compared to a wavelength of the field. For the present, the cylinder will be assumed not to carry current, so that the field intensity is derivable from a scalar potential function ψ. The boundary conditions which must be satisfied at the surface of the cylinder by the static potential ψ_o outside the cylinder and the static potential ψ_1 inside are

$$\psi_o = \psi_1 \tag{5-1}$$

and

$$\mu_o \frac{\partial \psi_o}{\partial r} = \mu_1 \frac{\partial \psi_1}{\partial r} \tag{5-2}$$

These conditions are simply reiterations of the well-known facts that the tangential component of the magnetic intensity, and the normal component of the magnetic flux density, must be continuous across any boundary. Radius vector r is centered on the axis of the cylinder. Almost any book on electromagnetic theory (e.g., [29, Sec. A.03] gives the solution for the corresponding problem of a dielectric cylinder in an electrostatic field. Because of the analogy between magnetic and electric quantities, the results may be carried directly over in the present case by substituting B for D, H for E, and μ_r for ϵ_r [23, p. 288f]. Thus we show that, in this case, ψ_0 and ψ_1 may be written as

$$\left.\begin{aligned} \psi_0 &= -H_0 \left[1 - \frac{r_1^2}{r^2}\left(\frac{\mu_1 - \mu_0}{\mu_1 + \mu_0}\right)\right](r \cos\theta) \quad \text{(a)} \\ \psi_1 &= \frac{-2\mu_0}{\mu_1 + \mu_0} H_0 r \cos\theta \quad \text{(b)} \end{aligned}\right\} \quad (5\text{-}3)$$

where

r_1 = radius of the cylinder, meters

r = radial distance from the cylindrical axis, meters

θ = angle between $\vec{H}_0$ and radius vector $\vec{r}$

and the other quantities have been previously defined. Now if the gross structure is periodic, then the macroscopic value of whatever parameter is sought is the same over any period ΔA, and must not be a function of the location of ΔA.

ΔA is now taken for convenience with its center on the axis of the cylinder, and we proceed to find the average value of μ over ΔA.

To do this we find first an average value of $\vec{B}$. A difficulty immediately presents itself: because of the distortion of the field due to the presence of magnetic material; $\vec{B}$ does not have the same direction throughout ΔA. However, along the line through the center of the cylinder perpendicular to the external field (along the y-axis in this case) $\vec{B}$ has the same direction both inside and outside the cylinder, and is maximum. Then the assumption is made that a value for the flux threading the periodic volume (ΔA times unit length) can be obtained by finding the flux threading the rectangle b times unit length, where b is the height of ΔA and of the periodic volume. Let us reason as follows:

$$\left.\begin{aligned} \text{Flux, } \phi &= \int_A \vec{B}\ dA \\ &= (\overline{\vec{B}})(b)(1) \\ &= 2\int_0^{r_1} \mu_1 \vec{H}_1\ dy + 2\int_{r_1}^{b/2} \mu_o \vec{H}_o\ dy \end{aligned}\right\} \quad (5\text{-}4)$$

So that

$$\overline{B} = \frac{\phi}{b \cdot 1}$$

and

$$\overline{\mu} = \frac{\overline{B}}{H_o} \quad (5\text{-}5)$$

where the overbar denotes an average value. The integration in (5-4) should, of course, be taken from $-b/2$ to $b/2$. In order to shorten the algebra, advantage is taken of the symmetry of ϕ about the x-axis by integrating over half the distance and doubling the result, as shown.

The field intensity $\vec{H}$ is obtainable from the potentials as

$$\vec{H} = -\nabla \psi \tag{5-6}$$

and in polar coordinates,

$$\nabla \psi = \frac{\partial \psi}{\partial r}\, \vec{u}_r + \frac{1}{r}\, \frac{\partial \psi}{\partial \varphi}\, \vec{u}_\varphi \tag{5-7}$$

where $\vec{u}_r$ and $\vec{u}_\varphi$ are the unit vectors in the r- and φ-directions respectively. Since $\vec{H}_0$ has been taken for convenience parallel to the x-axis, the angle θ between the radius vector $\vec{r}$ and $\vec{H}_0$ is identical to the angle φ of the polar coordinate system. Since the integration of (5-4) is to be taken along the y-axis, $\vec{H}$ must be evaluated at $\theta = \varphi = \pi/2$. In general, the intensity inside the ferromagnetic cylinder is, from (5-3b) and (5-7)

$$\begin{aligned} \vec{H}_1 &= -\nabla \varphi_1 \\ &= \frac{2\mu_0}{\mu_1 + \mu_0}\, H_0\, (\vec{u}_r \cos\varphi - \vec{u}_\varphi \sin\varphi) \end{aligned} \tag{5-8}$$

and along the y-axis

$$\vec{H}_1 = -\nabla \varphi_1 \Big|_{\varphi = \pi/2} = -\frac{2\mu_0}{\mu_1 + \mu_0}\, H_0\, \vec{u}_\varphi \tag{5-9}$$

The general expression for the intensity over the rest of $\triangle A$ is, from (5-3a) and (5-7)

$$\vec{H}_o = -\nabla \psi_o$$

$$= H_o \left[(\cos \varphi) \left(1 + \frac{r_1^2}{r^2} \frac{\mu_1 - \mu_o}{\mu_1 + \mu_o} \right) \vec{u}_r + \left(-r \sin \theta + \frac{r_1^2}{r} \frac{\mu_1 - \mu_o}{\mu_1 + \mu_o} \sin \theta \right) \frac{\vec{u}_\varphi}{r} \right] \quad (5\text{-}10)$$

Evaluating (5-10) along the y-axis gives

$$\vec{H}_o = -\nabla \psi_o \Big|_{\varphi = \pi/2} = -H_o \left(1 - M \frac{r_1^2}{r^2} \right) \vec{u}_\varphi \quad (5\text{-}11)$$

where, for convenience, we define $M = \frac{\mu_1 - \mu_o}{\mu_1 + \mu_o}$

Both $\vec{H}_1$ and $\vec{H}_o$ are seen to lie here entirely in the negative $\vec{u}_\varphi$ - direction, which, for $\varphi = \pi/2$, is just the positive $\vec{u}_1$ - direction of rectangular coordinates. Thus the vector notation may now be dropped and the remainder of the analysis carried out in terms of magnitude only.

Substituting (5-9) and (5-11) in (5-4),

$$\bar{B}b = 2\mu_1 \int_0^{r_1} \frac{2\mu_o H_o}{\mu_o + \mu_1} dy + 2\mu_o \int_{r_1}^{b/2} H_o \left(1 - M \frac{r_1^2}{y^2} \right) dy \quad (5\text{-}12)$$

Straightforward integration and algebraic manipulation then yield

$$\bar{B} = \mu_o H_o \left(1 + 4M \frac{r_1^2}{b^2} \right) \quad (5\text{-}13)$$

and hence, from (5-5),

$$\bar{\mu} = \mu_0 \left(1 + 4 \frac{r_1^2}{b^2} \frac{\mu_1 - \mu_0}{\mu_1 + \mu_0} \right) \qquad (5\text{-}14)$$

If the dimensions of ΔA are large with respect to the radius of the cylinder, the value of r_1^2/b^2 on the circumference of ΔA will be small compared with unity. The contribution of the ferromagnetic material will be small and $\bar{\mu}$ will approach μ_0. Unfortunately, the value of r_1^2/b^2 will not be small in the present instance.

The exact value of $\bar{\mu}$ depends very much on the size and shape of ΔA, which is itself open to debate. To get some feel for the size of $\bar{\mu}$, let us assume a convenient but reasonable ΔA. Reference to Figure 5-4 shows that, if a woven braid is to be described by this periodic approximation, the rectangle ΔA must be at least $4r_1$ meters square. This is a convenient shape in that it simplifies the mathematics, yet at the same time its size provides a realistic and not overly favorable case. If ΔA should turn out in practice to be larger so much the better, for the effects of proximity to the strand will thereby be lessened.. With the above choice of size and shape for ΔA, b (and also a) will be $4r_1$ meters and there results

$$\bar{\mu} = \mu_0 \left(1 + \frac{M}{4} \right), \quad b = 4r_1 \qquad (5\text{-}15)$$

Thus we have a general idea of the magnitude of $\bar{\mu}$: if the strands are nonmagnetic, or small with respect to the spacing between them, $\bar{\mu}/\mu_o$ could be as small as unity; if the permeability of the strands is at all appreciable and/or they are tightly woven, $\bar{\mu}$ is increased somewhat; for the case above and a strand permeability $\mu_1 = 100\,\mu_o$, $\bar{\mu} = 1.245\,\mu_o$.

The factor r_1^2/b^2 may be written in terms of the cross-sectional areas ΔA and A. Doing so may appear to introduce an unnecessary complication, but the reason for it will become evident shortly. The area of ΔA is ab, and that of A_1 πr_1^2. Then

$$\frac{A_1}{\Delta A} = \frac{\pi r_1^2}{ab} = \frac{\pi b}{a}\ \frac{r_1^2}{b^2} \qquad (5\text{-}16)$$

so that

$$\frac{r_1^2}{b^2} = K\ \frac{A_1}{\Delta A} \qquad (5\text{-}17)$$

where

ΔA = cross-sectional area of the periodic volume

A_1 = cross-sectional area of the ferromagnetic cylinder

$K = \frac{a}{\pi b}$, a constant depending on the proportions of ΔA

Then (5-14) may finally be written in the alternate form

$$\bar{\mu}_1 = \mu_o \left(1 + K_A\ \frac{A_1}{\Delta A}\ \frac{\mu_1 - \mu_o}{\mu_1 + \mu_o}\right) \qquad (5\text{-}18)$$

where $K_A = \frac{4}{\pi} \frac{a}{b}$ and the subscript on $\bar{\mu}$ denotes that H_o is perpendicular to the axis of the cylinder.

At first it may seem surprising that the steel should have so little effect on average permeability, even when it constitutes a fairly large percentage of the shield volume, but this is a consequence of the fact that the field is required to satisfy boundary conditions involving a unity-permeability medium. In other words, it is a consequence of the demagnetizing effect.

In the foregoing, it was assumed for convenience that no current was flowing in the metal within ΔA, so that curl $H = 0$ inside as well as outside the metal, and the conditions of continuity were as given. But these conditions must hold even when one (or both) of the media forming the interface carry current. (The application of the boundary conditions when curl $H \neq 0$ is discussed in [15, Chap. 12].) But our purpose so far has not been to describe the total field around a strand when the braid carries current; it was to arrive at a basis for assigning an average value for the permeability of the braided conductor by examining a field in a section of this composite material. The existence of the field was given and, if one likes, can be thought of as being set up by some other strand.

It seems best to pause here to review the analysis so far, and to recapitulate the assumptions. The braided conductor which is to be described is assumed to be made up of

a large number of identical building blocks, of the form of or similar to Figure 5-5, which are placed end-to-end and side-by-side, and are possibly also stacked "vertically", i.e., in the radial direction, in the most general case. Each block consists of bimetal conductors surrounded by a dielectric. At the moment, we are searching for an average permeability which can be assigned to a hypothetical homogeneous conductor which fills the block. To this end we have arrived at an average permeability for a block containing a straight, circular, cylindrical, ferromagnetic conductor; the block is situated in a uniform field so that the cylindrical axis is perpendicular to the field. (Implicitly in such an arrangement, the composite conductor is "developed", i.e, unwrapped and straightened out flat, but this causes no great concern since we reiterate that the interest at the moment is in the macroscopic properties of the material, and not in the field of a given current distribution.)

It was seen that the average permeability of the braid depends in part on the fraction of the volume of the block occupied by ferromagnetic material. In addition, if the braid structure is periodic then integrating over the volume (Δ A times unit length) gives the same result no matter where the volume is taken. Or, what is the same thing, the result is the same no matter where within Δ A

the cross-section of the cylinder lies (as long as the cylindrical axis remains perpendicular to the field). These assertions form the basis of the next two approximations: (1) as far as its effect on the value of $\bar{\mu}$ is concerned, we may ignore the fact that the cylinder is not straight, especially since its curvature will be periodic in the long run, and (2) the presence of two cylinders (strands) in ΔA is conveniently handled by simply doubling the area of the single cylinder in the formula for $\bar{\mu}$. Again, both assertions carry the qualification that the cylindrical axis is perpendicular to the field.

This qualification represents the remaining discrepancy between the building block which we wish to analyze and the building block for which we have an analysis. In Figure 5-5, the strands cross, and neither has its axis perpendicular to the plane in which the field vector is taken to lie. To take account of this, it will be helpful to return to the idealized straight cylinder at the center of ΔA. This time, however, let the field be parallel to the cylindrical axis. Then the H-field is not distorted by the cylinder, and by the condition that $\psi_0 = \psi_1$ on the boundary it is the same inside and outside the cylinder. Then $H = H_0 = H_1$. Now, if $\mu = \mu_0$ throughout ΔA, we could write $\bar{B} = \mu_0 H$, but in fact $B = \mu_1 H$ within the cylinder; therefore

$$\bar{B} = \mu_0 H_0 + \frac{\mu_1 - \mu_0}{\Delta A} \int_{A_1} H_1 \, dA \qquad (5\text{-}19)$$

Since H_1 is constant over the area of the cylinder,

$$B = \mu_0 H_0 + (\mu_1 - \mu_0) H_0 \frac{A_1}{\Delta A} \qquad (5\text{-}20)$$

which leads to

$$\bar{\mu}_{\parallel} = \mu_0 \left(1 + \frac{A_1}{\Delta A} \frac{\mu_1 - \mu_0}{\mu_0}\right) \qquad (5\text{-}21)$$

Thus it is seen that the average permeability of a building block containing a ferromagnetic cylinder depends very much on the direction from which the block is viewed. The same effect is obtained if the cylinder is canted at an angle θ to the z-axis of the periodic volume. Then the field H_0 makes the same angle θ with the normal to the cylindrical axis, and H_0 can be resolved into components tangent and normal to the cylinder which are given by $H_0 \sin \theta$ and $H_0 \cos \theta$ respectively. It is seen that the average permeability $\bar{\mu}$ of the block of Figure 5-4 will have some intermediate value between $\bar{\mu}_{\perp}$ and $\bar{\mu}_{\parallel}$, depending upon the volume of the steel and the angle at which it is laid. The basis for the final assumption lies in the principle of superposition and the expression for the energy in a magnetic field, which was given earlier,

$$U = \tfrac{1}{2} \int_V \mathrm{Re}\, \vec{B} \cdot \vec{H}^* \, dv \qquad (2\text{-}16)$$

Remember that $\bar{\mu}_\perp$ and $\bar{\mu}_{||}$ are average values over the entire periodic volume, derived for two specific directions; we calculate the total energy as

$$U = \tfrac{1}{2}\bar{\mu}H_o^2 = \tfrac{1}{2}\mu_{||}(H_o \sin\theta)^2 + \tfrac{1}{2}\mu_\perp(H_o\cos\theta)^2 \qquad (5\text{-}22)$$

from which follows

$$\bar{\mu} = \mu_\perp \cos^2\theta + \mu_{||}\sin^2\theta \qquad (5\text{-}23)$$

or, in its complete form,

$$\bar{\mu} = \bar{\mu}_o\left[\left(1 + K_A\frac{A_1}{\Delta A}\frac{\mu_1 - \mu_o}{\mu_1 + \mu_o}\right)\cos^2\theta + \left(1 + \frac{A_1}{\Delta A}\frac{\mu_1 - \mu_o}{\mu_1 + \mu_o}\right)\sin^2\theta\right] \qquad (5\text{-}24)$$

where

μ_1 = permeability of ferromagnetic material in the braid

μ_o = permeability of the rest of the material (including air gaps or space) of the braid

$\frac{A_1}{\Delta A}$ = fraction of the (periodic) volume of the braid occupied by ferromagnetic material

θ = angle between axis of the braid strands and axis of the cable

K_A = a constant, $(4/\pi)(a/b)$, where a and b are respectively the width and the height of the unit volume

There still remains the question of an average value for the conductivity of the composite conductor. This is easily handled by the following procedure, which is readily seen to be an extension of the method used to adjust the conductivity of the all-copper line in the previous chapter.

Here, however, we will continue to work with the periodic cross-section ΔA, rather than the entire braid cross-sectional area, which consists of some integer number of identical ΔA's. The conductance of the periodic volume is given by

$$g = \frac{\bar{\sigma} \Delta A}{\ell} \tag{5-26}$$

where

g = conductance (per unit length)

$\bar{\sigma}$ = average conductivity

ℓ = (unit) length

If all calculations are made on a per-unit-length basis, $\ell = 1$ and need not be carried along. The area ΔA contains some number of conductors of steel, having together a total area of A_{fe}, and the same number of copper conductors, having together a total area of A_{cu}. Conductivity of the steel is σ_{fe}, and of the copper σ_{cu}. All these conductors are in parallel, so that their conductivities add directly.

Then

$$\begin{aligned} g &= \bar{\sigma} \Delta A \\ &= \sigma_{fe} A_{fe} + \sigma_{cu} A_{cu} \end{aligned} \tag{5-27}$$

which leads immediately to

$$\bar{\sigma} = \sigma_{fe} \frac{A_{fe}}{\Delta A} + \sigma_{cu} \frac{A_{cu}}{\Delta A} \tag{5-28}$$

where

$\bar{\sigma}$ = average conductivity of the bimetal braid, mhos/meter

σ_{fe} = conductivity of the steel, mhos/meter

σ_{cu} = conductivity of the copper, mhos/meter

$\frac{A_{fe}}{\Delta A}$ = fraction of the (periodic) volume of the braid occupied by steel

$\frac{A_{cu}}{\Delta A}$ = corresponding quantity for copper

Armed with the above two constants, $\bar{\mu}$ and $\bar{\sigma}$, we now assume that the braid is replaced by a homogeneous tubular conductor to which these constants apply, and compute the transmission characteristics as we have done in previous chapters.

The reader may be left with some apprehension as to the validity and rigor of the approach just presented for computing the braid characteristics. Probably the best defense that can be given lies in the following two points: (1) As mentioned previously, almost any reasonable guess is preferable to the task of computing the fields exactly (if it can be done at all); to use a metaphor common among engineers, we have at least narrowed the search for first base to the ball park; and (2) the most important fact to be gained from the foregoing analysis is that the effective permeability of the braided structure will be considerably less than the permeability of the steel

itself, and will not vary widely from that of nonmagnetic material; something less than an order of magnitude should generally be the rule for strands laid on at small angles (20 degrees or less).

There is one other factor which serves to make the struggle for great accuracy unnecessary, at least in the present circumstances, and that is the variability of μ (and σ) for a given steel wire from batch to batch and from manufacturer to manufacturer. But it is seen that in the present configuration the effect of the permeability of the steel is reduced to a relatively minor importance.

The dimensions and other vital statistics of the bimetal-braided cable are presented in Table 5-2. Calculated results for both the sample and the corresponding all-copper case appear in Figures 5-5 and 5-6. Breaking strength of this sample was about 70 pounds.

D. Copper Coaxial Line with Steel Overbraid

The last steel-bearing cable to be considered is a combination of types previously encountered. Its base is a coaxial line like that of Chapter 3, with a stranded copper center conductor and a ring of bare copper wires in contact as the innermost layer of the outer conductor. Over the copper is woven a braid of high-tensile steel strands to provide strength. The cable has no jacket, so

that in operation the sea will penetrate into it as far as the outer surface of the dielectric. Since seawater is so much less conductive than either steel or copper, it is ignored amid the metallic strands for simplicity. After conductivities and permeability are adjusted in accordance with techniques previously described, there results a cable with an outer conductor of three laminations: copper, steel, and sea. Other than the labor of computation, the configuration presents no particular difficulties.

The advantage of an arrangement of conductors such as that occurring in the present sample is that the high-conductivity material (copper) is located in just the regions into which skin effects tend to crowd the current as frequency rises; the steel is placed on the outside, where it has less effect and soon tends to fall out of the picture altogether. The price paid for this, of course, is that if the overall cable diameter must be held to an upper bound, then only two choices are possible, both of which tend to raise the attenuation of the line. Either the spacing between the conductors is made smaller, which increases capacitance and reduces inductance (both bad), or the diameter of the center conductor is reduced from the value it would have in an all-copper line in order to maintain the optimum 3.6:1 ratio of conductor radii. This increases resistance (again bad). Naturally these comments

do not apply if the overall diameter can be increased when adding the strength member; in that case the only price paid for this configuration is the additional cost of the cable.

A diagram of the cable construction is shown in Figure 5-7. Dimensions are given in Table 5-3. Graphs of characteristic impedance and attenuation appear in Figures 5-8 and 5-9 respectively. Instead of the corresponding all-copper case, computations have been carried through for a line consisting of the core, dielectric, and innermost layer of the outer conductor only, i.e., the configuration of Chapter 3.

VI. DATA TRANSMISSION

Now that the electrical properties of the bimetal path are known, the next most important question becomes, "How good (or bad) is the channel for the transmission of data? What can we reasonably expect to accomplish, and what, if anything, can be done to improve matters?" This, of course, is a big question, and any answers given here are certainly not going to exhaust the subject. Much depends upon the character and strength of the signal, the character and strength of the noise, and the terminal equipment at the ends of the line. Let us first, then, enumerate some boundary conditions which we will assume to limit and simplify the discussion:

1. The effects of cable self-generated noise and amplifier noise figure will not be considered. This simplification implies that the signal-to-noise ratio at the output of the amplifier terminating the line is sufficiently high at all important frequencies, and hence the large attenuations encountered in these small-diameter cables can be overcome without penalty by sufficient amplification.

2. The information to be transmitted is digital. It is a binary (two-level) non-return-to-zero (NRZ) data stream. The desired transmission rate is constant and for discussion purposes will be taken as 400 kilobits per second.

3. Transmission over the cable is in one direction only.

4. Appropriate sampling and pulse-reshaping circuitry is available at the receiver, if needed. Hence, it is not necessary that the data stream at the output end of the cable be as clean, square, and noisefree as it was at the input end, as long as the signal-to-noise ratio exceeds certain definite minimum values determined by such considerations as channel capacity and error rate (see below).

The temptation to regard the transmission path as simply an RC line, of which an analysis has been made [13, p. 307ff] must be resisted if the bit rate is to be as high as 400 kbps, for it has been seen in previous chapters that inductance becomes appreciable at the higher frequencies, giving an inductance loading effect to improve transmission signal resolution, but at the cost of still greater signal attenuation. The dividing line is the point at which the inequality $\omega \ll \frac{2R}{L}$ is no longer a valid assumption.

The signal-to-noise ratio required to transmit binary information at a given rate and for a prescribed error probability can be computed assuming Gaussian noise. A ratio of about 18 to 20 db is required for error probabilities in the range 10^{-4} to 10^{-6} [26, p. 384] . But the question immediately arises as to the bandwidth of the channel. Harman [16, p. 154] shows that, for binary data, the channel

capacity remains constant at the Nyquist rate for any signal-to-noise ratio greater than 10 db. In the case of a coaxial cable, one may define a 3 db bandwidth, or a 20 db bandwidth, or any other convenient figure, but the point is that some definition is necessary, for previous chapters have shown that attenuation is minimum at d.c. and increases with frequency at an almost constant rate from there. For this reason, the bandwidth concept does not appear very profitable; a better approach would seem to be on the basis of pulse resolution. The two concepts are related, of course, but the latter will have broader application here, primarily because of the conditions stipulated earlier in this chapter. Specifically, because of condition 4, our requirements will be satisfied if a series of level changes, occurring at the minimum transition spacing, can be detected and then regenerated to produce a replica of the original data stream. This criterion would be met, for instance, if a repetitive 101010...data stream at the input were represented at the output by a sinusoid. To avoid later confusion, it should be noted in passing at this point that a steady stream of alternate ones and zeros at a 400 kilobit rate looks like a 200 KC square wave. If such a signal is represented at the output of a transmission path by a sinusoid, it only means that the higher-frequency components of the input

have been attenuated by the path, and we would expect the sinusoid to have a frequency of 200 KC.

A moment's reflection will lead one to the conclusion that a square wave is not a very good pattern to test the data transmission capabilities of a channel with, because it allows the channel to settle down to a steady-state condition, and this is a state it will never see in practice with data consisting of random ones and zeros. Besides, a sinusoid will probably be easier to detect than other more complicated patterns. A more valid test would be the system's ability to pass a pulse. But because the pulse can spread in time, an even more meaningful test would be the system's ability to transmit, and resolve at the output, two pulses separated by the minimum spacing which will be encountered. For NRZ data, this condition would be produced by a pattern of the form 101 in the midst of an infinite (or at least long) string of zeros, or its complement. If the system can handle this pattern, it should be able to handle anything, for the whole question of required bandwidth can be stated in terms of the ability to resolve two minimally-spaced pulses [20, p. 78]. If the minimum spacing (and minimum pulse width) is τ seconds, the (flat) bandwidth must be equal to or greater than $1/(2\tau)$ cps for resolution, i.e., $\geq$ 200 KC in the present instance. With the minimum possible bandwidth, Freeman [12, p. 25] shows that about 90% of the pulse energy will be transmitted if there is no

attenuation in the passband.

Now since a digital data stream has such a large bandwidth, and the cable that will carry it exhibits such wide parameter variations with frequency, it would be desirable to get some idea of what the cable will do to the signal and how bad the result will be. An actual plot of the waveform is especially useful, since the eye is a better resolver of degraded signals than electronic circuitry is. The means of obtaining such a plot is available in the technique of Fourier analysis.

Consider then a pattern having the form 101 followed by seventeen (17) zeros (which will be written as 1010_{17}). While 17 zeros is something short of an infinite string, it is mathematically more tractable, and is felt to be sufficiently long to provide a valid test. The line is driven with a signal V_g which is a continuous repetition of this 20-bit pattern. Then, a Fourier analysis of the driving waveform yields a function of the form

$$\left.\begin{aligned} V_g &= a_o + \sum_{n=1}^{\infty} a_n \cos n\omega_o t \\ &= a_o + \sum_{n=1}^{\infty} \mathrm{Re}\, \overset{\times}{V}_{g_n} e^{jn\omega_o t} \end{aligned}\right\} \quad (6\text{-}1)$$

where a_o is the average d.c. value of the waveform, in which we are not interested at the moment, and $a_n = \overset{\times}{V}_{g_n}$ is the Fourier coefficient of the n^{th} harmonic (which is

of angular frequency $n\omega_o$). The d.c. component will be important when it comes to the design of a cable driver and signal receiving and regenerating circuits (which are beyond the scope of the present discussion), but it is not a factor when considering pulse resolution and will be dropped in all equations from this point on. No sine terms appear in (7-1), because the stipulated pulse pattern can be made an even function by suitable choice of origin, and can therefore be represented by a sum of even functions only.

The propagation characteristics of the signal path (the cable) are known. Specifically, any signal at the input will suffer attenuation $\alpha\ell$ and phase shift $\beta\ell$ in the course of its travel along the cable, where ℓ is the length of the cable. The only difficulty is that α and β are functions of frequency. This means first that the component cosinusoids of equation (6-1) will not be attenuated proportionally, and second, that they will not add in their proper phases at the load. The result is easily determined; if the cable is terminated in its characteristic impedance at all frequencies, there are no reflections and the load voltage is (equation (A-12), Appendix A)

$$\overset{\times}{V}_{load} = \overset{\times}{V}_g \, e^{-\gamma\ell} \qquad (6\text{-}2)$$

where

ℓ = length of the line in meters

$\gamma = \alpha + j\beta$ = propagation constant, (nepers + j radians)/unit length

Now, $\overset{x}{V}_{gn} = a_n$; therefore $\overset{x}{V}_{load_n} = a_n e^{-\gamma \ell}$ and $V_{load_n} = \mathcal{R}_e\, a_n e^{-\gamma \ell} e^{jn\omega_o t}$. In view of the form of the applied signal from (6-1), the load voltage (less d.c. term) may be written by superposition of individual harmonic components as

$$V_{load} = \sum_{n=1}^{\infty} a_n e^{-\alpha_n \ell} \cos(n\omega t - \beta_n \ell) \qquad (6\text{-}3)$$

Other than the great deal of labor involved in the actual calculations, (6-3) presents no problems. For the signal stipulated, a 20-bit repetitive pattern at a bit rate of 400 kbps, the fundamental cosinusoid is at 20 KC, and $\gamma_n = \alpha_n + j\beta_n$ is merely γ of the line evaluated at harmonics of 20 KC.

Equation (6-3) was programmed for the IBM 7090 computer. Provisions were made to automatically terminate the summation at the value of n for which $a_n e^{-\gamma_n s}$ becomes less than one percent of $a_1 e^{-\gamma_1 s}$, where s is the distance, along the line from the source, at which the voltage is being computed. Computations were made at 1-kilometer intervals along the line (total length: 4 kilometers) for two pulse patterns, 1010_{17} and 10_{19}. The results are shown as Figures 6-2 through 6-9. The deterioration in the waveforms as they travel along the line is readily apparent, and it is seen that the signals at the load are totally unacceptable.

Obviously, something must be done.

In terms of bandwidth rather than pulse resolution, the conclusions of Espenscheid and Strieby [3] concerning the data transmission problem are summed up (paraphrastically) in two statements:

1. For a given cable size, "bandwidth" increases nearly as the square of the reduction in length.

2. For a given length, "bandwidth" increases approximately as the square of the conductor diameter. As mentioned in the introduction, cable outside diameter is severely limited in the present application; thus increasing the cable size is not likely to represent a practical solution. Nevertheless, it is seen that holding the diameter to the maximum allowable limit will be worthwhile.

Short of giving up all hope of transmitting over such distances or at such high bit rates, the most obvious solution is the installation of repeaters. Such a course of action may or may not be feasible, depending upon many factors which are not of immediate concern in the present discussion. If repeaters are to be used, equation (6-3) provides a convenient starting point for determining their spacing, for the computer program as written has provision for graphing the function on a Calcomp plotter, as well as printing the results in tabular form. Thus the signal deterioration may be seen at a glance, at any distance from the source.

If repeaters are not to be used, the next best answer is equalization. A network (or networks) can be placed at the load end of the line, which will delay the lower frequencies more than the higher ones, thus allowing the latter to catch up and add in their proper phase at the load. It may be shown, although the demonstration is beyond the scope of this discussion (as is the whole subject of equalizer design), that an equalizer which adjusts the phase relationships properly will also automatically adjust the amplitude relationships. This is not necessarily true in general, but it is true for a transmission line, which is a minimum-phase system.

If an equalization network is placed between the line and the load, and if there are no mismatch problems, equation (6-2) becomes

$$\overset{\times}{V}_{load} = K \overset{\times}{V}_g \, e^{-\gamma \ell} \, e^{-\zeta} \qquad (6\text{-}4)$$

where

ζ = complex transfer constant of the equalization network, analogous to γ of the line

K = some multiplying factor

Now it is not difficult to postulate an equalizer whose transfer characteristic is the inverse of that of the line, so that $\zeta = -\gamma\ell$. It is quite another matter to build one. Techniques do exist, however, for the design of approximations which give reasonably good results over a frequency range as

wide as one cares to take the trouble to make it. Reference [6] gives an outline of the procedure. The equalizer consists of cascaded bridged-Tee networks, the number depending on the frequency range and the degree of accuracy required.

Another computer program was written to take into account the effects of (physically realizable) equalization. The network configuration employed consists of two cascaded sections, each having two R-C combinations in the bridging arm. A diagram is shown in Figure 6-10. Plots of the resulting output waveforms for the 4-km distance and patterns are shown in Figures 6-11 and 6-12. It is granted that additional amplification will be necessary because the equalizers are passive networks; nevertheless, these are results we can reasonably expect to accomplish in practice.

All the above predictions are based on the correctness of equation (6-2). The absence of a positive exponential term in this expression implies that the line is matched to its load at all frequencies. We have seen in earlier sections that the characteristic impedance of a line varies widely with frequency, approaching its high-frequency value asymptotically. Therefore, any matching network between the line and the load-equalizer combination must vary in the same manner. The design of suitable terminations, which are simpler to build than equalizing networks, is also

covered in reference [6], and their presence is taken for granted here.

As a final note to this section, it may be of some interest to the reader to have the Fourier coefficients of the two test patterns used in the computer studies described above. They are, for the pattern 10_{19}:

$$a_n = \frac{2A}{n\pi} \sin \frac{n\pi}{20} \tag{6-5}$$

and for the pattern 1010_{17}:

$$a_n = \frac{4A}{n\pi} \cos \frac{n\pi}{10} \sin \frac{n\pi}{20} \tag{6-6}$$

where A is the peak-to-peak excursion of the NRZ data stream, and was taken to be unity in this study. Time-origins were chosen in the center of the pulse for the 10_{19} pattern, and midway between the pulses for the 1010_{17} pattern. Then the patterns are even functions and their Fourier coefficients are easily obtainable from half-range expansions [32, Sec. 5.4].

VII. EXPERIMENTAL RESULTS

Not all the lines whose characteristics have been computed in the foregoing sections have been fabricated and tested for this investigation. As explained in the introduction, one of the purposes of the work that has been done was to acquire a feel for the behavior of various line configurations in these small diameters, and an idea of the magnitude of the characteristic impedances and attenuations to be expected. This has been done by calculation, largely performed on the IBM-7090 computer. The analyses on which these calculations are based have been thoroughly checked by several investigators, and the conclusions corroborated beyond any need for further verification here. Samples have been obtained, however, of the first two steel-bearing configurations discussed in Chapter V, and a considerable quantity of the third was also manufactured.

Before the actual results are presented, a word is in order about the methods of measurement. Two quantities were sought: characteristic impedance and attenuation. The former was obtained in all cases by one of the simplest and most convenient methods: open and short-circuit measurements. Most references on the subject [20, p. 433; 27, p. 163] show that the characteristic impedance of a network (or a transmission line, which is just a distributed network) is given by

$$Z_o = \sqrt{Z_{oc}\, Z_{sc}} \qquad (7\text{-}1)$$

where

Z_o = characteristic impedance of network, ohms

Z_{oc} = impedance looking into network with output open-circuited

Z_{sc} = corresponding impedance with output short-circuited

The general measurement setup is shown diagrammatically in Figure 7-1. Measurements were made of the input impedance of the cable samples under open- and short-circuited conditions over the frequency range of interest. Three instruments were used to cover this range: (1) a Technology Instrument Corporation (now Acton Laboratories) Type 310A Z-Angle Meter; (2) a Type 311A RF Z-Angle Meter by the same manufacturer; and (3) a General Radio Type 916-AL Radio Frequency Bridge. Detector for the last-named instrument was a VTVM. The RF Z-Angle meter is no longer being built, nor is a similar instrument being offered by the manufacturer as a replacement. The instrument was used, however, since it was available.

From the open- and short-circuit measurements, characteristic impedance was calculated using equation (7-1). Series RC networks having an impedance equal to Z_o were then built and used to terminate the line. Regardless of their exact value, the networks were adjusted until they produced the same readings whether connected directly across the impedance-measuring terminals or with the line interposed.

Then with the bridge or meter removed, voltages were measured across the line at the input and at the output, and their ratio taken to calculate the attenuation. A diagram of the procedure is shown in Figure 7-2.

There was some overlap of frequency ranges in the three instruments used for measurements. In fact, the range could have been covered satisfactorily with only the two Z-Angle Meters, but it was thought desirable to check the results with a different type of instrument. In general, the impedance bridge gave results which appeared to be reasonably accurate, as judged by direct measurement of resistors, capacitors, and RC networks. Thus, the values of Z_{oc} and Z_{sc} of the lines as given by the bridge probably represent the true values. Somewhat more inaccuracy in readings was noted with the Z-Angle meters, however, because they are inherently less accurate instruments than the bridge. But regardless of the individual readings, it was noted in every case that the values calculated for Z_o from them showed good agreement no matter what the equipment used. Coupled with the well-behaved nature of the variation in Z_o and α with frequency, it is felt that the measurements are satisfactory as intended for the purposes here. It is for this reason that only the Z-Angle meters have been taken to the field, for they are small, portable, self-contained, and relatively easy to operate for repetitive

measurements. In contrast, the General Radio Bridge, while more accurate, is bulky, requires an external detector, and is very time-consuming to operate if more than just a few readings are to be taken. In addition, the bridge should rest on a copper ground plane for best results. All three instruments require an external source of excitation.

No measurements were taken in seawater for the second sample cable because it had an outer nylon jacket which effectively insulated it from the surrounding water. Attempts were made, however, to take measurements on the unjacketed steel-cored cable in the Chesapeake Bay. A steel watertight bottle was fixed on one end and the cable suspended vertically from the side of a boat. Wet measurements showed no difference from their dry counterparts. It is felt that this is largely due to the fact that only sample lengths of these cables were available (100 feet in the case of the cable measured in water); this is much too short a length to produce the fields in seawater associated with a very long line, upon which all the foregoing analysis was based, without terminal disks or other means to avoid end effects. It has been mentioned previously that some long lengths of cable were also eventually manufactured. In many tests, the number and length of samples was extremely limited, being primarily the fortuitous result of experiments with the manufacturing processes. It is for this reason that

we are forced to content ourselves here with the knowledge that the theory of the effects of surrounding seawater has been well established, and has ample experimental justification [1, 34, 36] .

The results of attenuation measurements of the steel-cored cable are presented graphically in Figure 7-3. The computed curve is redrawn from Figure 5-2 of Chapter V. Plotted points represent values computed according to the procedure described above, based on readings taken with the RF Z-Angle meter and the impedance bridge. No readings were taken at the lower frequencies with this cable, first because of the labor involved in the procedure and the time element involved, and second, because of the greater magnitude and importance of attenuation in the high-frequency range. Within the limits of experimental error (probably influenced unfavorably by the fact that the available cable samples were so short) and the variability of values for μ and σ as given by the manufacturer, the results appear to agree satisfactorily with the predicted figures over the range in which a comparison was made. Figure 7-4 is a graph of computed characteristic impedance of the steel-core cable, again with measured values plotted as points. Agreement is reasonably close.

Attenuation measurements of the second cable sample (the bimetal braid) are plotted in Figure 7-5, along with the calculated attenuation. The calculated curve for the corresponding all-copper case is also shown for comparison. Again, within the limits of experimental accuracy and material variation, it is felt that agreement is sufficiently close to justify the analysis. Since the computations have been performed, it has been noted that there is a second-order effect that was neglected, and that would tend to pull the upper curve closer to the measured points at the higher frequencies. In the actual braided bimetal conductor, skin effect will tend to crowd the current more and more into the copper as frequency increases, and the reduced conductivity of the steel core in each strand will exert less and less effect. Therefore, while it is still necessary to adjust the conductivity of the equivalent homogeneous conductor, the adjustment factor is now a function of frequency and must be computed anew at each frequency. The procedure is straightforward and employs the techniques outlined in Chapter IV, but is tedious and has not been programmed for the computer as yet. Figure 7-6 presents the calculated and measured results of characteristic impedance.

The attentuation characteristics of all the coaxial samples computed exhibit a characteristic spoon-shaped depression at the high end of the frequency range, as it is

presented here. Actually this is part of the transition region commonly found in such curves, and is to be expected. Reference [6] discusses this behavior at some length, and presents a characteristic attenuation curve over a frequency range wide enough to demonstrate the phenomenon. In a few words, it is shown that attenuation varies as the square root of frequency at low frequencies, and that as skin effects become appreciable, it again varies as the square root of frequency, but with a different constant of proportionality. The transition region corresponds to the frequency range in which neither the low-frequency nor the high-frequency approximation formulas, all of which are to be found in any text on transmission lines, are applicable, and its appearance both in the calculated and measured curves is comforting rather than disquieting. There is, it is true, a factor in the high-frequency attenuation expression which varies directly with frequency, but it does not become of importance until considerably higher frequencies, and is of no concern here, at least in the coaxial lines. In the sea-return line, this is not true, for the slope of the attenuation characteristic is already seen from Figure 2-3 to be close to unity by the time frequency has increased to one megacycle.

One further result, which is not really an experimental result, may be worth including at this point because it logically fits better in this chapter than anywhere else.

The reader may by this time have begun to wonder just how accurate are the approximations (4-12) compared to the exact expressions (4-9). Even if the justifications for them sound plausible, no approximations are ever really wholly satisfying. The time comes eventually when one must roll up the sleeves, resign oneself to the labor involved, and check a few points to satisfy one's curiosity. The effort will be largely wasted, unless one has access to at least a desk calculator and fairly detailed tables of the Thomson functions, for the complex algebra leads to small differences in large quantities and many transformations of the complex quantities between rectangular and polar form. A slide rule is useless.

In this age of the digital computer the situation is not as hopeless as it would have been a few years ago. Once equations (4-9) are programmed, the work is essentially finished. There are still difficulties involved, for the Thomson functions of the second kind do not converge rapidly, and tend to overflow the computer registers for all but the smallest values. McElroy [37] has written a routine which calculates all the Thomson functions to an accuracy of at least four places. Using this routine, a program was written to compute and compare the approximate and exact internal, external, and transfer impedances of a laminated outer conductor. It consists of a copper inner layer surrounded by the sea, and is the outer conductor of one of the cables

calculated in an earlier chapter. The results are presented in Table 7-1; it may be seen that the difference is slight, and that therefore use of the approximations is justified.

As a final note to the experimental results, it must be mentioned that all calculations have been made using room-temperature (25°C) conductivities, because this was the approximate ambient temperature at which the experimental work was carried out. (It is also the temperature for which conductivities of materials are most often tabulated.) However, as has already been pointed out, the average temperature over a long deeply submerged cable is more likely to be in the neighborhood of 4 degrees centigrade. The effect of reduced temperature on attenuation can be calculated as follows. At 25°C, the temperature coefficient of copper is 0.00385 per degree centigrade. Then the resistance of a copper conductor at any temperature can be found from the formula

$$R_t = R_{25} \left[1 + 0.00385 \, (t - 25) \right] \qquad (7\text{-}2)$$

where

R_t = resistance at temperature t

R_{25} = resistance at 25°C

t = temperature in °C

Calculation for a temperature of 4°C yields

$$\frac{R_{25}}{R_4} = 1.087 \qquad (7\text{-}3)$$

Thus, the d.c. resistance as computed is almost nine per cent too high.

The general expression for the attenuation of the cable is the real part of equation (1-2b). It is conveniently listed in [31, p. 552] as

$$\alpha = \sqrt{\tfrac{1}{2}\left[\sqrt{(R^2+\omega^2L^2)(G^2+\omega^2C^2)} + RG - \omega^2LC\right]} \qquad (7\text{-}4)$$

In all the work here, we have assumed $G = 0$; for low frequencies where $\omega L \ll R$, one can approximate one's way through equation (7-4) to the conclusion that

$$\frac{\alpha_{25}}{\alpha_4} \approx \sqrt{\frac{R_{25}}{R_4}} = 1.043 \ , \ \omega L \ll R \qquad (7\text{-}5)$$

Thus the low frequency attenuation as calculated is about 4% greater than would be experienced in practice. Similarly, for high enough frequency, (7-4) reduces to

$$\frac{\alpha_{25}}{\alpha_4} \approx 1 \ , \ R \ll \omega L \qquad (7\text{-}6)$$

The best way to handle this error, of course, is not to introduce it in the first place. Its presence in the results given here has been explained; the subject was brought up only to point out that failure to take proper account of temperature effects <u>can</u> be a mistake of significance.

VIII. CONCLUSIONS

In the preceding sections, several types of small diameter coaxial transmission lines have been analyzed. As detailed in the introduction, the investigation was limited to a consideration of coaxial lines because they promised to have the least attenuation for a given size. The next most likely configuration, a parallel conductor line with an oval shield, would have about 30% greater loss, and if the shield were round the increase would be 50%. Some effects of steel have been looked at, and the nature of waveform deterioration, with a view to characterizing suitability of the lines for data transmission, has been treated. A limited amount of experimental work has been performed, where possible, and was found in general to corroborate the predictions of the analyses. From this work, several significant points have emerged; these are recapitulated below.

First of all, it has been seen that characteristic impedance of a transmission line varies widely with frequency. It is inversely proportional at low frequencies to the square root of frequency, gradually "breaking" much as an RC network does. As f increases, it eventually becomes asymptotic to the value $\sqrt{L/C}$, which is commonly taken as the impedance of a transmission line. The characteristic impedance of small-diameter cables is lower than

that of the standard sizes more commonly met with, whose characteristics are tabulated in handbooks such as reference [31]. The exception to this is the sea-return cable, which will have an impedance much higher than a corresponding coaxial line.

Attenuation of small-diameter coaxial lines is considerably higher than that of larger sizes, but otherwise their behavior is quite similar and predictable. In the sizes of interest here, it is seen that the attenuation at 200 KC will probably be between 4 and 9 db per thousand feet, depending on size and material of the line.

The sea-return line causes the smallest attenuation of any configuration as long as frequency is low. There soon comes a point, however, where attenuation begins to rise steeply; beyond a certain point the sea-return line is lossier than its coaxial equivalent, and losses increase faster with frequency. The crossover point is at about 250 KC for the cables considered here.

The effects of the sea in contact with the outer metallic conductor of a coaxial line produce an attenuation characteristic midway between those of the sea-return line and its coaxial counterpart. The comparison is made in Figure 8-1, which shows the attenuation characteristics of the first three lines considered. At low frequencies, the behavior is that of a sea-return line. As frequency

increases, the copper outer conductor provides more and more shielding of the fields from the seawater until, when skin effects are sufficiently pronounced, essentially all the outer conductor current flows in the copper. For the sizes of cables investigated, this effect becomes complete at just about the frequency at which the attenuation characteristic enters the transition region.

The effects of steel in a cable, when in the center conductor, are easily handled and quite predictable, assuming that the effective values of μ and σ of the steel are known. When the steel appears in a bimetal braided conductor, its greatest effect is to increase the resistance of the line; the increased permeability is of relatively minor importance. This provides a convenient method of increasing a cable's strength without increasing its diameter, if the added resistance poses no problem. For greater strength, the steel may be moved further to the outside as a separate layer over the copper. This yields the double advantage of having minimum effect on the signal transmission properties and providing, for the strength member, maximum cross-sectional area for a given thickness. When the tradeoffs between strength, size, and attenuation are closely balanced, it is felt that the work done so far indicates such a configuration to be the best design. Several long lengths of the steel-overbraid cable described in Section C

of Chapter V are currently being manufactured and tested.

If digital data, in the form of pulses or a non-return-to-zero (NRZ) data stream, is sent over small-diameter transmission lines, the speed of transmission is severely limited unless the distance is short. Straightforward methods exist, however, for equalizing the attenuation and phase-shift characteristics of such lines, which with suitable amplification will compensate for these effects. Terminating networks can also be designed, which will match the widely-varying characteristic impedance of the line to a fixed load.

"Bandwidth" is not strictly definable in the usual sense when talking about cables, but it is often spoken of anyway. For digital data transmission, the term can be taken to mean the frequency range over which the cable is equalized sufficiently well to allow the transmission, reception, and proper reconstruction of pulses. This is the frequency range over which <u>both</u> the amplitude response is reasonably flat and the phase shift is reasonably linear with frequency. (For the equalizer design presented here, the range of flat amplifier response will include, and be greater than, the range of linear phase shift.) Theoretical minimum bandwidth needed to transmit random NRZ digital data at a rate of f kilobits per second is $1/(2f)$ cycles; for the postulated 400 kbps rate this means an absolute minimum

bandwidth of 200 KC (and practical considerations beyond the scope of this discussion will dictate a larger figure.) A final determination of the required value cannot be undertaken without a thorough knowledge of the noise characteristics of the system, which have not been investigated here.

The information collected and developed in the foregoing pages by no means exhausts the subjects treated, and in fact, many points remain to be answered in the course of the continuing investigation of which the work presented here forms only a part. Nevertheless, some helpful guidelines have been laid down.

In summary, the behavior of coaxial cables can be predicted with reasonable accuracy. A systematic procedure for calculating their propagation characteristics has been set forth, and the results obtained for several miniature cables, both in and out of seawater, are given. The effects of steel, seawater, and variation of size on electrical properties, as well as the actual magnitude of these effects and properties, have been presented for ready comparison. Out of these results has come a cable design which appears to offer the best compromise between strength, size, and electrical requirements, for which a patent application has been filed. In the implementation of the above work, several programs and subroutines have been written for the IBM 7090

computer. They are quite general, and can handle a wide variety of coaxial configurations. Separately, or together they provide for computation of impedances, attenuation, and network response. Finally, to the extent that the assumptions encountered above are valid (or can be made so), no phenomena have been uncovered which will necessarily preclude the transmission of digital data at the desired speeds over coaxial cables of the postulated length, diameter, and strength.

APPENDIX A

SOME BASIC TRANSMISSION LINE EQUATIONS

Reference to Figure 1-1 shows that the differential equations describing a uniform transmission line with losses at any instant are:

$$\frac{\partial V}{\partial s} = -L\frac{\partial I}{\partial t} - RI \qquad (A\text{-}1)$$

$$\frac{\partial I}{\partial s} = -C\frac{\partial V}{\partial t} - GV$$

where

V = instantaneous voltage across the line as measured from the reference point

I = instantaneous current in the line at the same point

L = series inductance
R = series resistance
G = shunt conductance
C = shunt capacitance
} per unit length

s = distance along the line

t = time

Strictly speaking, the equations as written are for a point, and for the purposes of this appendix Figure 1-1 should be thought of as representing an infinitesimal length ds of the line, i.e., $\Delta s = ds$. If the line is driven with a

sinusoidal function and steady-state conditions prevail, equations (A-1) have a general phasor solution of the form

$$\overset{\times}{V} = Ae^{-\gamma s} + Be^{\gamma s} \qquad \text{(A-2)}$$

where

$\overset{\times}{V}$ = peak phasor representation of V, i.e., $V(s,t) = \mathcal{R}_e \hat{V} e^{j\omega t}$

γ = line propagation constant $\sqrt{(R + j\omega L)(G + j\omega C)}$ $= \alpha + j\beta$

and A and B are complex constants to be evaluated from the terminal conditions. The evaluation is carried out in standard texts on transmission line theory; one reference [21, p. 221] gives as a result:

$$\overset{\times}{V} = \tfrac{1}{2}(\overset{\times}{V}_r + \overset{\times}{I}_r Z_o)e^{-\gamma s} + \tfrac{1}{2}(\overset{\times}{V}_r - \overset{\times}{I}_r Z_o)e^{\gamma s} \qquad \text{(A-3)}$$

where

$\overset{\times}{V}$ = voltage across the line at distance s from the reference point

$\overset{\times}{V}_r$ = voltage at a reference point, at which s = 0

$\overset{\times}{I}_r$ = current at the reference point, at which s = 0

Z_o = characteristic impedance of the line = $\sqrt{(R + j\omega L)(G + j\omega C)}$

γ = propagation constant = $\sqrt{(R + j\omega L)(G + j\omega C)}$

s = distance from the reference point (see below)

and the overcross denotes peak phasor values. A similar relationship exists for the current.

Equation (A-3) is general in that it allows the use of either the sending end or the receiving end of the line as a reference point. When the reference point $s = 0$ is taken at the generator and E is reckoned at or toward the load, s is assigned a positive value. When the reference point is taken at the load and s is reckoned toward the generator, it is given a negative numerical value. It is most convenient for the exposition here to take the reference at the sending end. Then the voltage at distance s along the line can be written in terms of the line constants and terminal conditions as

$$\overset{\times}{V} = \tfrac{1}{2}\left(\overset{\times}{V}_g + \frac{\overset{\times}{V}_g Z_o}{Z_{in}}\right) e^{-\gamma s} + \tfrac{1}{2}\left(\overset{\times}{V}_g - \frac{\overset{\times}{V}_g Z_o}{Z_{in}}\right) e^{\gamma s} \quad (A\text{-}4)$$

where

$\overset{\times}{V}_g$ = peak phasor generator voltage

Z_{in} = input impedance of the line

The input impedance of the line will depend upon several factors, as will be brought out shortly. Manipulation of equation (A-4) gives

$$\overset{\times}{V} = \left(\frac{\overset{\times}{V}_g}{2}\right)\left(1 + \frac{Z_o}{Z_{in}}\right)\left[e^{-\gamma s} + \frac{1 - Z_o/Z_{in}}{1 + Z_o/Z_{in}} e^{\gamma s}\right] \quad (A\text{-}5)$$

From this equation can be seen the manner in which the line modifies the generator voltage throughout its length. In particular, the two exponentials show that the actual voltage

at distance s is composed of two waves traveling in opposite directions on the line: one toward the load (an $e^{-\gamma s}$ effect, as the reference point has been assumed here) and one away from the load (an $e^{+\gamma s}$ effect). Physically the latter wave arises as a reflection from the load because (and if) the load is not exactly equal to the characteristic impedance of the line. The factor multiplying $e^{\gamma s}$ must then be some sort of measure of how bad (or good) this reflection is. Unfortunately it is not in a very convenient form, because Z_{in} depends on so many things, and one usually has no idea what this impedance is until one computes it. This may be done from the formula

$$Z_{in} = Z_o \left[\frac{Z_L \cosh \gamma\ell + Z_o \sinh \gamma\ell}{Z_o \cosh \gamma\ell + Z_L \sinh \gamma\ell} \right] \qquad \text{(A-6)}$$

where

Z_{in} = line input impedance

Z_o = line characteristic impedance

Z_L = line terminating (load) impedance

γ = line propagation constant

ℓ = line length

which is also available in all standard references. A better feel for the physical picture may be had by substituting (A-6) into (A-5), but first the hyperbolic functions in the former expression are rewritten in exponential form

and terms collected; this leads to the equivalent expression

$$Z_{in} = Z_o \left[\frac{(Z_L + Z_o) + (Z_L - Z_o)\, e^{-2\gamma\ell}}{(Z_L + Z_o) - (Z_L - Z_o)\, e^{-2\gamma\ell}} \right] \quad \text{(A-7)}$$

which may be simplified still further into

$$Z_{in} = \left[\frac{1 + \rho\, e^{-2\gamma\ell}}{1 - \rho\, e^{-2\gamma\ell}} \right] \quad \text{(A-8)}$$

by use of the well-known and ubiquitous reflection coefficient, ρ , defined as

$$\rho = \frac{Z_L - Z_o}{Z_L + Z_o} \quad \text{(A-9)}$$

Then (A-8) is substituted into (A-5), and after some straightforward algebraic manipulation yields

$$\overset{\times}{V} = \frac{\overset{\times}{V}_g}{1 + \rho\, e^{-2\gamma\ell}} \left[e^{-\gamma s} + \rho\, e^{-2\gamma\ell}\, e^{\gamma s} \right] \quad \text{(A-10)}$$

Then it is seen that the generator voltage is modified in several ways: first, it is augmented or diminished by the load mismatch, as modified by the length of the line (the factor $1/\left[1 + \rho\, e^{-2\gamma\ell}\right]$); second, it is attenuated and phase-shifted with distance (the factor $e^{-\gamma s} = e^{-\alpha s}\, e^{-j\beta s}$); and third, there is added to it a wave reflected from the mismatched termination (the factor $\rho\, e^{-2\gamma\ell}\, e^{\gamma s}$).

Obviously, from equation (A-9), if the line is terminated in its characteristic impedance, $Z_L = Z_o$, $\rho = 0$,

and (A-10) becomes

$$\overset{\times}{V} = \overset{\times}{V}_g \, e^{-\gamma s} \quad , \quad Z_L = Z_o \qquad \text{(A-11)}$$

showing that the generator voltage is only attenuated and phase-shifted along the line. Specifically, the load voltage is

$$\overset{\times}{V}_{load} = \overset{\times}{V}_g \, e^{-\gamma \ell} \qquad \text{(A-12)}$$

If, in some frequency range or for some other reason, Z_L is not equal to Z_o, the line will not be terminated correctly and a mismatch loss at the receiving end must be accepted as a cost of doing business. Moreover, the input impedance as seen by the generator will now be different, and will probably not match the generator impedance. Reflections from the receiving end will be re-reflected at the sending end, and a further mismatch loss must be taken between line and generator. To account for these factors as well as the attenuation inherent in the line, it is convenient to view the line as a network inserted between the generator and the load and compute the insertion loss.

Because the design of the transmitter and receiver at the two ends of the line can often be made a part of the overall data transmission problem (certainly true here), adjustment of the generator output impedance and the load impedance are under control. A not unreasonable choice is to make $Z_g = Z_L$. Then, without the line between them, the

load and generator are matched and maximum transmission occurs.

If I_L is the current that flows in the load without the line interposed, and I_L' is the current that flows in the load when the line is inserted, then straightforward two-port network analysis shows that the ratio of these currents is given [15, p. 119 and 239] by

$$\frac{\overset{\times}{I}_L}{\overset{\times}{I}_{L'}} = \frac{F_1 F_4}{F_2 F_3} e^{\gamma \ell} \qquad \text{(A-13)}$$

where

$\overset{\times}{I}_L$ = load current without transmission line inserted

$\overset{\times}{I}_{L'}$ = load current with transmission line inserted

$F_1 = \frac{2\sqrt{Z_g Z_L}}{Z_g + Z_L}$ = reflection factor for Z_g and Z_L

$F_2 = \frac{2\sqrt{Z_g Z_{in}}}{Z_g + Z_{in}}$ = reflection factor for Z_g and Z_{in}

$F_3 = \frac{2\sqrt{Z_g Z_{out}}}{Z_g + Z_{out}}$ = reflection factor for Z_g and Z_{out}

$F_4 = 1 - \left(\frac{Z_g - Z_{in}}{Z_g + Z_{in}}\right)\left(\frac{Z_L - Z_{out}}{Z_L + Z_{out}}\right) e^{-2\gamma \ell}$ = interaction factor due to a mismatch at both ends of the line.

Z_{in} = impedance seen by the generator looking into the line

Z_{out} = impedance seen by the load looking into the line

Note that the reflection factors are not the same as ρ, the reflection coefficient. Equation (A-13) is a general expression; note also that $F_1 = 1$ here because the assumption has been made that $Z_g = Z_L$. If Z_g and Z_L are not very different from Z_o, or if $e^{-2\gamma\ell}$ is small (which will always be true in the cases under investigation here), F_4 is close to unity, and may be taken to be so. (For $Z_L = Z_g = Z_o$, of course, F_4 is identically unity).

Equation (A-13) is known as the <u>insertion ratio</u>; insertion loss is then defined as the natural logarithm of the absolute magnitude of this ratio. In general

$$\text{Loss} = \ln \frac{1}{|F_2|} + \ln \frac{1}{|F_3|} - \ln \frac{1}{|F_1|} - \ln \frac{1}{|F_4|} + \ln e^{\alpha\ell} \quad \text{(A-14)}$$

Specifically, for the case in which $F_1 = 1$, which implies that $Z_g = Z_L$, $Z_g \approx Z_{in}$, and $Z_L \approx Z_{out}$,

$$\text{Loss} = 2 \ln \frac{|Z_o + Z_g|}{2\sqrt{|Z_g||Z_o|}} + \alpha\ell \text{ nepers} \quad \text{(A-15)}$$

If $Z_o = Z_g$, the line is matched and the insertion loss is simply $\alpha\ell$ nepers. For the matched case, the same result could have easily been obtained from equation (A-12) merely by taking the natural logarithm of the ratio of the generator and load voltages.

Insertion loss can also be expressed in db. For reference, the formula is presented here:

$$\text{Loss} = 20\left(\log\frac{1}{F_2} + \log\frac{1}{F_3} - \log\frac{1}{F_1} - \log\frac{1}{F_4} + 0.434\,\alpha\ell\right) \qquad \text{(A-16)}$$

In general, loss or gain in db = (8.686)(Loss or gain in nepers).

APPENDIX B

THE MODIFIED BESSEL FUNCTIONS

The discussion will be limited here to the case where n is an integer, since this corresponds to a physical field which is always periodic in 2π in its φ-dependence. A more complete treatment of Bessel functions may be found in references [22] or [32].

Bessel's Equation, of order n with (unrestricted) parameter λ is a differential equation customarily written as

$$\frac{d^2y}{dx^2} + \frac{1}{x}\frac{dy}{dx} + \left(\lambda^2 - \frac{n^2}{x^2}\right) y = 0 \qquad \text{(B-1)}$$

One general solution to this equation is

$$y = A\, J_n(\lambda x) + B\, Y_n(\lambda x) \qquad \text{(B-2)}$$

where

J_n = the Bessel function of the first kind and of order n

Y_n = the Bessel function of the second kind and of order n

A, B = constants

n = an integer which may be positive, negative, or zero

Quite often $\lambda = 1$.

Certain equations closely resembling (B-1) occur quite often; one of these is

$$\frac{d^2y}{dx^2} + \frac{1}{x}\frac{dy}{dx} - \left(1 + \frac{n^2}{x^2}\right) y = 0 \qquad \text{(B-3)}$$

which may be rewritten in the form

$$\frac{d^2y}{dx^2} + \frac{1}{x}\frac{dy}{dx} + \left(j^2 - \frac{n^2}{x^2}\right) = 0 \qquad \text{(B-4)}$$

which shows that this is merely Bessel's equation with parameter j. From equation (B-2) the solution to (B-4) may be written

$$y = A\, J_n(jx) + B\, Y_n(jx) \qquad \text{(B-5)}$$

which is inconvenient to use in practice because of the imaginary arguments. Two new functions $I_n(x)$ and $K_n(x)$, which are entirely real, may be defined, so that another solution to (B-4) is

$$y = A\, I_n(x) + B\, K_n(x) \qquad \text{(B-6)}$$

where

$I_n(x)$ = modified Bessel function of first kind, of order $n = J_n(jx)/(j)^n$

$K_n(x)$ = modified Bessel function of second kind, of order $n = \frac{\pi}{2}\, j^{n+1}\left[J_n(jx) + jY_n(jx)\right]$

$\left.\begin{matrix} A \\ B \end{matrix}\right\}$ = constants

As indicated, I_n and J_n are quite simply related, but K_n is a complex linear sum of $J_n + Y_n$; hence it is <u>not</u> true that $J_n(jx) = I_n(x)$, or that $Y_n(jx) = K_n(x)$.

A second equation which closely resembles (B-1) is

$$\frac{d^2y}{dx^2} + \frac{1}{x}\frac{dy}{dx} + \left(-j - \frac{n^2}{x^2}\right) y = 0 \qquad \text{(B-7)}$$

which can be considered either as the Bessel equation of order n with parameter $\sqrt{-j}$, or the modified n^{th}-order equation with parameter $\sqrt{+j}$. Noting that $\sqrt{-j} = (\sqrt{-1})(\sqrt{j}) = j^{3/2}$, the solution to (B-7) may be written as

$$y = A\, J_n(j^{3/2} x) + B\, Y_n(j^{3/2} x) \qquad \text{(B-8)}$$

or in the form

$$y = C\, I_n(x\sqrt{j}) + D\, K_n(x\sqrt{j}) \qquad \text{(B-9)}$$

If the argument $(j^{3/2} x)$ is substituted in the series expansion for J_n, the terms may then be collected into two series; one purely real and the other purely imaginary, i.e.,

$$J_n(j^{3/2} x) = \mathrm{ber}_n x + j\, \mathrm{bei}_n x \qquad \text{(B-10)}$$

A similar procedure for the second solution to Bessel's modified equation yields

$$-j^n K_n(j^{\frac{1}{2}} x) = \mathrm{ker}_n x + j\, \mathrm{kei}_n x \qquad \text{(B-11)}$$

Equations (B-10) and (B-11) are the definitions of the ber, bei, ker, and kei functions. These functions were first suggested by Sir William Thomson, Lord Kelvin. They are all real and have been tabulated [17,22].

The Thomson functions of the first kind also have a close relation, naturally, to the modified functions in equation (B-9). Specifically, for both kinds,

$$j^{\nu} I_{\nu}(x\sqrt{j}) = \mathrm{ber}_{\nu}(x) + j\,\mathrm{bei}_{\nu}(x) \qquad \text{(B-12)}$$

and

$$j^{-\nu} K_{\nu}(x\sqrt{j}) = \mathrm{ker}_{\nu}(x) + j\,\mathrm{kei}_{\nu}(x) \qquad \text{(B-13)}$$

The subscript ν is purposely used here instead of n to emphasize the fact that, although it was stipulated at the outset that discussion would be restricted to integer n, there is no mathematical restriction in (B-12) or (B-13) on the value of ν. If ν (or n) is zero, it is customary to omit the subscript when writing the Thomson functions. Thus, $\mathrm{ber}_0\, y$ is written ber y, etc. Some other useful relationships, which will often be needed, are

$$\left.\begin{aligned}
&I_0'(x) = I_1(x)\\
&K_0'(x) = -K_1(x)\\
&j^{\frac{1}{2}} I_1(j^{\frac{1}{2}}x) = \mathrm{ber}'\, x + j\,\mathrm{bei}'\, x\\
&-j^{\frac{1}{2}} K_1(j^{\frac{1}{2}}x) = \mathrm{ker}'\, x + j\,\mathrm{kei}'\, x\\
&\frac{d}{dx}(\mathrm{ber}_{\nu}\, x + j\,\mathrm{bei}_{\nu}\, x) = \mathrm{ber}'_{\nu}\, x + j\,\mathrm{bei}'_{\nu}\, x\\
&\frac{d}{dx}(\mathrm{ker}_{\nu}\, x + j\,\mathrm{kei}_{\nu}\, x) = \mathrm{ker}'_{\nu}\, x + j\,\mathrm{kei}'_{\nu}\, x
\end{aligned}\right\} \qquad \text{(B-14)}$$

Reference 22 contains an extensive collection of formulas and handy relationships between the Thomson functions at the rear of the book, as well as tables of the functions ber', bei', ker', and kei'.

One often finds that approximations to the Thomson functions are often used "if the argument is sufficiently small." Unfortunately, "sufficiently" is all too often left undefined; this can be remedied with only the aid of a desk calculator and a little time. It is worth the effort to anyone who is going to compute the fields surrounding cables in seawater, for the argument of the Thomson functions will be small. The following approximations provide accuracy to one percent or better. In these expressions, γ is Euler's Constant; $\gamma = 0.5772157$, and $(\ln 2 - \gamma) = 0.1159315$

For an Argument $z \leq 1.5$, within 1%

$$\left.\begin{aligned}
&\text{ber } z = 1 - z^4/64 \\
&\text{bei } z = z^2/4 - z^6/2304 \\
&\text{ker } z = (\ln 2 - \gamma - \ln z)\ \text{ber } z + \pi/4\ \text{bei } z - 3z^4/128 \\
&\text{kei } z = (\ln 2 - \gamma - \ln z)\ \text{bei } z - \pi/4\ \text{ber } z + z^2/4 \\
&\qquad\qquad - 1.833z^6/2304 \\
&\text{ber}' z = -z^3/16 + z^7/18432 \\
&\text{bei}' z = z/2 - z^5/384 \\
&\text{ker}' z = (\ln 2 - \gamma - \ln z)\ \text{ber}' z - \frac{\text{ber } z}{z} \\
&\qquad\qquad + \pi/4\ \text{bei}' z - 3z^3/32 \\
&\text{kei}' z = (\ln 2 - \gamma - \ln z)\ \text{bei}' z - \frac{\text{bei } z}{z} \\
&\qquad\qquad - \pi/4\ \text{ber}' z + z/2 - 1.833z^5/384
\end{aligned}\right\} \quad \text{(B-15)}$$

For the ber, bei, ber', and bei' functions, the above approximations are good up to $z = 2$. The second terms of the bei and ber' expressions are not really necessary. For an Argument $z \leq 0.1$, within 1%

$$\begin{aligned} \text{ber } z &= 1 \\ \text{bei } z &= z^2/4 \\ \text{ker } z &= \ln 2 - \gamma - \ln z \\ \text{kei } z &= -\pi/4 \\ \text{ber}' z &= -z^3/16 \\ \text{bei}' z &= z/2 \\ \text{ker}' z &= -1/z \\ \text{kei}' z &= (\tfrac{1}{2} + \ln 2 - \gamma - \ln z)\, z/2 \end{aligned} \qquad \text{(B-16)}$$

There are some simplifications possible to the expressions (2-6) and (2-7) for the cases where the argument is fairly large or fairly small. The following expressions are due to von Aulock [33, p. 12].

If

$$\left.\begin{aligned} &u < 2, \\ &R = R_{dc}(1 + u^4/192) \\ &L = L_{dc} \end{aligned}\right\} \qquad \text{(B-17)}$$

If

$$\left.\begin{aligned} &u > 10, \\ &R = R_{dc}(u/2\sqrt{2}) \\ &L = L_{dc}(2\sqrt{2}/u) \end{aligned}\right\} \qquad \text{(B-18)}$$

where $u = b\sqrt{\omega\mu\sigma}$ as defined in those expressions. The second of equations (B-18) is actually good down to $u = 5$.

APPENDIX C

DERIVATION OF BESSEL'S EQUATION TO DESCRIBE THE FIELD IN A CONDUCTOR OF A COAXIAL TRANSMISSION LINE

Maxwell's equations may be written at any point (and irrespective of coordinate systems) as:

$$\left.\begin{aligned} \nabla \wedge \vec{E} &= \frac{-\partial \vec{B}}{\partial t} && \text{(a)} \\ \nabla \wedge \vec{H} &= J + \frac{\partial \vec{D}}{\partial t} && \text{(b)} \\ \nabla \wedge \vec{B} &= 0 && \text{(c)} \\ \nabla \wedge \vec{D} &= \rho && \text{(d)} \end{aligned}\right\} \quad \text{(C-1)}$$

where

$\vec{E}$ = electric intensity in volts/meter

$\vec{H}$ = magnetic intensity in amperes/meter

$\vec{B}$ = magnetic flux density in webers/meter^2

$\vec{D}$ = electric displacement in coulombs/meter^2

$\vec{J}$ = current density in amperes/meters^2

In addition, there are the relationships, true anywhere

$$\left.\begin{aligned} \vec{D} &= \epsilon \vec{E} && \text{(a)} \\ \vec{B} &= \mu \vec{H} && \text{(b)} \end{aligned}\right\} \quad \text{(C-2)}$$

and the expression of Ohm's Law at a point, also true anywhere but normally thought of as applying to a conductor

$$\vec{J} = \sigma \vec{E} \qquad \text{(C-3)}$$

where

ϵ = permittivity in farads/meter

μ = permeability in henries/meter

For steady-state ac conditions, all field vectors become periodic sinusoidal time functions of a common angular frequency $\omega = 2\pi f$. Then a phasor representation is convenient to simplify the equations; for instance,

$$\vec{E}(t) = \mathrm{Re}\, \overset{\times}{\vec{E}} e^{j\omega t} \qquad \text{(C-4)}$$

where

$\overset{\times}{\vec{E}}$ = peak phasor representation of $\vec{E}(t)$, a complex vector function independent of t

Under these conditions $\frac{\partial}{\partial t}$ is equivalent to "$j\omega$" and equations (C-1) become

$$\left.\begin{aligned} \nabla \wedge \overset{\times}{\vec{E}} &= -j\omega \overset{\times}{\vec{B}} && \text{(a)} \\ \nabla \wedge \overset{\times}{\vec{H}} &= \overset{\times}{\vec{J}} + j\omega \overset{\times}{\vec{D}} && \text{(b)} \\ \nabla \cdot \overset{\times}{\vec{B}} &= 0 && \text{(c)} \\ \nabla \cdot \overset{\times}{\vec{D}} &= \rho && \text{(d)} \end{aligned}\right\} \qquad \text{(C-5)}$$

Substitution of (C-2) and (C-3) into (C-5) yield, for the first two equations

$$\left.\begin{aligned} \nabla \wedge \overset{\times}{\vec{E}} &= -j\omega\mu \overset{\times}{\vec{H}} && \text{(a)} \\ \nabla \wedge \overset{\times}{\vec{H}} &= \sigma \overset{\times}{\vec{E}} + j\omega\epsilon \overset{\times}{\vec{E}} && \text{(b)} \end{aligned}\right\} \qquad \text{(C-6)}$$

Then (C-6b) is substituted in (C-6a):

$$-j\omega\mu\vec{H}^{*} = \nabla\wedge\left(\frac{\nabla\wedge\vec{H}^{*}}{\sigma + j\omega\epsilon}\right) = \frac{1}{\sigma + j\omega\epsilon}\,\nabla\wedge\nabla\wedge\vec{H}^{*}$$

$$= \frac{1}{\sigma + j\omega\epsilon}\left[\nabla(\nabla\cdot\vec{H}^{*}) - \nabla^{2}\vec{H}^{*}\right] \qquad \text{(C-7)}$$

From equations (C-2b) and (C-1c) $\vec{B} = \mu\vec{H}$ and $\nabla\cdot\vec{B} = 0$, therefore, taking μ constant, $\nabla\cdot\mu\vec{H} = \mu\,\nabla\cdot\vec{H} = 0$, $\nabla(0)$ is always zero, and (C-7) becomes

$$\nabla^{2}\vec{H}^{*} = (j\omega\mu)(\sigma + j\omega\epsilon)\,\vec{H}^{*} \qquad \text{(C-8)}$$

Since it is usually true that $\omega\epsilon \ll \sigma$ for all frequencies of interest within a conductor, it is permissible to write, within a good conductor,

$$\nabla^{2}\vec{H}^{*} = j\omega\mu\sigma\,\vec{H}^{*} \qquad \text{(C-9)}$$

So far the use of vector notation has allowed us to keep the discussion general. To press on to more specific results, we must speak more concretely: the time has come to choose a coordinate system. Since the structures under investigation are coaxial transmission lines, cylindrical coordinates are chosen as shown in Figure 4-1. Now, unfortunately the Laplacian of a vector is not as simple as that of a scalar in any but the rectangular system of coordinates, but the additional labor can be minimized by stopping to take a look at the physical system we are describing and getting rid of anything not needed.

In the first place coaxial cables, as normally energized, have circular magnetic fields; $\vec{H}$ has a component in the φ-direction only. The electric field has two components: $\vec{E}_r$ in the radial direction and $\vec{E}_z$ along the axis of the cable. For the moment, the latter will be ignored; the reasons will be given later. Secondly, because of the circular symmetry, all derivatives with respect to φ are zero, and implicit in ignoring $\vec{E}_z$ is the assumption that the same is true of all partials with respect to z.

In cylindrical coordinates, $\nabla^2\vec{H}$ may be defined as

$$\nabla^2\vec{H} = \nabla\cdot(\nabla\vec{H})$$

where (C-10)

$$\nabla\vec{H} = \frac{\partial\vec{H}}{\partial r}\vec{u}_r + \frac{1}{r}\frac{\partial\vec{H}}{\partial\varphi}\vec{u}_\varphi + \frac{\partial\vec{H}}{\partial z}\vec{u}_z$$

The quantities $\vec{u}_r$, $\vec{u}_\varphi$, and $\vec{u}_z$ are unit vectors in the three directions of the cylindrical coordinate system. It is most convenient to work with one component $\nabla\vec{H}$ at a time

$$\frac{\partial\vec{H}}{\partial r} = \frac{\partial}{\partial r}\left[H_r\vec{u}_r + H_\varphi\vec{u}_\varphi + H_z\vec{u}_z\right] \qquad \text{(C-11)}$$

$$= \frac{\partial H_r}{\partial r}\vec{u}_r + H_r\frac{\partial\vec{u}_r}{\partial r} + \frac{\partial H_\varphi}{\partial r}\vec{u}_\varphi + H_\varphi\frac{\partial\vec{u}_\varphi}{\partial r} + \frac{\partial H_z}{\partial r}\vec{u}_z + H_z\frac{\partial\vec{u}_z}{\partial r}$$

$$= \frac{\partial H_r}{\partial r}\vec{u}_r + \frac{\partial H_\varphi}{\partial r}\vec{u}_\varphi + \frac{\partial H_z}{\partial r}\vec{u}_z$$

since, in cylindrical coordinates, the partial derivatives of all unit vectors with respect to r are zero. It is found that the same is true of all partials with respect to z; therefore, there is no point in computing $\frac{\partial \vec{H}}{\partial z}$.

Even though H_r and H_z are assumed here to be zero, they will be carried along for the time being. The next partial is

$$\frac{\partial \vec{H}}{\partial \varphi} = \frac{\partial H_r}{\partial \varphi} \vec{u}_r + H_r \frac{\partial \vec{u}_r}{\partial \varphi} + \frac{\partial H_\varphi}{\partial \varphi} \vec{u}_\varphi + H_\varphi \frac{\partial u_\varphi}{\partial \varphi} + \frac{\partial H_z}{\partial \varphi} \vec{u}_z + H_z \frac{\partial \vec{u}_z}{\partial \varphi} \tag{C-12}$$

This time, however, there are two partials of unit vectors which are not zero (the only two which occur in cylindrical coordinates):

$$\frac{\partial \vec{u}_r}{\partial \varphi} = \vec{u}_\varphi \tag{C-13}$$

and

$$\frac{\partial \vec{u}_\varphi}{\partial \varphi} = -\vec{u}_r$$

so that

$$\frac{\partial \vec{H}}{\partial \varphi} = \left(\frac{\partial H_r}{\partial \varphi} - H_\varphi\right)\vec{u}_r + \left(\frac{\partial H_\varphi}{\partial \varphi} + H_r\right)\vec{u}_\varphi + \frac{\partial H_z}{\partial \varphi} \vec{u}_z \tag{C-14}$$

Then, neglecting z-derivatives,

$$\nabla \vec{H} = \left[\frac{\partial H_r}{\partial r} \vec{u}_r + \frac{\partial H_\varphi}{\partial r} \vec{u}_\varphi + \frac{\partial H_z}{\partial r} \vec{u}_z\right] \vec{u}_r + \frac{1}{r}\left[\left(\frac{\partial H_r}{\partial \varphi} - H_\varphi\right)\vec{u}_r + \left(\frac{\partial H_\varphi}{\partial \varphi} + H_r\right) \vec{u}_\varphi + \frac{\partial H_z}{\partial \varphi} \vec{u}_z\right] \vec{u}_\varphi \tag{C-15}$$

In cylindrical coordinates the divergence of a vector $\vec{A}$ is defined as

$$\nabla \cdot \vec{A} = \frac{1}{r} \frac{\partial}{\partial r} \left[r(A_r) \right] + \frac{1}{r} \frac{\partial (A\varphi)}{\partial \varphi} + \frac{\partial (A_z)}{\partial z} \qquad \text{(C-16)}$$

Equations (C-15) and (C-16) are then combined to yield

$$\nabla \cdot \nabla \vec{H} = \frac{1}{r} \frac{\partial}{\partial r} \left[r \left(\frac{\partial H_r}{\partial r} \vec{u}_r + \frac{\partial H_\varphi}{\partial r} \vec{u}_\varphi + \frac{\partial H_z}{\partial r} \vec{u}_z \right) \right] + \qquad \text{(C-17)}$$

$$+ \frac{1}{r} \frac{\partial}{\partial \varphi} \left[\frac{1}{r} \left(\left[\frac{\partial H_r}{\partial \varphi} - H_\varphi \right] \vec{u}_r + \left[\frac{\partial H_\varphi}{\partial \varphi} + H_r \right] \vec{u}_\varphi \right. \right.$$

$$\left. \left. + \frac{\partial H_z}{\partial \varphi} \vec{u}_z \right) \right]$$

Now that there is no doubt about the procedure being followed, let us dispense with the rest of the quantities which are assumed to be zero. Then (C-17) becomes

$$\nabla^2 \vec{H} = \nabla \cdot \nabla \vec{H} = \frac{1}{r} \frac{\partial}{\partial r} \left(r \frac{\partial H_\varphi}{\partial r} \vec{u}_\varphi \right) + \frac{1}{r^2} \frac{\partial}{\partial \varphi} (-H_\varphi \vec{u}_r) \qquad \text{(C-18)}$$

Performing the indicated differentiations and making use of (C-13) yields, for the non-zero quantities

$$\nabla^2 \vec{H} = \left(\frac{\partial^2 H_\varphi}{\partial r^2} + \frac{1}{r} \frac{\partial H_\varphi}{\partial r} \right) \vec{u}_\varphi - \frac{H_\varphi}{r^2} \vec{u}_\varphi \qquad \text{(C-19)}$$

Thus it is seen that $\nabla^2 \vec{H}$ is a vector whose only component is in the φ-direction, and whose magnitude is

$$\left| \nabla^2 \vec{H} \right| = \frac{\partial^2 H_\varphi}{\partial r^2} + \frac{1}{r} \frac{\partial H_\varphi}{\partial r} - \frac{H_\varphi}{r^2} \qquad \text{(C-20)}$$

Since there is now only one variable in the expression, the partials are written as total derivatives; and an equivalent form of (C-20) is

$$|\nabla^2 \vec{H}| = \frac{d}{dr}\left[\frac{1}{r}\ \frac{d}{dr}\ (rH_\varphi)\right] \qquad \text{(C-21)}$$

which is best shown by performing the differentiations. Now $\vec{H}$ has only a component in the φ-direction (as does $\nabla^2\vec{H}$) and its magnitude is H_φ. For steady-state sinusoidal conditions, (C-21) can be written in peak phasor form as

$$\frac{d}{dr}\left[\frac{1}{r}\ \frac{d}{dr}\ (r\overset{\times}{H}_\varphi)\right] = j\omega\mu\sigma\overset{\times}{H}_\varphi \qquad \text{(C-22)}$$

which is Bessel's equation, and exactly equation (4-2).

Two assumptions were made in the derivation in this appendix, viz., that all partial derivatives with respect to z are zero and that all field intensities vary as $e^{j\omega t}$. These imply a lossless line and a steady-state ac transmission. In truth, the field quantities do not vary as $e^{j\omega t}$ alone; they vary as $e^{-\gamma z + j\omega t}$, where $\gamma = \alpha + j\beta$ is the well-known longitudinal propagation constant and one of the very things that this whole investigation is about. If γ is not neglected and the partials with respect to z are carried along, it will be found that the exact form of (C-22) is, in peak phasor notation,

$$\frac{\partial}{\partial r}\left[\frac{1}{r}\ \frac{\partial}{\partial r}\ (r\overset{\times}{H}_\varphi)\right] + \frac{\partial^2 H_\varphi}{\partial z^2} = \Gamma^2 H_\varphi \qquad \text{(C-23)}$$

where $\Gamma = \sqrt{j\omega\mu\sigma}$. Since $\frac{\partial}{\partial z}$ is equivalent to "$-\gamma$", this leads to

$$\frac{d}{dr}\left[\frac{1}{r}\frac{d}{dr}(r\overset{\times}{H}_\varphi)\right] = (\Gamma^2 - \gamma^2)\overset{\times}{H}_\varphi \qquad (C\text{-}24)$$

The longitudinal propagation constant γ will be very small compared to Γ (e.g., by about 5 orders of magnitude or better in copper up to 100 mc [8]) and may therefore safely be ignored in (C-24). Then the results of this appendix naturally follow.

APPENDIX D

A NOTE ON THE CONDUCTIVITY OF SEA WATER

The conductivity σ of sea water is open to some debate. A good average value is approximately 4 mhos/meter; this is the value given by most authors [20, p. 115; 24, p. 277; 31, p. 714]. Stratton [20, p. 606] gives the range 3-5, with a representative value of 4.3 in the Atlantic. Conductivity is very much a function of two factors, temperature and salinity, both of which vary with depth. Conductivity is strongly affected by temperature, and to a much lesser extent by salinity. To arrive at a single value of σ which will yield meaningful results over 10,000- to 20,000-foot lengths of cable suspended vertically in various regions of the ocean, the variation of these two factors with depth and latitude must be known. Reference [11] provides a ready answer to this question. A few minutes spent in perusal of the excellent profile charts there will lead one rapidly to the conclusion that a good round value for temperature is 4°C and, similarly, 35 parts per thousand for salinity. Entering the appropriate conversion table [35, p. 104] with these values yields an average conductivity of about 3.3 mhos/meter.

APPENDIX E

SIMPLIFICATION OF THE EXPRESSION FOR AC RESISTANCE OF A SEAWATER RETURN

Equation (4-20) gives, for the impedance of a the water path in a sea-return line

$$Z_{sea} = \frac{-jv}{2\pi\sigma a} \frac{\text{ker } va + j \text{ kei } va}{\text{ker}' va + j \text{ kei}' va} \qquad \text{(E-1)}$$

Rationalizing the denominator yields (arguments of the Thomson functions are dropped for conciseness of notation)

$$Z = \frac{-jv}{2\pi\sigma a} \frac{(\text{ker} + j \text{ kei})(\text{ker}' - j \text{ kei}')}{(\text{ker}')^2 + (\text{kei}')^2} \qquad \text{(E-2)}$$

Expanding the numerator and collecting terms,

$$\mathcal{R}_e Z = \frac{v}{2\pi\sigma a} \frac{\text{kei ker}' - \text{ker kei}'}{(\text{ker}')^2 + (\text{kei}')^2} \qquad \text{(E-3)}$$

Advantage may be taken of the fact that va will be small in seawater. By definition $v = \sqrt{\omega\mu\sigma} = 5.11 \times 10^{-3}\sqrt{f}$. At one megacycle, the highest frequency considered here $v = 5.11$. If the radius a of the outer conductor is 0.068", as predicated in some of the examples, $a = 1.73 \times 10^{-3}$ meters and $va = 8.85 \times 10^{-3}$ at 1 mc. (It is smaller at lower frequencies.)

Assume that va is as large as 0.1; then by the approximations of Appendix B

$$(\text{ker}'\ va)^2 + (\text{kei}'\ va)^2 \doteq \left(\frac{1}{va}\right)^2 + (0.61593 + \ln va)^2\ \frac{(va)^2}{4}$$

$$\doteq 100 + (0.61593 + 2.3026)^2\ (10^{-2}/4)$$

$$\doteq 100 + 0.0213$$

$$\doteq 100$$

Thus for the usual size of cables in seawater, it is a safe assumption as long as frequency is not too high that

$$(\text{ker}'\ va)^2 + (\text{kei}'\ va)^2 = (1/va)^2 \qquad \text{(E-4)}$$

Similar calculations using the approximations of Appendix B show that, for $z = 0.1$

$$z(\text{kei}\ z\ \text{ker}'\ z - \text{ker}'\ z\ \text{kei}'\ z) = \pi/4 \qquad \text{(E-5)}$$

When $z = 0.1$, the error in (E-5) is about 3%, but rapidly decreases as z decreases. Substituting (E-4) and (E-5) in (E-3) yields for the latter

$$R_e\ Z = \frac{va}{2\pi\sigma a^2}\ \frac{(1/va)(\pi/4)}{\left(\frac{1}{va}\right)^2}$$

$$= \frac{v^2a^2}{2\pi\sigma a^2}\ \frac{\pi}{4} = \frac{v^2}{8\sigma} \qquad \text{(E-6)}$$

And since $v = \sqrt{\omega\mu\sigma}$, (E-6) becomes

$$R_e\ Z = R_{sea} = \frac{\omega\mu}{8} \qquad \text{(E-7)}$$

APPENDIX F

DERIVATION OF RECURSION FORMULAS FOR THE IMPEDANCES OF A LAMINATED CONDUCTOR

Consider a conductor having k laminations in all. Let Z_{am} and Z_{bm} be the surface impedances at the inner and outer surfaces of the m^{th} layer respectively, and let Z_{tm} be the transfer impedance of the m^{th} layer. Denote by z_{am}, z_{bm}, and z_{tm} the corresponding impedances of the first m layers taken together; let I_m be the total current flowing in these first m layers in the positive z-direction. Remember that in equations (4-8), which will be used presently, the current $I_a + I_b$ was defined as flowing in the positive direction in the tubular conductor, the current $+I_a$ returns to the source in the hole within the tube, and the current $+I_b$ does the same outside. The important point is that currents are defined to flow in the positive direction as shown by the arrowheads in Figure 4-1, and equations (4-8) were derived using these definitions.

For convenience, consider the m^{th} layer of a laminated outer conductor, in which the laminations are numbered beginning with the outermost one and increasing inward. By the definition of I_m, the current in the m^{th} layer must be $I_m - I_{m-1}$. Now use equations (4-8) to write the longitudinal

field intensity at the two surfaces of the m^{th} layer. Assuming $(I_m - I_{m-1})$ to be flowing in the positive z-direction, one can think of two currents flowing closer to the conductor axis: I_k in the return direction (physically, $-I_k$ in the positive z-direction), and $I_k - I_m$ in the same direction as $I_m - I_{m-1}$. Then the net return current internal to the m^{th} layer, in the direction of the I_a-arrowhead of Figure 4-1, is $I_k - (I_k - I_m)$ or simply I_m. Since all the current I_{m-1} external to the m^{th} layer has the same physical direction as the current in the m^{th} layer, the net external return current I_{m-1} in the direction of the I_b-arrowhead of Figure 4-1 is $-I_{m-1}$. Then in equations (4-8), I_a corresponds to I_m and I_b to $-I_{m-1}$, and we have

$$\left.\begin{aligned} \overset{\times}{E}_m(a) &= Z_{am}\,\overset{\times}{I}_m - Z_{tm}\,\overset{\times}{I}_{m-1} && (a)\\ \overset{\times}{E}_m(b) &= Z_{tm}\,\overset{\times}{I}_m - Z_{bm}\,\overset{\times}{I}_{m-1} && (b) \end{aligned}\right\} (F\text{-}1)$$

The fields at the surfaces of the m^{th} layer may also be written in terms of the combined impedances of the first m and m-1 layers. There is, of course, no conduction current I_b flowing outside this path. Then, since $E_m(b) = E_{m-1}(a)$,

$$\left.\begin{aligned} \overset{\times}{E}_m(a) &= z_{am}\,\overset{\times}{I}_m && (a)\\ \overset{\times}{E}_m(b) &= \overset{\times}{E}_{m-1}(a) = z_{a,m-1}\,\overset{\times}{I}_{m-1} && (b) \end{aligned}\right\} (F\text{-}2)$$

The quantity $\overset{\times}{E}_m(a)$ may be eliminated between (F-1a) and (F-2a) to yield an expression for the ratio $\overset{\times}{I}_m/\overset{\times}{I}_{m-1}$; next $\overset{\times}{E}_m(b)$ is eliminated between (F-1b) and (F-2b); the latter result is substituted into the former and, after some manipulation, there results the desired expression

$$z_{am} = Z_{am} - \frac{Z_{tm}^2}{Z_{bm} + z_{a,m-1}} \qquad (F\text{-}3)$$

This describes the surface impedance for internal return current of the first m layers of a laminated outer conductor. The iteration procedure is begun with the outermost lamination, for which, of course, $z_{a1} = Z_{a1}$.

Now return to equation (4-8b), and consider the case where $I_b = 0$ (which holds here since we are considering the m outermost laminations, and there is no return conduction current external to them). The m outermost layers themselves form a tube, which carries a current I_m in the positive z-direction. Within the hollow of this tube there flows a current $I_k - I_m$ in the same direction as I_m, and a return current I_k in the opposite direction. The net return current internal to the first m layers is then $I_k - (I_k - I_m)$ or just I_m, so that from (4-8b),

$$\overset{\times}{E}_1(b) = z_{tm}\,\overset{\times}{I}_m \qquad (F\text{-}4)$$

where now z_{tm} must be used instead of Z_{tm} because the first m layers are being considered compositely. But the field at the outer surface of the first m layers is the

same field as that at the outer surface of the first m-1 layers; therefore it is just as true that

$$\overset{\times}{E}_1(b) = z_{t,m-1}\,\overset{\times}{I}_{m-1} \qquad \text{(F-5)}$$

Equations (F-4) and (F-5) may now be combined to yield another expression for the ratio $\overset{\times}{I}_m/\overset{\times}{I}_{m-1}$. This result is substituted in the previous expression for the same ratio, obtained just above, yielding

$$z_{tm} = \frac{Z_{tm}\, z_{t,m-1}}{Z_{bm} + z_{a,m-1}} \qquad \text{(F-6)}$$

which is the transfer impedance for internal return current of the first m layers of a laminated outer conductor. Again, the iteration procedure is begun with the outermost lamination, and $z_{t1} = Z_{t1}$.

For convenience a laminated outer conductor was considered in deriving the recursion formulas presented here, for that is the configuration encountered in this investigation. Identically the same procedure may be followed, however, for a laminated inner conductor. Since there is no current flowing inside the innermost lamination, it is considered first and laminations are numbered progressively outward from the axis (in contrast to the outer conductor, in which we proceeded in the other direction). Recursion formulas are quite similar to (F-3) and (F-6), differing only in the subscripts; they are listed below for reference:

$$\left.\begin{aligned} z_{bm} &= Z_{bm} - \frac{Z_{tm}^2}{Z_{am} + z_{b,m-1}} \\ z_{tm} &= \frac{Z_{tm}\, z_{t,m-1}}{Z_{am} + z_{b,m-1}} \end{aligned}\right\} \qquad \text{(F-7)}$$

where the method and direction of numbering the laminations are as set forth above.

	Smaller Cable	Larger Cable
Center Conductor:		
Strand Number	7	7
Strand Diameter	0.010"	0.0142"
"Calipered" Diameter	0.030"	0.045 "
Dielectric Diameter	0.050"	0.065 "

Table 2-1: Dimensions of Two Miniature Sea-Return Lines

	Smaller Cable	Larger Cable
Center Conductor:		
Strand Number	7	7
Strand Diameter	0.010"	0.010"
Dielectric Diameter	0.050"	0.065"
Shield:		
Strand Number	42	56
Strand Diameter	0.004"	0.004"

Table 3-1: Dimensions of Two Miniature Coaxial Cables

Center Conductor:	
Strand Number	7
Strand Diameter	0.008"
Strand Material	Carbon Steel ("Rocket Wire")
Dielectric Diameter	0.044"
Shield:	
Strand Number	32
Strand Radius	0.004"
Strand Material	Copper

Table 5-1: Dimensions of a Miniature Steel-Cored Coaxial Cable

Center Conductor:	
Strand Number	7
Strand Diameter	0.0063"
Strand Material	Copper
Dielectric Diameter	0.038"
Braid:	
Strand Number	32
Strand Diameter	0.0044"
Strand Material	Copper-Coated Steel
Strand Steel-Core Diameter	0.0040"

Table 5-2: Dimensions of a Miniature Coaxial Cable With a Bimetal Braid

Center Conductor:	
Strand Number	7
Strand Diameter	0.005"
Strand Material	Copper
Dielectric Diameter	0.038"
Shield:	
Inner Layer:	
Strand Number	16
Strand Diameter	0.005"
Strand Material	Copper
Overbraid:	
Strand Number	32
Strand Diameter	0.004"
Strand Material	Carbon Steel ("Rocket Wire")

Table 5-3: Dimensions of a Miniature Coaxial Cable With a Steel Overbraid

FREQ	EXACT R	APPROX R
10.	1.036841E-05	9.508338E-06
20.	2.161646E-05	2.078246E-05
50.	6.009964E-05	5.919673E-05
100.	1.387172E-04	1.376923E-04
200.	3.451612E-04	3.437777E-04
500.	1.300037E-03	1.296612E-03
1000.	3.722065E-03	3.713781E-03
2000.	9.952036E-03	9.937480E-03
5000.	2.469620E-02	2.470766E-02
10000.	3.366783E-02	3.372363E-02
20000.	3.783623E-02	3.791951E-02
50000.	3.966858E-02	3.976472E-02
100000.	4.023701E-02	4.033663E-02
200000.	4.100806E-02	4.111165E-02
500000.	4.506674E-02	4.518867E-02
1000000.	5.704279E-02	5.716479E-02

FREQ	X	X
10.	1.428938E-04	1.428551E-04
20.	2.769366E-04	2.768782E-04
50.	6.624664E-04	6.622629E-04
100.	1.277443E-03	1.277047E-03
200.	2.449675E-03	2.449000E-03
500.	5.659920E-03	5.659118E-03
1000.	1.010791E-02	1.010994E-02
2000.	1.577774E-02	1.579475E-02
5000.	1.812588E-02	1.818277E-02
10000.	1.373419E-02	1.379355E-02
20000.	9.142807E-03	9.185006E-03
50000.	6.827453E-03	6.853358E-03
100000.	8.456878E-03	8.481870E-03
200000.	1.407204E-02	1.410586E-02
500000.	3.220740E-02	3.227529E-02
1000000.	5.868685E-02	5.875973E-02

Table 7-1: Comparison of a Representative Impedance Calculation From Approximate and Exact Formulas. The structure is an outer conductor in contact with the sea. $R = \mathcal{R}_e\, z_{a2}$; $X = \mathcal{I}_m\, z_{a2}$ Read 1.23E-04 as 1.23×10^{-4}.

	EXACT	APPROX
FREQ	RA	RA
10.	4.005914E-02	4.015792E-02
20.	4.005914E-02	4.015970E-02
50.	4.005914E-02	4.015864E-02
100.	4.005914E-02	4.015829E-02
200.	4.005913E-02	4.015794E-02
500.	4.005914E-02	4.015795E-02
1000.	4.005915E-02	4.015801E-02
2000.	4.005922E-02	4.015806E-02
5000.	4.005964E-02	4.015848E-02
10000.	4.006114E-02	4.015999E-02
20000.	4.006715E-02	4.016603E-02
50000.	4.010923E-02	4.020830E-02
100000.	4.025926E-02	4.035897E-02
200000.	4.085464E-02	4.095716E-02
500000.	4.483368E-02	4.495416E-02
1000000.	5.686601E-02	5.698462E-02
FREQ	XA	XA
10.	6.581863E-07	6.347337E-07
20.	1.316390E-06	1.316977E-06
50.	3.291013E-06	3.290732E-06
100.	6.581884E-06	6.590499E-06
200.	1.316392E-05	1.319116E-05
500.	3.290952E-05	3.298145E-05
1000.	6.581960E-05	6.596421E-05
5000.	3.290954E-04	3.298238E-04
10000.	6.581826E-04	6.596425E-04
20000.	1.316317E-03	1.319234E-03
50000.	3.289898E-03	3.297162E-03
100000.	6.572776E-03	6.587755E-03
200000.	1.309468E-02	1.312336E-02
500000.	3.187350E-02	3.193983E-02
1000000.	5.863990E-02	5.871300E-02

Table 7-1, continued: Comparison of a Representative Impedance Calculation from Approximate and Exact Formulas. RA = $\mathcal{R}_e Z_{a_2}$; XA = $\mathcal{I}_m Z_{a2}$. Read 1.23E-04 as 1.23 x 10^{-4}.

	EXACT	APPROX
FREQ	RB	RB
10.	4.005914E-02	4.017367E-02
20.	4.005914E-02	4.017521E-02
50.	4.005914E-02	4.017430E-02
100.	4.005914E-02	4.017399E-02
200.	4.005913E-02	4.017369E-02
500.	4.005914E-02	4.017370E-02
1000.	4.005915E-02	4.017375E-02
2000.	4.005920E-02	4.017380E-02
5000.	4.005957E-02	4.017415E-02
10000.	4.006086E-02	4.017546E-02
20000.	4.006606E-02	4.018068E-02
50000.	4.010243E-02	4.021720E-02
100000.	4.023192E-02	4.034737E-02
200000.	4.074654E-02	4.086417E-02
500000.	4.418500E-02	4.431736E-02
1000000.	5.430374E-02	5.471103E-02
FREQ	XB	XB
10.	5.687263E-07	5.483754E-07
20.	1.137466E-06	1.137797E-06
50.	2.843673E-06	2.843013E-06
100.	5.687298E-06	5.693832E-06
200.	1.137466E-05	1.139644E-05
500.	2.843650E-05	2.849417E-05
1000.	5.687344E-05	5.698949E-05
2000.	1.137461E-04	1.139803E-04
5000.	2.843647E-04	2.849498E-04
10000.	5.687225E-04	5.698952E-04
20000.	1.137403E-03	1.139746E-03
50000.	2.842725E-03	2.848569E-03
100000.	5.679595E-03	5.691461E-03
200000.	1.131481E-02	1.133787E-02
500000.	2.754120E-02	2.759428E-02
1000000.	5.059357E-02	5.072484E-02

Table 7-1, continued: Comparison of a Representative Impedance Calculation from Approximate and Exact Formulas. RB = $\mathcal{R}_e\, Z_{b2}$; XB = $\mathcal{I}_m\, Z_{b2}$. Read 1.23E-04 as 1.23×10^{-4}.

FREQ	EXACT RT	APPROX RT
10.	4.005914E-02	4.016622E-02
20.	4.005914E-02	4.016787E-02
50.	4.005914E-02	4.016689E-02
100.	4.005914E-02	4.016657E-02
200.	4.005913E-02	4.016624E-02
500.	4.005913E-02	4.016625E-02
1000.	4.005912E-02	4.016628E-02
2000.	4.005907E-02	4.016622E-02
5000.	4.005873E-02	4.016587E-02
10000.	4.005751E-02	4.016464E-02
20000.	4.005262E-02	4.015973E-02
50000.	4.001843E-02	4.012536E-02
100000.	3.989649E-02	4.000286E-02
200000.	3.941313E-02	3.951700E-02
500000.	3.620325E-02	3.629145E-02
1000000.	2.667315E-02	2.683720E-02

FREQ	XT	XT
10.	-3.054309E-07	-3.341979E-07
20.	-6.108459E-07	-6.310590E-07
50.	-1.527095E-06	-1.544204E-06
100.	-3.054286E-06	-3.070848E-06
200.	-6.108442E-06	-6.138260E-06
500.	-1.527133E-05	-1.533247E-05
1000.	-3.054214E-05	-3.065868E-05
2000.	-6.108501E-05	-6.131467E-05
5000.	-1.527112E-04	-1.532846E-04
10000.	-3.054179E-04	-3.065623E-04
20000.	-6.107852E-04	-6.130755E-04
50000.	-1.526137E-03	-1.531856E-03
100000.	-3.046662E-03	-3.057797E-03
200000.	-6.046194E-03	-6.068653E-03
500000.	-1.433978E-02	-1.439099E-02
1000000.	-2.387904E-02	-2.416787E-02

Table 7-1, continued: Comparison of a Representative Impedance Calculation From Approximate and Exact Formulas. RT = $\mathcal{R}_e\, Z_{t_2}$; XT = $\mathcal{I}_m\, Z_{t_2}$. Read 1.23E-04 as 1.23×10^{-4}.

FREQ	R(SEA)	X(SEA)
10.	9.869604E-06	1.411277E-04
20.	1.973921E-05	2.735451E-04
50.	4.934802E-05	6.550766E-04
100.	9.869604E-05	1.266602E-03
200.	1.973921E-04	2.446100E-03
500.	4.934802E-04	5.827388E-03
1000.	9.869604E-04	1.121926E-02
2000.	1.973921E-03	2.156748E-02
5000.	4.934802E-03	5.104010E-02
10000.	9.869605E-03	9.772502E-02
20000.	1.973921E-02	1.867397E-01
50000.	4.934802E-02	4.380631E-01
100000.	9.869604E-02	8.325745E-01
200000.	1.973921E-01	1.578046E-00
500000.	4.934802E-01	3.657253E-00
1000000.	9.869604E-01	6.878988E-00

Table 7-1, continued: Comparison of a Representative Impedance Calculation From Approximate and Exact Formulas.

$$R(SEA) = \mathcal{R}_e\, z_{al} = \mathcal{R}_e\, Z_{al}$$

$$X(SEA) = \mathcal{I}_m\, z_{al} = \mathcal{I}_m\, Z_{al}$$

Read 1.23E-04 as 1.23×10^{-4}.

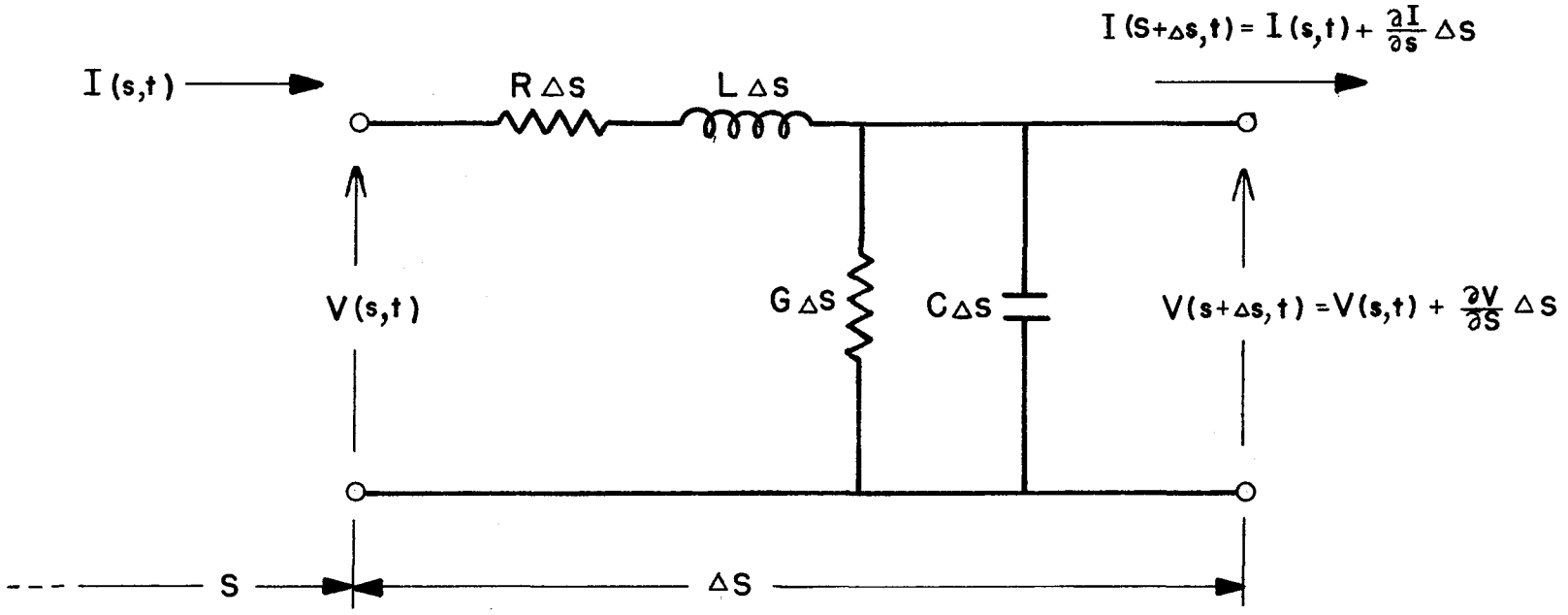

Figure 1-1: Lumped-Circuit Representation of a Small Length of Transmission Line

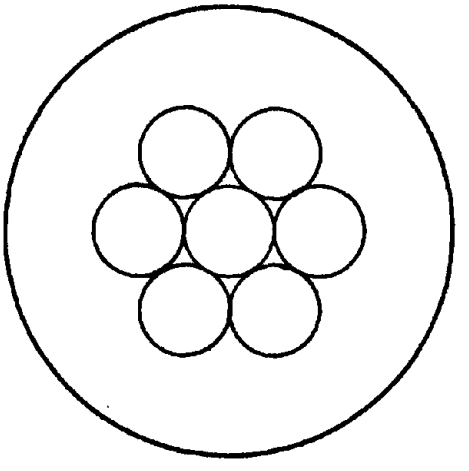

Figure 2-1: Cross-section of a Sea-Return Line. The cable consists of a stranded copper center conductor surrounded by a dielectric. When immersed, the surrounding sea forms the outer conductor.

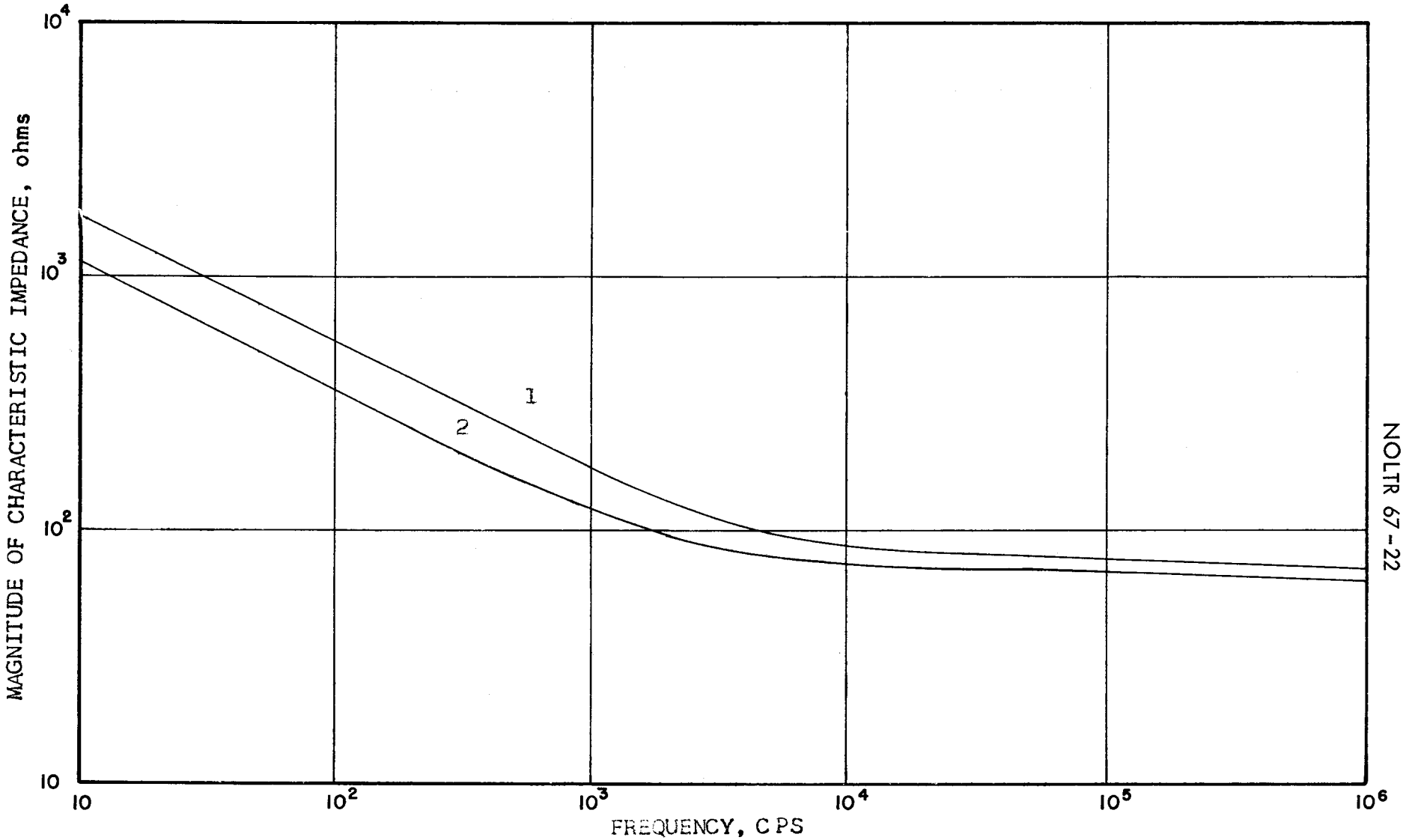

Figure 2-2: Comparison of Characteristic Impedence of Two Miniature Sea-Return Lines. 1--Smaller diameter. 2--Larger diameter.

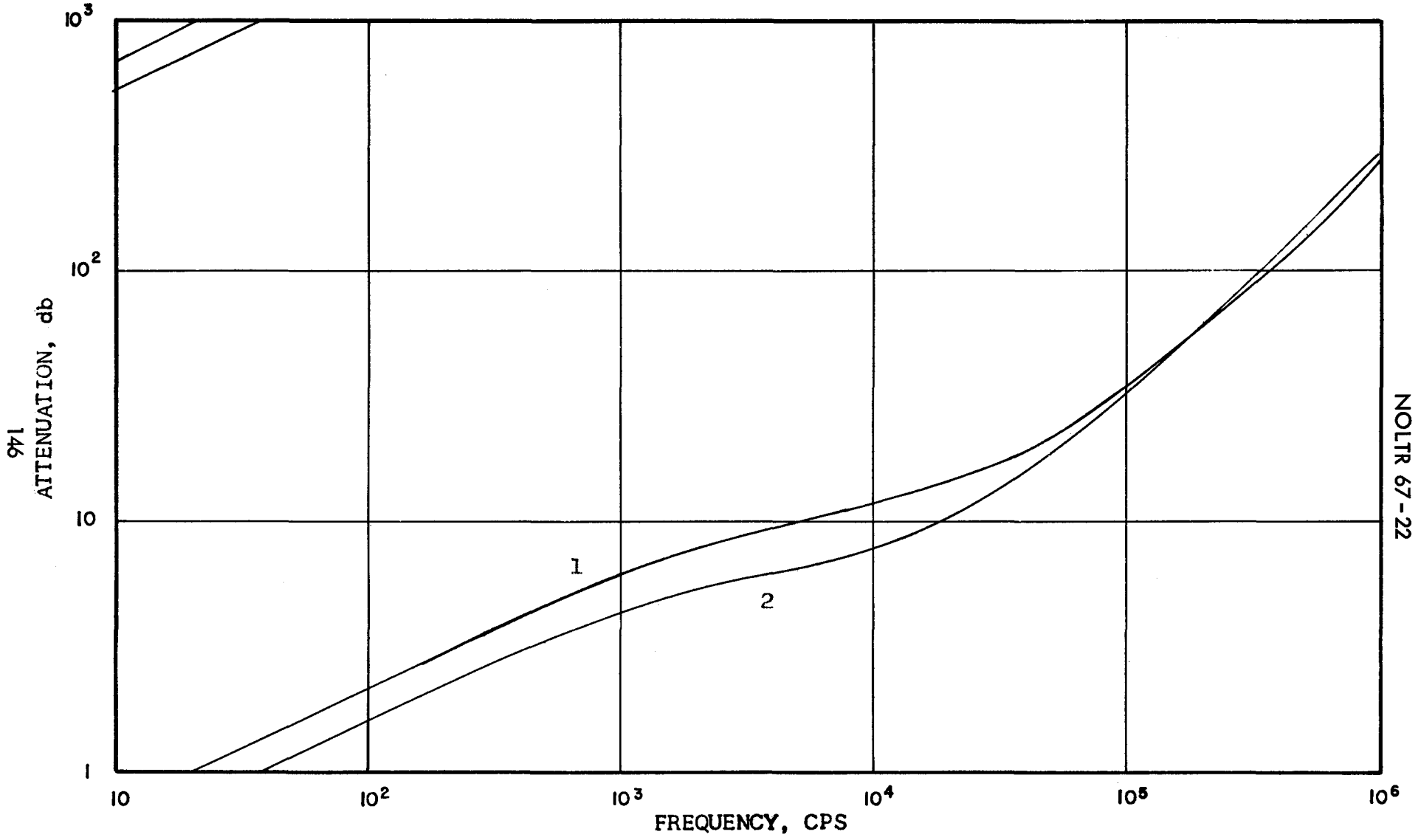

Figure 2-3: Comparison of Insertion Loss of Two Miniature Sea-Return Lines. Figures based on a line length of 4 kilometers. 1--Smaller diameter. 2--Larger diameter.

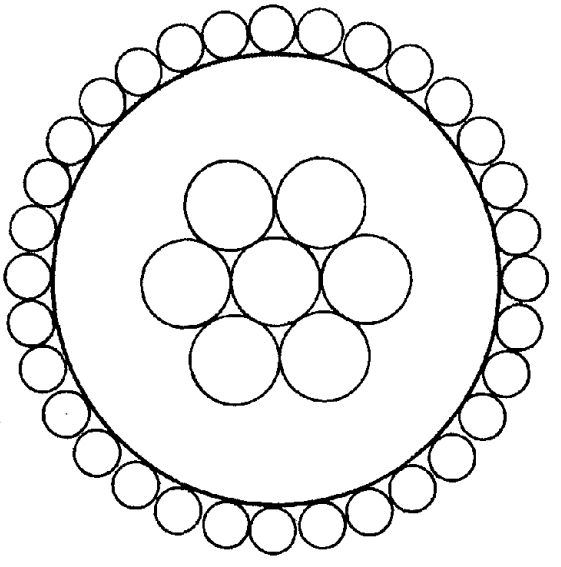

Figure 3-1: Cross-section of One Type of Coaxial Cable. The inner and outer conductors, which are separated by a dielectric, are made up of strands of bare wire in contact throughout their length.

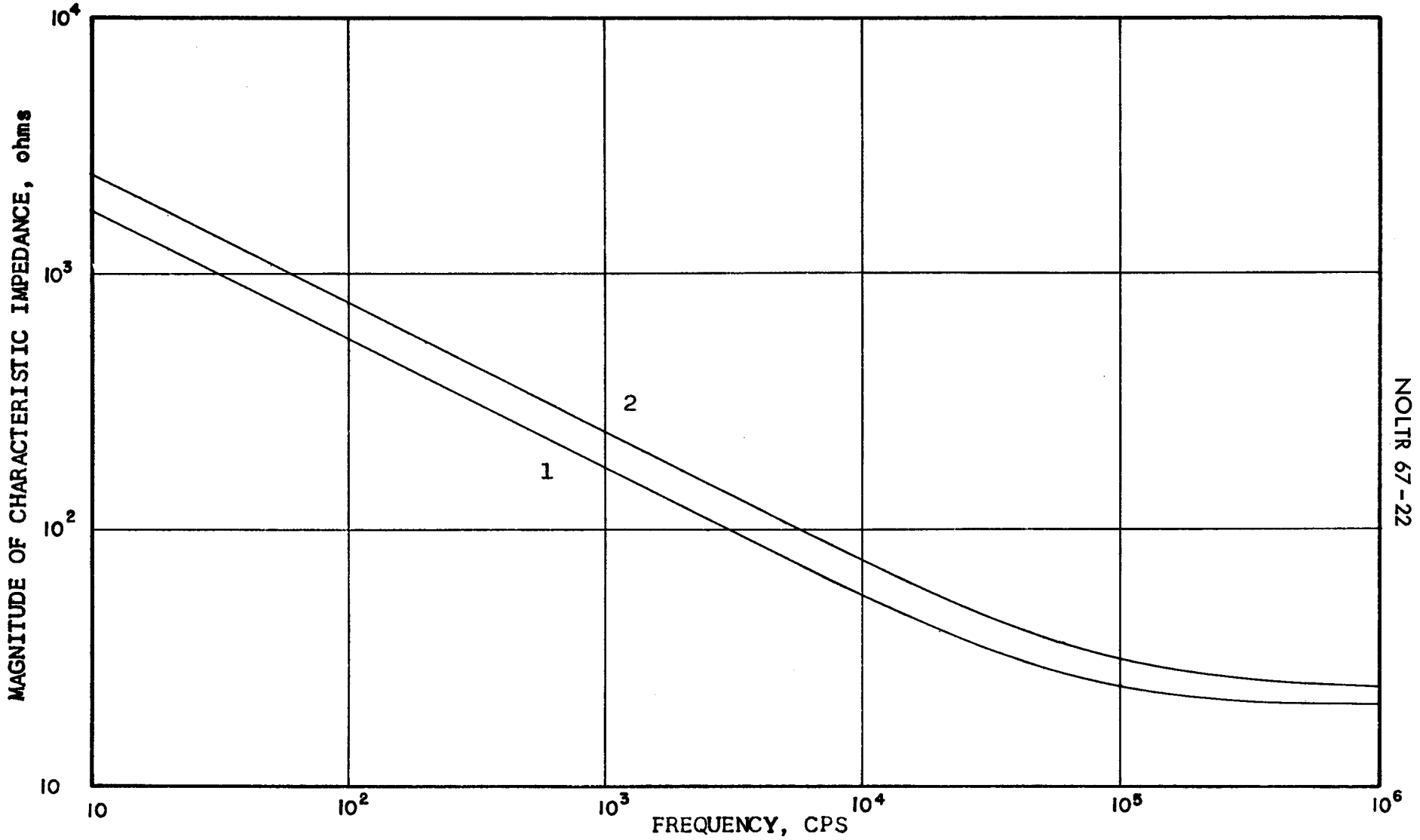

Figure 3-2: Comparison of Characteristic Impedance of Two Miniature Coaxial Cables. 1--Smaller diameter. 2--Larger diameter.

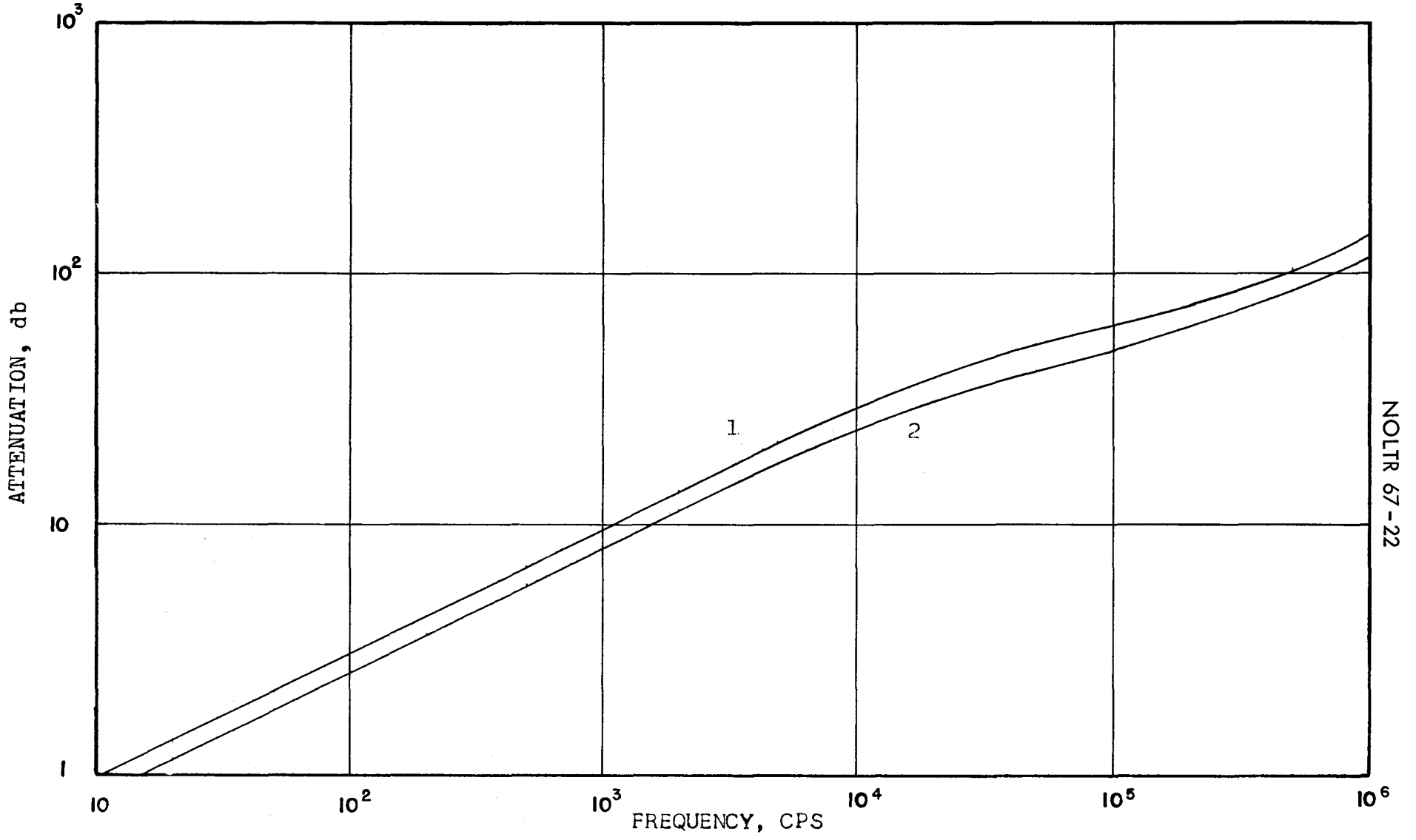

Figure 3-3: Comparison of Insertion Loss of Two Miniature Coaxial Cables. Figures based on a line length of 4 kilometers. 1--Smaller diameter. 2--Larger diameter.

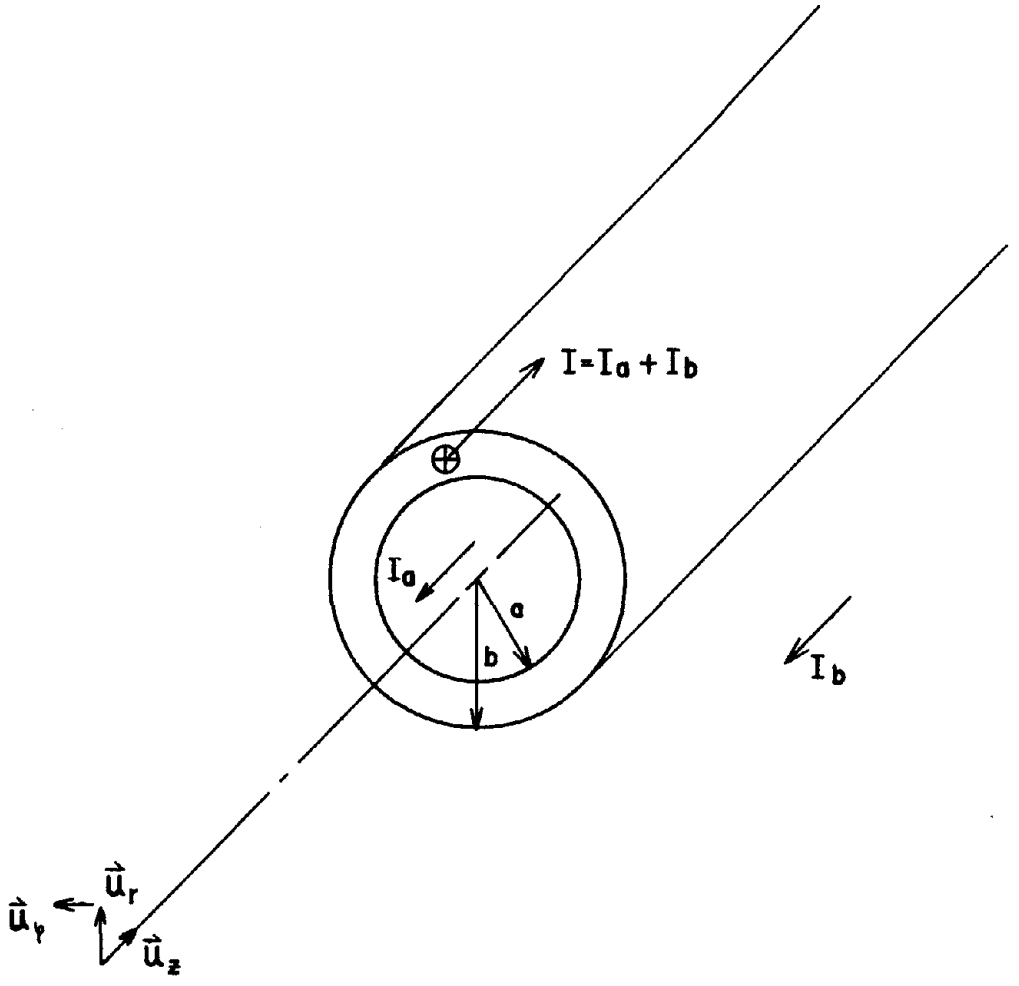

Figure 4-1: Cross-section of a Tubular Conductor, Showing Current Flow. In the positive z-direction, current flows within the material of the tube. The return paths are arbitrary, except for the constraint that I_a flows inside, and I_b outside, the tube.

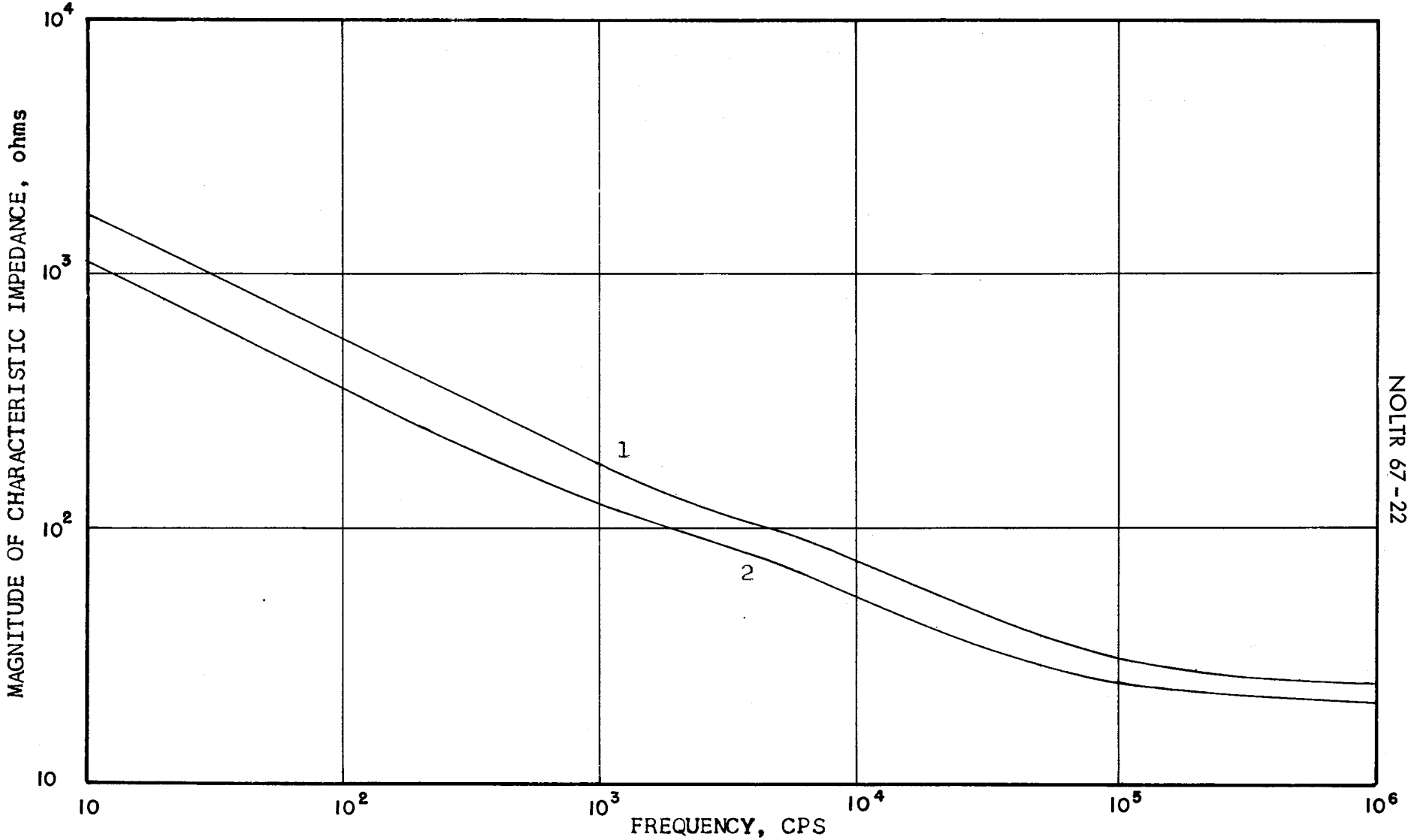

Figure 4-2: Comparison of Characteristic Impedance of Two Miniature Coaxial Cables Immersed in Seawater. 1--Smaller diameter. 2--Larger diameter.

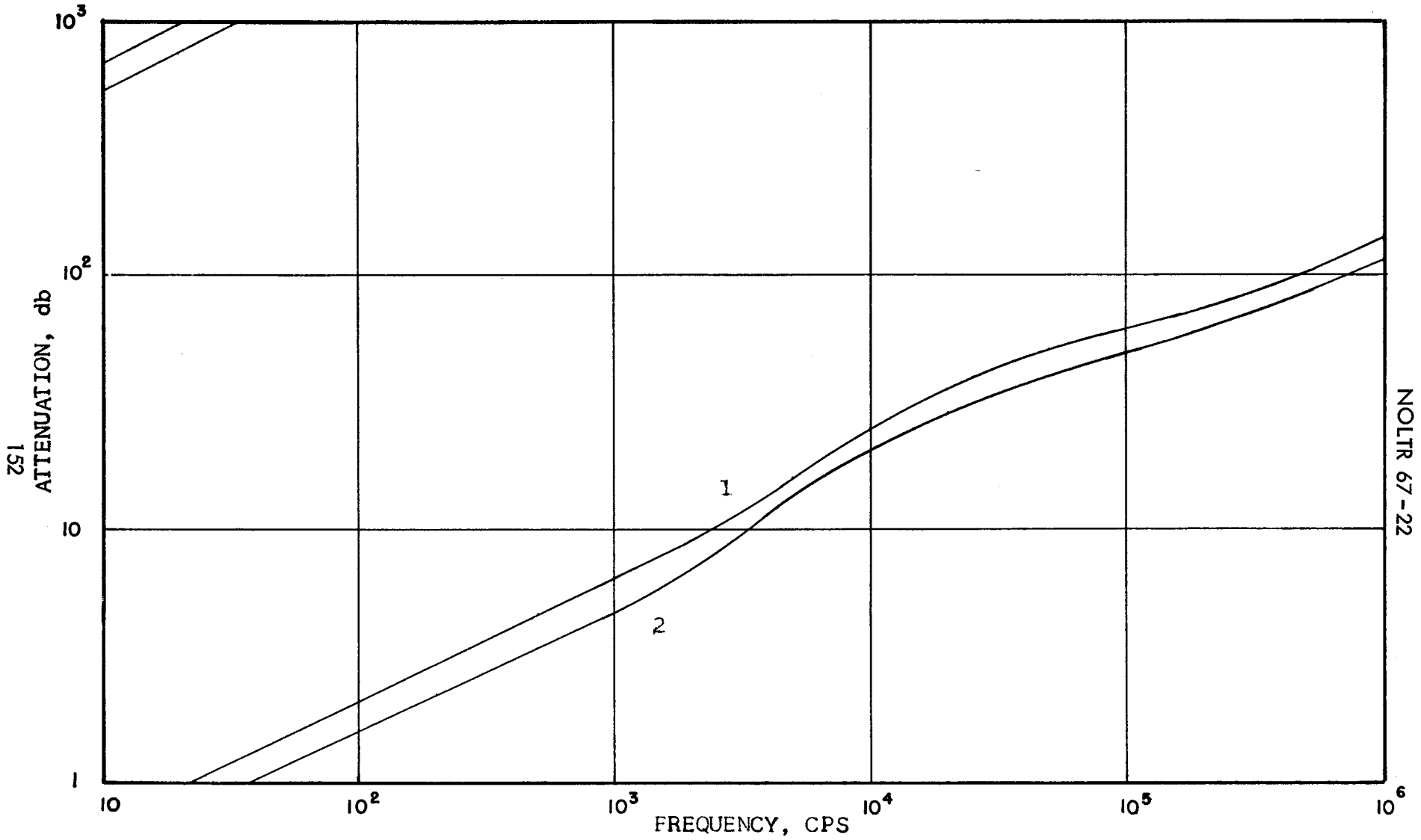

Figure 4-3: Comparison of Insertion Loss of Two Miniature Coaxial Cables Immersed in Seawater.
Figures based on a line length of 4 kilometers.
1--Smaller diameter. 2--Larger diameter.

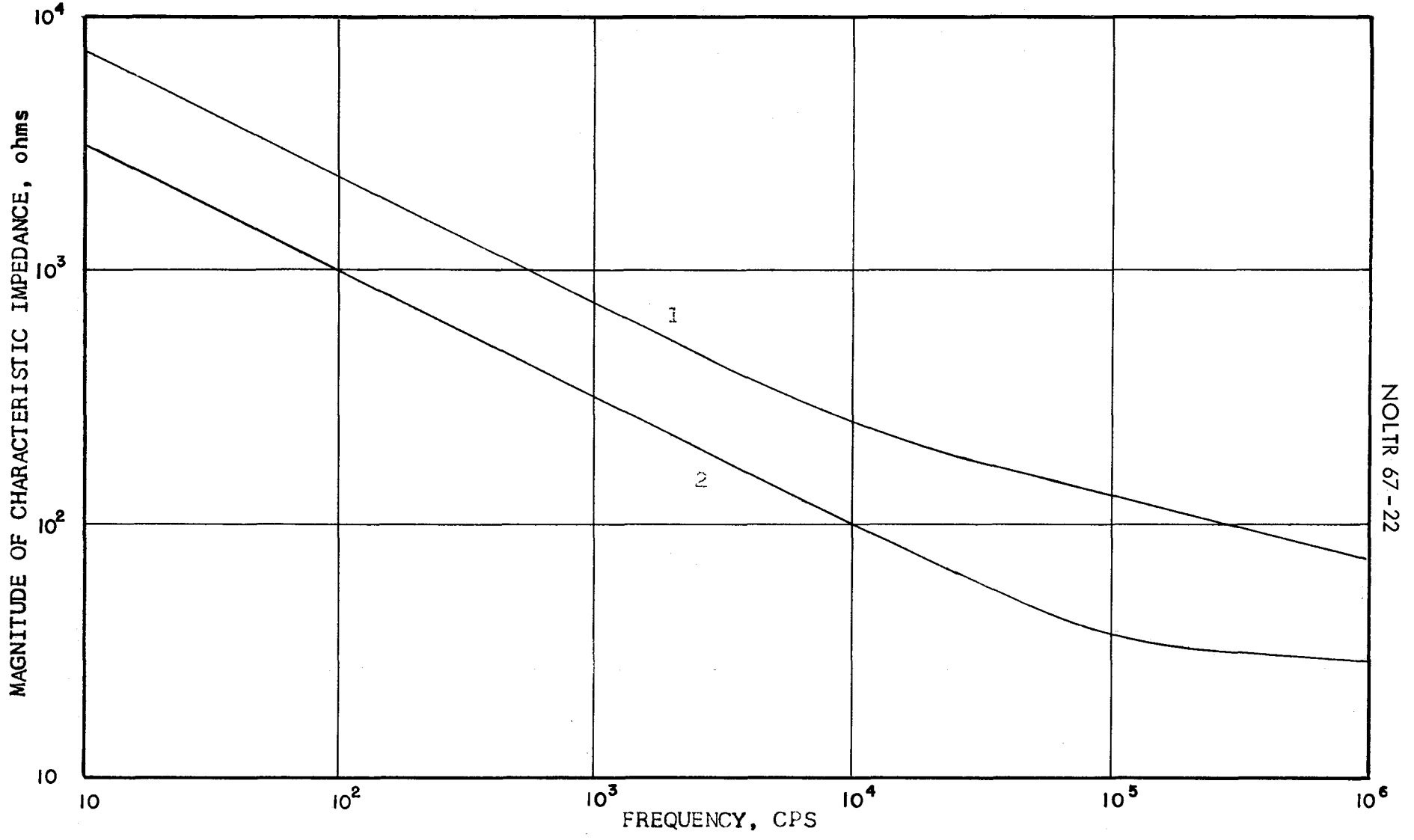

Figure 5-1: Characteristic Impedance of a Miniature Coaxial Cable Having a Steel Core. 1--Steel-core cable. 2--Corresponding all-copper cable.

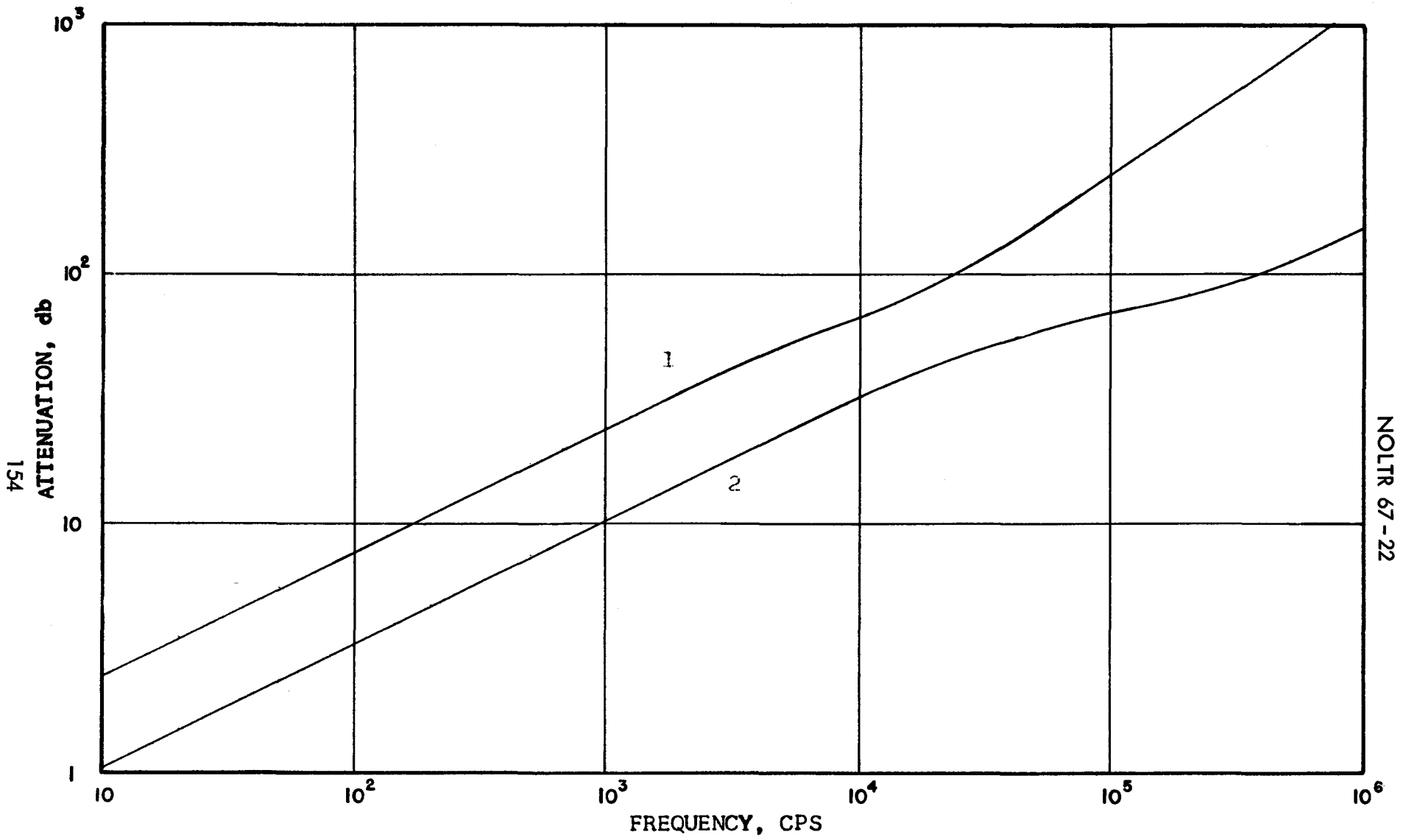

Figure 5-2: Insertion Loss of a Miniature Coaxial Cable Having a Steel Core. Figures based on a line length of 4 kilometers. 1--Steel-core cable. 2--Corresponding all-copper line.

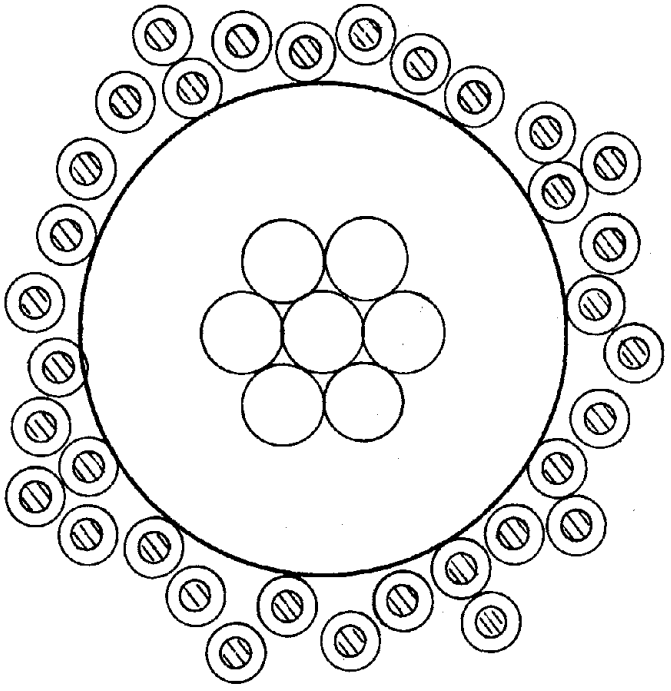

Figure 5-3: Cross-section of a Miniature Coaxial Cable With a Bimetal Braid. The outer conductor is a woven braid in which each strand consists of a steel core covered with a copper jacket. The center conductor is copper, the dielectric polyethylene.

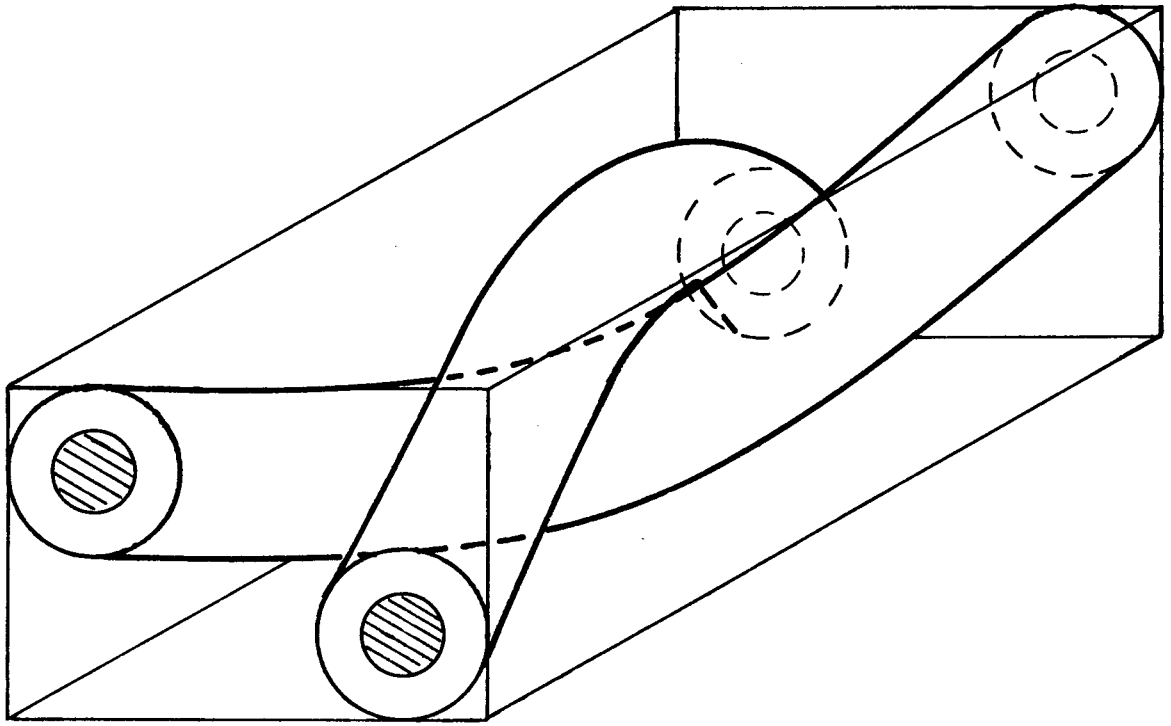

Figure 5-4: Simplified Representation of a Small Section of a Woven Braid. The strands shown are copper-covered steel.

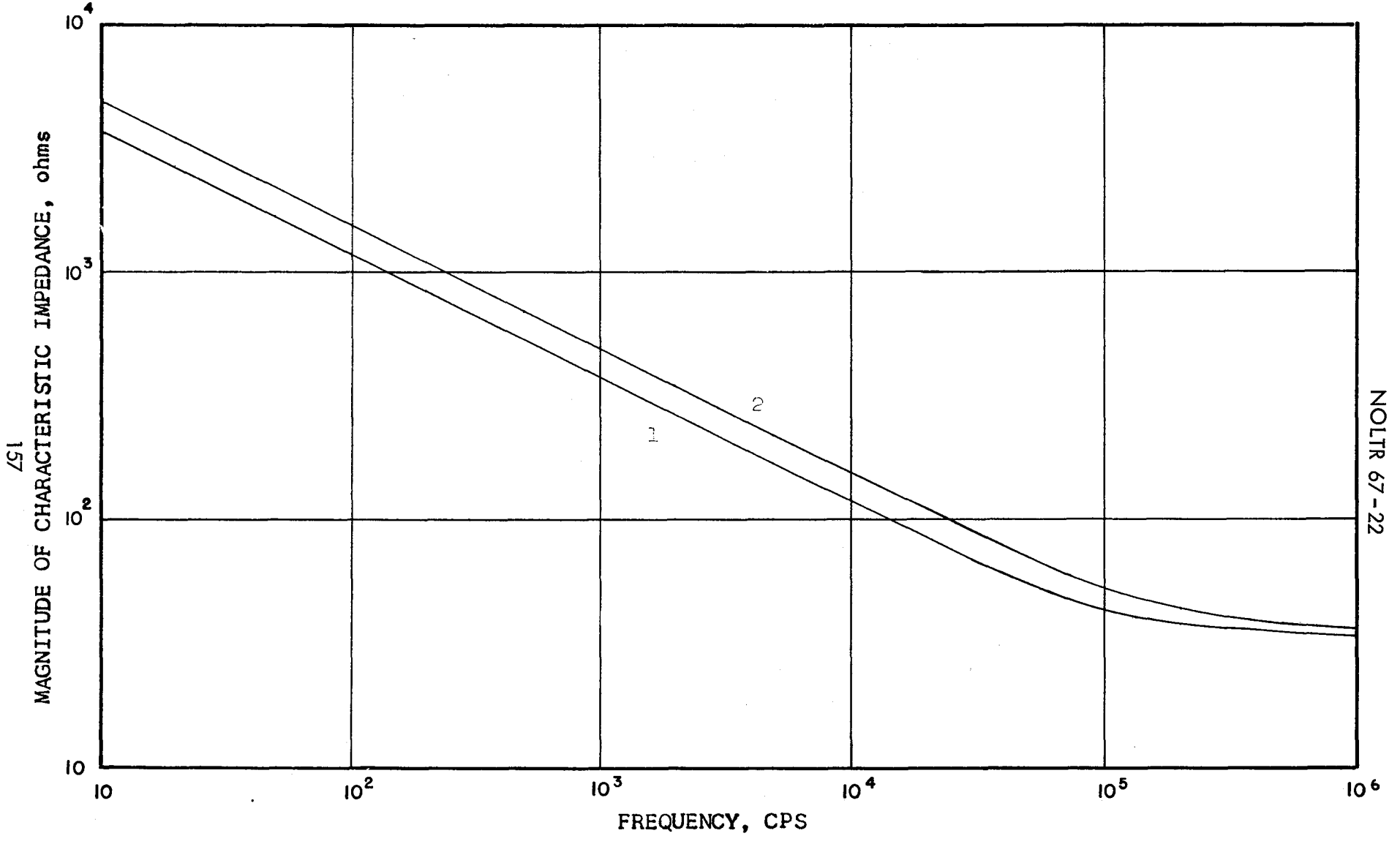

Figure 5-5: Characteristic Impedance of a Miniature Coaxial Cable Having a Bimetal Woven Braid. 1--Bimetal braid. 2--Corresponding cable with all-copper braid.

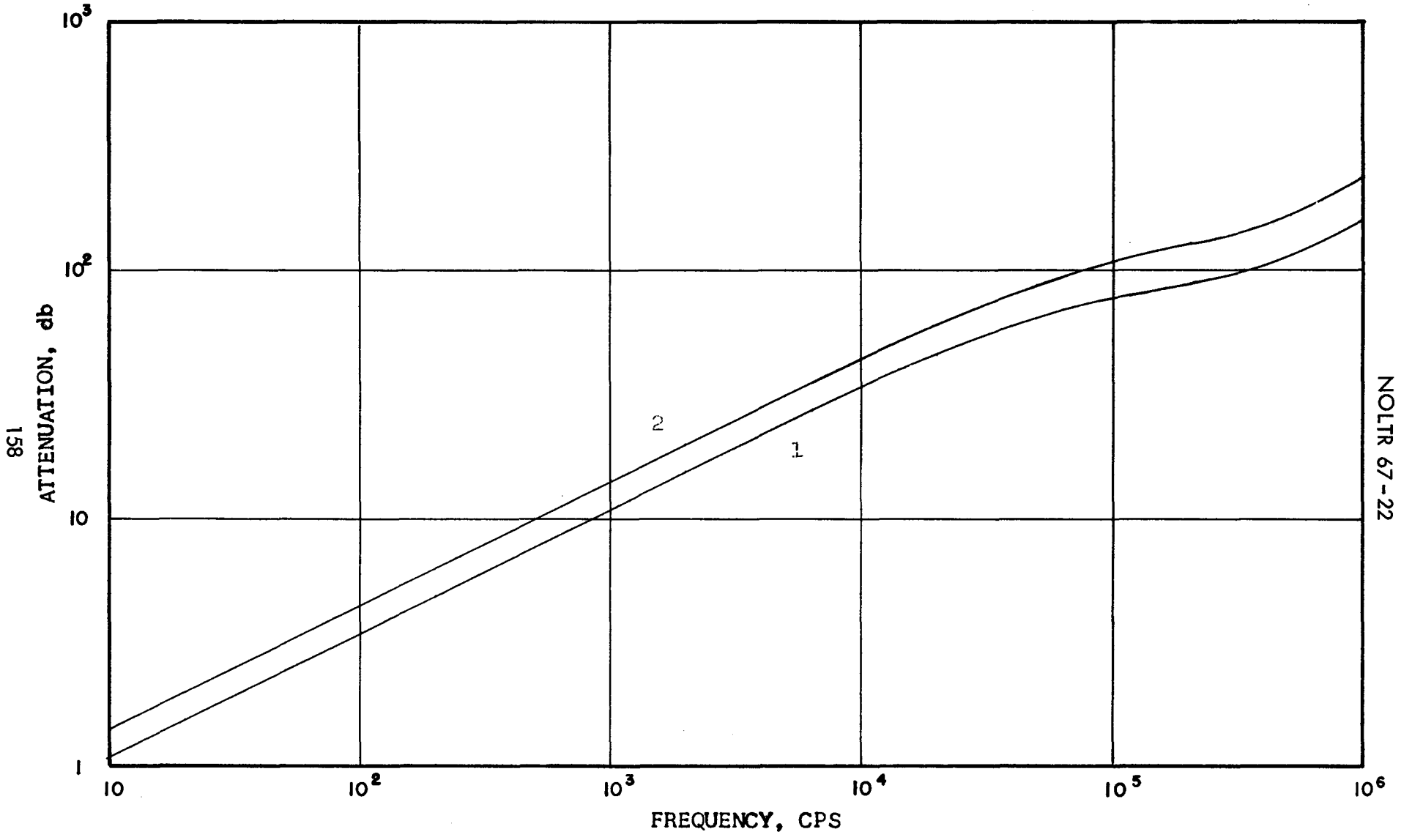

Figure 5-6: Insertion Loss of a Miniature Coaxial Cable Having a Bimetal Woven Braid. Figures based on a line length of 4 kilometers. 1--Bimetal braid. 2--Corresponding cable with all-copper braid.

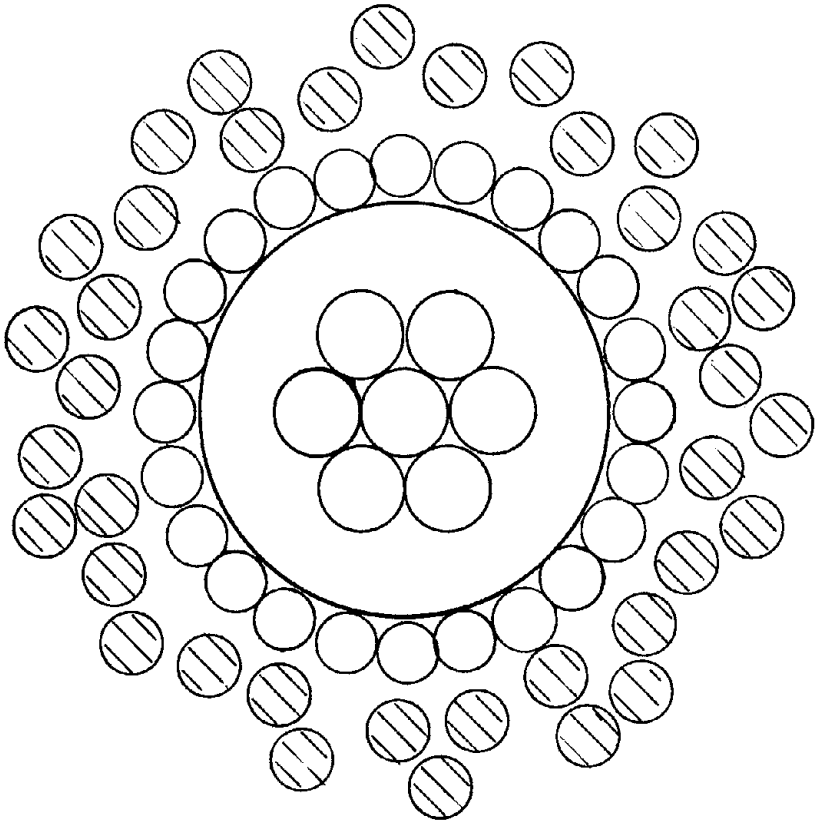

Figure 5-7: Cross-section of a Miniature Coaxial Cable Having a Steel Overbraid. The strands of the center conductor and inner shield are copper. Strands of the overlying braid (shown cross-hatched) are steel.

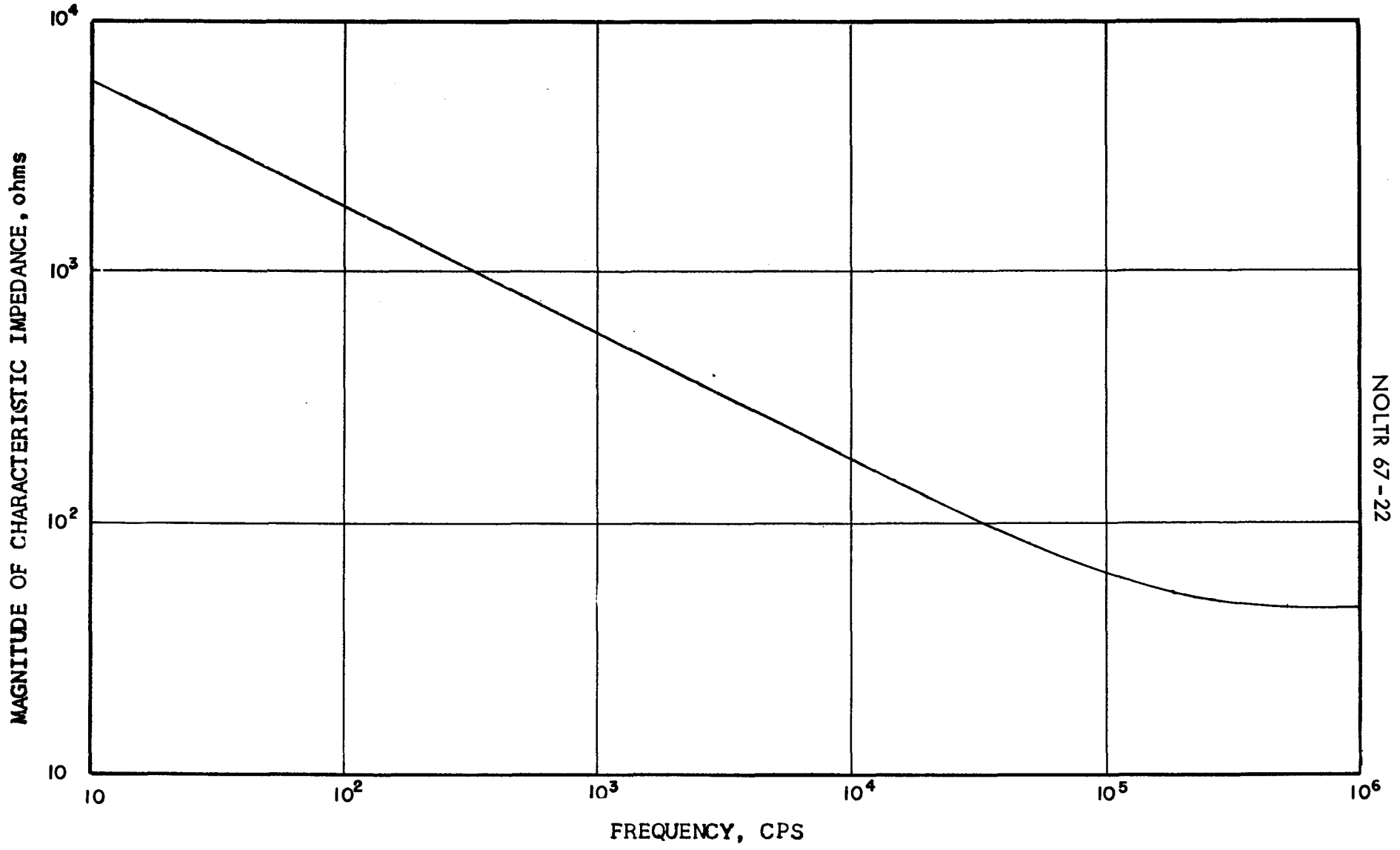

Figure 5-8: Characteristic Impedance of a Miniature Cable With and Without a Steel Overbraid. Curves are coincident.

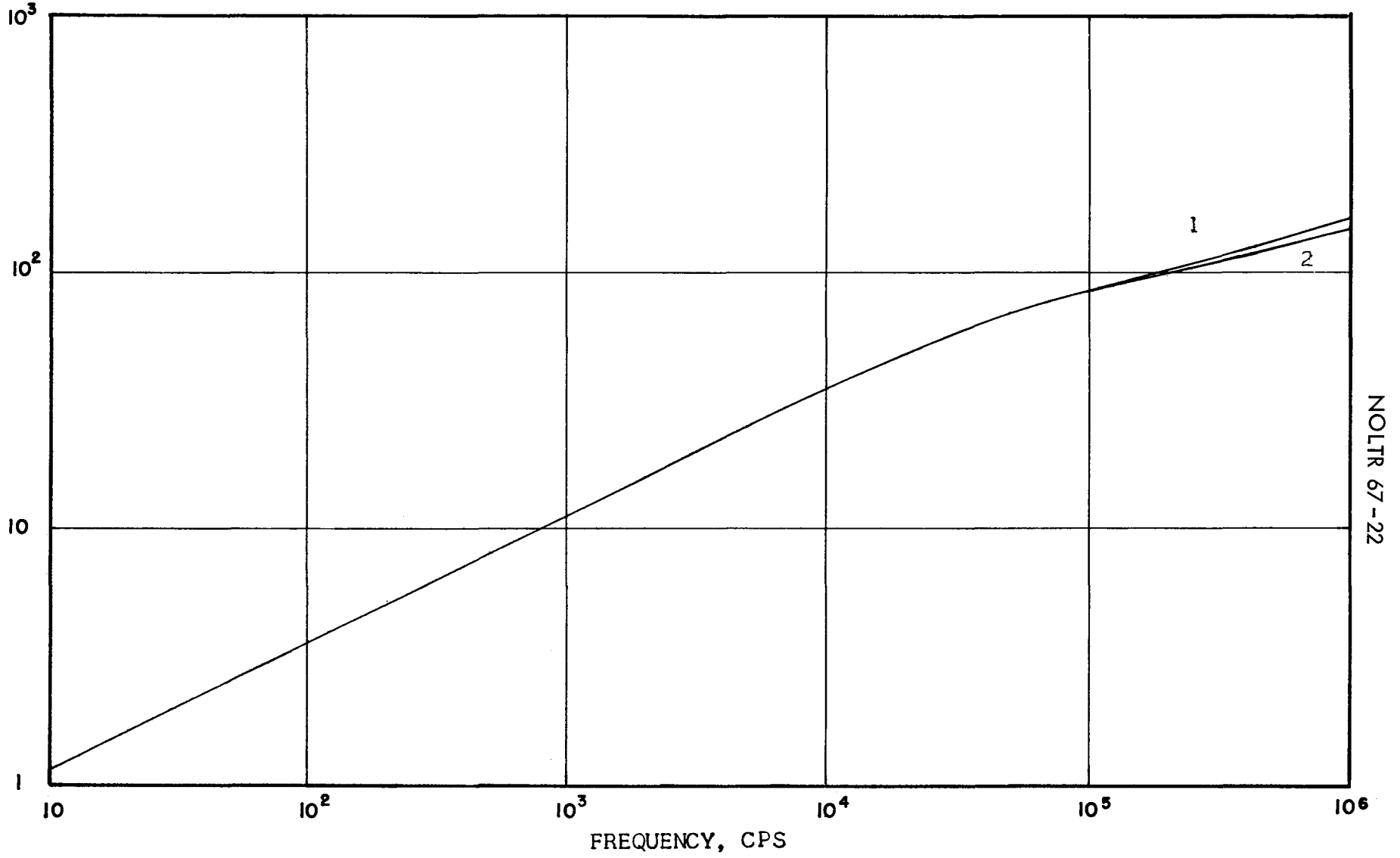

Figure 5-9: Comparison of Insertion Loss of Two Miniature Coaxial Cables. Figures based on a line length of 4 kilometers. 1--With steel overbraid. 2--Without steel overbraid.

1. The miniature coaxial line considered is the all-copper cable corresponding to the bimetal braid configuration of Chapter V, Section B.
2. The waveforms shown are Fourier reconstructions of two repetitive patterns of non-return-to-zero digital data at a rate of 400 kilobits per second. The first pattern is a "one" followed by 19 "zeros" (denoted 10_{19}). The second is "one-zero-one" followed by 17 "zeros" (1010_{17}).
3. All plots are drawn to the same physical size. Since the dc component is not considered, all magnitudes are scaled such that the maximum excursion from the x-axis occupies four divisions as marked on the vertical axis.
4. The number appearing at the upper right of each plot is the amplitude of the maximum excursion from the x-axis (<u>not</u> the maximum peak-to-peak excursion). Hence each vertical division is one-fourth of this amount. Read "TXP" as "times 10 to the power." An input signal of one volt peak-to-peak is assumed.
5. Since the 20-bit pattern runs at a 400 kbps rate, the fundamental Fourier component frequency is 20 KC. Each mark on the horizontal axis sets off one-sixth of a cycle of this component ($\pi/3$ radians) or, for this

Figure 6-1: Notes for Figures 6-2 through 6-12.

specific case, 8.33 μsec. No attempt should be made to correlate horizontal divisions with bit width, which is 2.5 μsec.

Figure 6-1, continued: Notes for Figures 6-2 through 6-12.

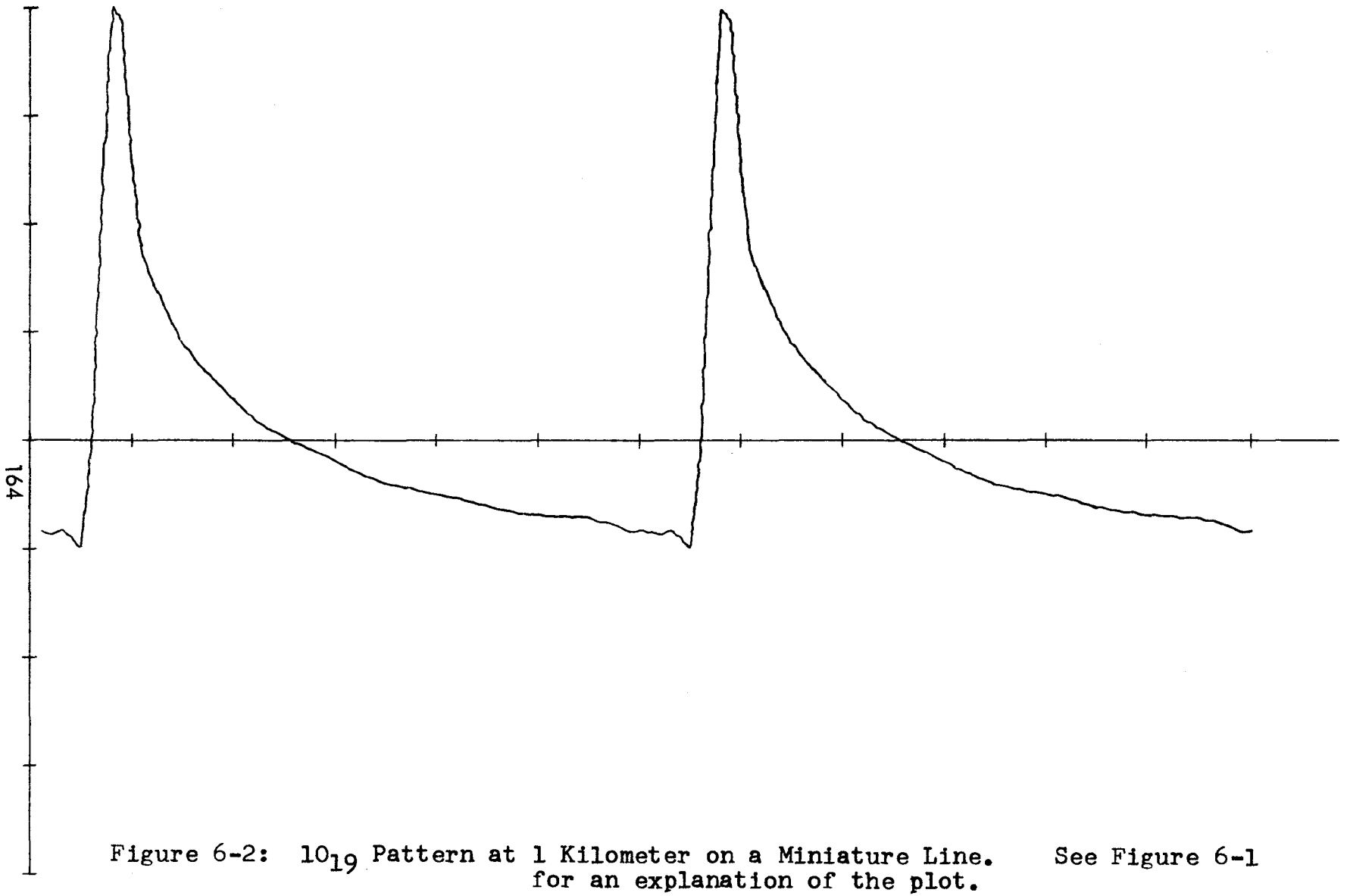

Figure 6-2: 10_{19} Pattern at 1 Kilometer on a Miniature Line. See Figure 6-1 for an explanation of the plot.

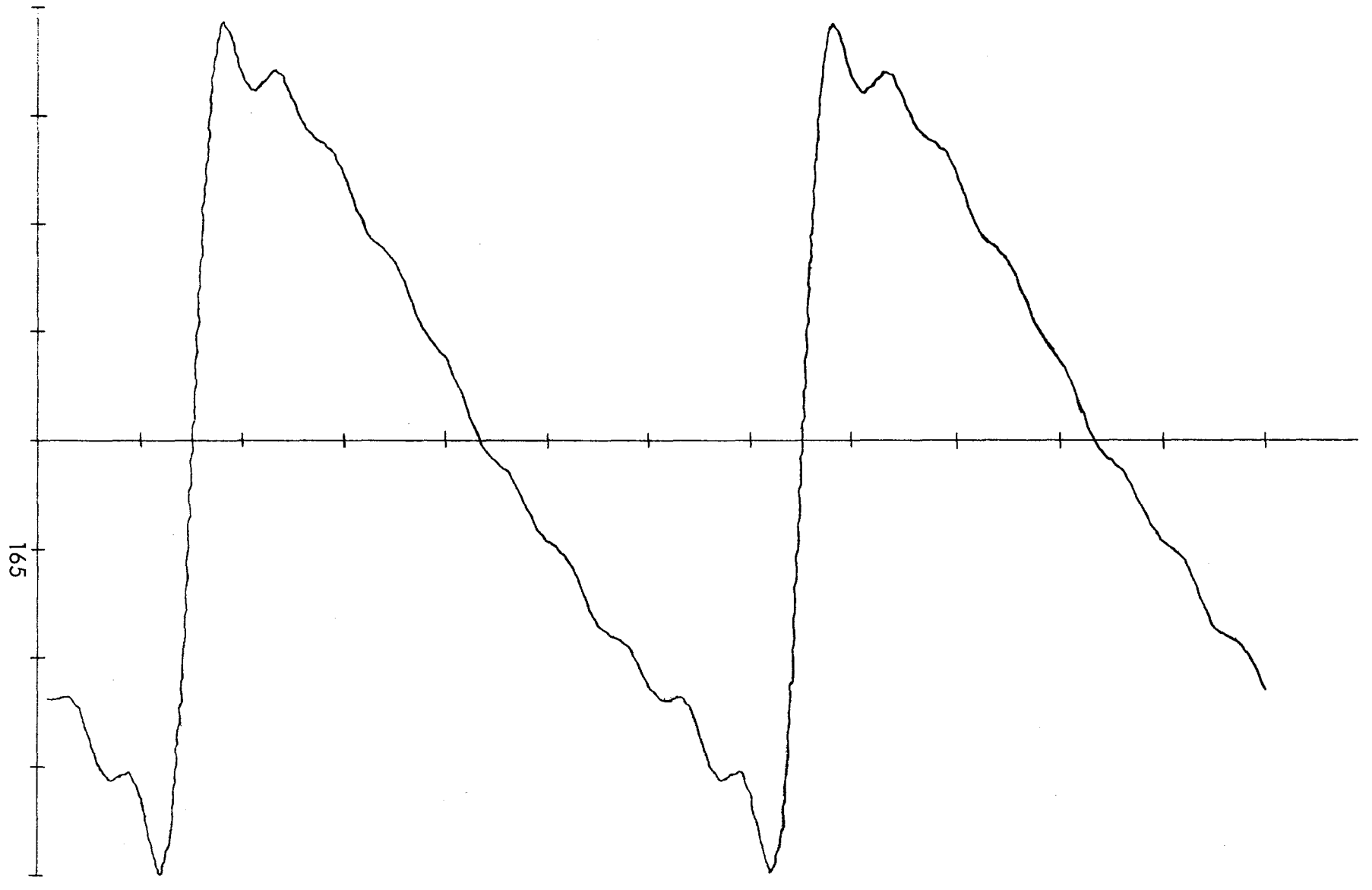

Figure 6-3: 10_{19} Pattern at 2 Kilometers on a Miniature Line. See Figure 6-1 for an explanation of the plot.

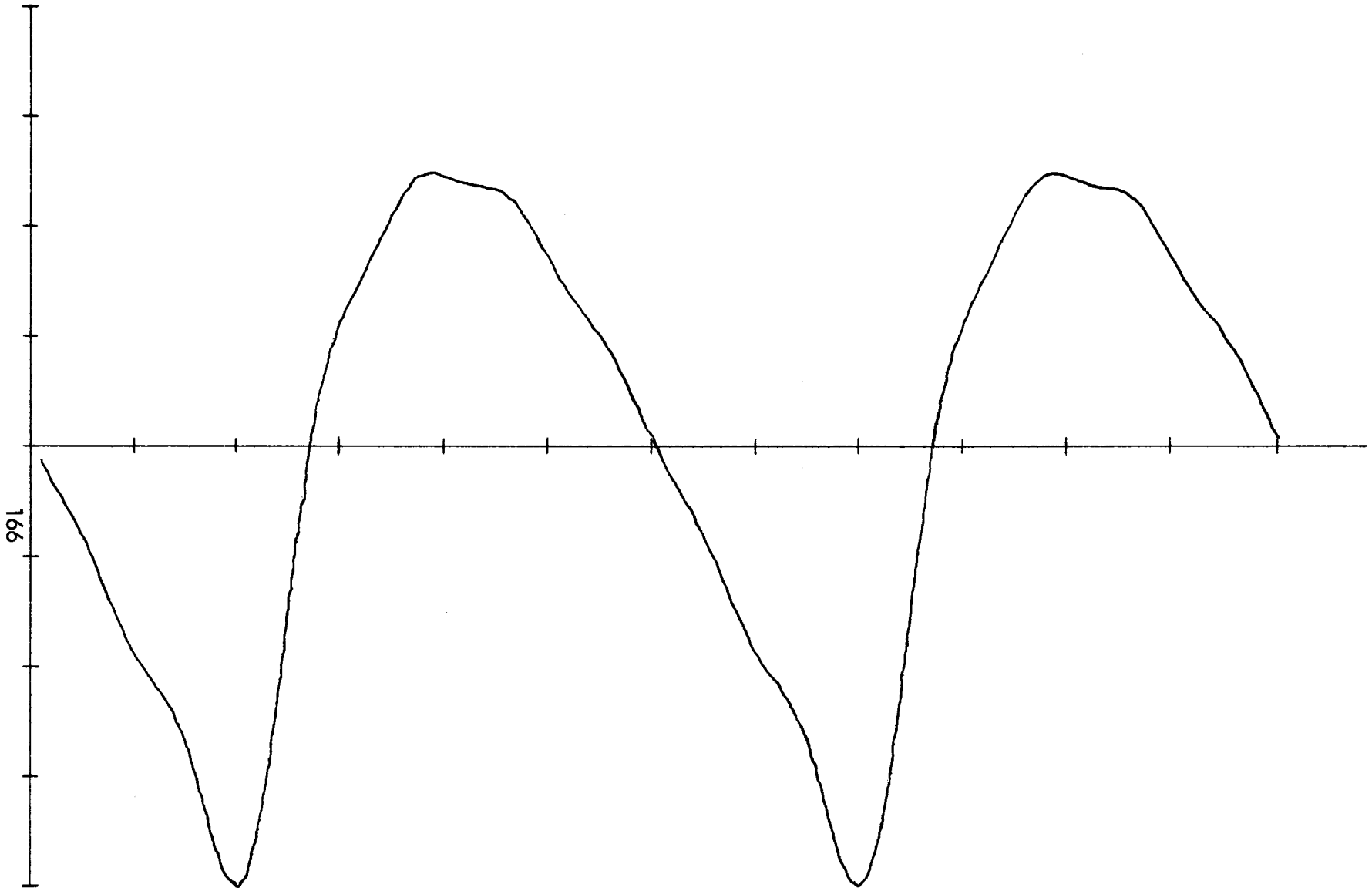

Figure 6-4: 10_{19} Pattern at 3 Kilometers on a Miniature Line. See Figure 6-1 for an explanation of the plot.

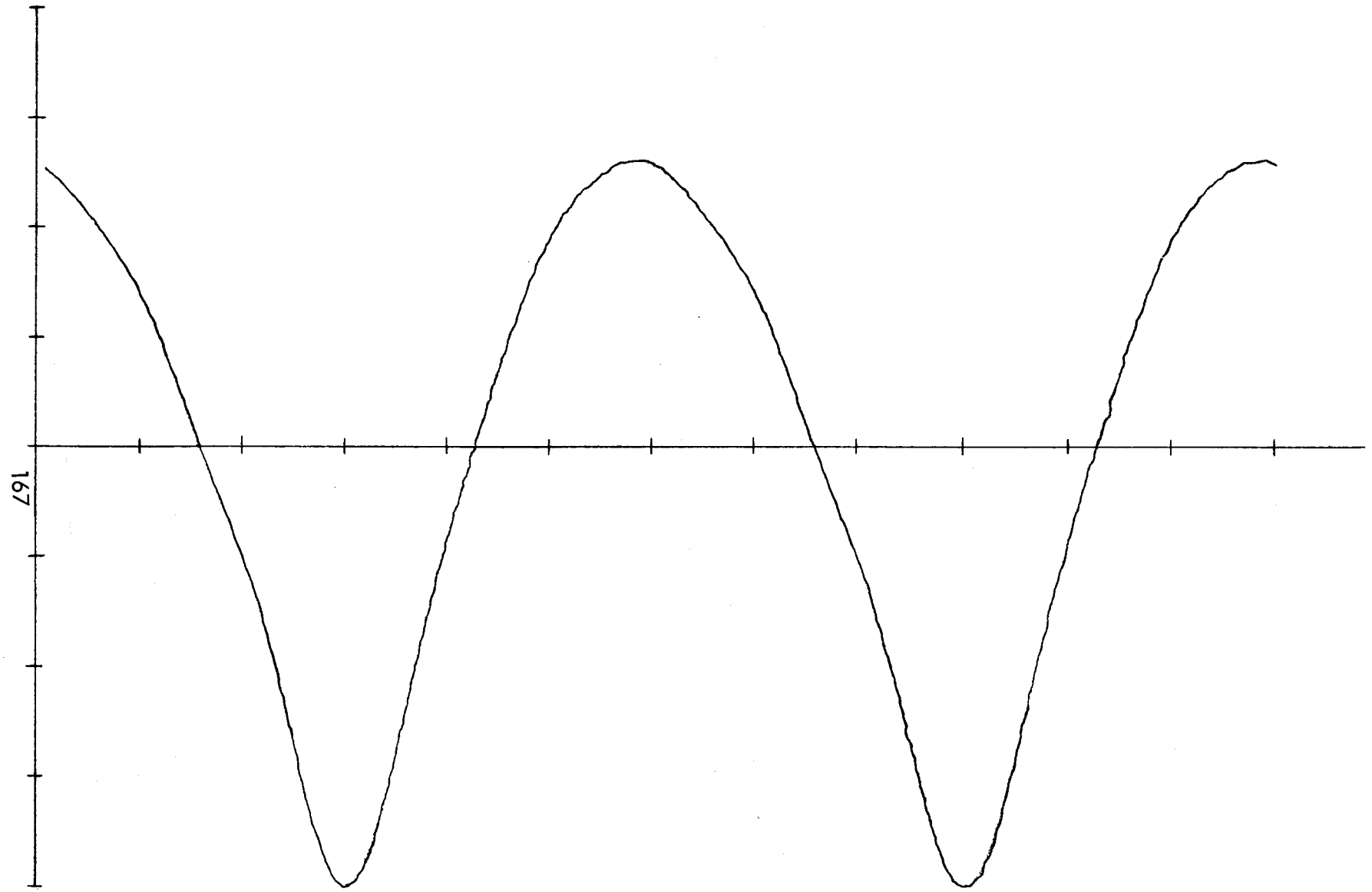

Figure 6-5: 10_{19} Pattern at 4 Kilometers on a Miniature Line, Unequalized. See Figure 6-1 for an explanation of the plot.

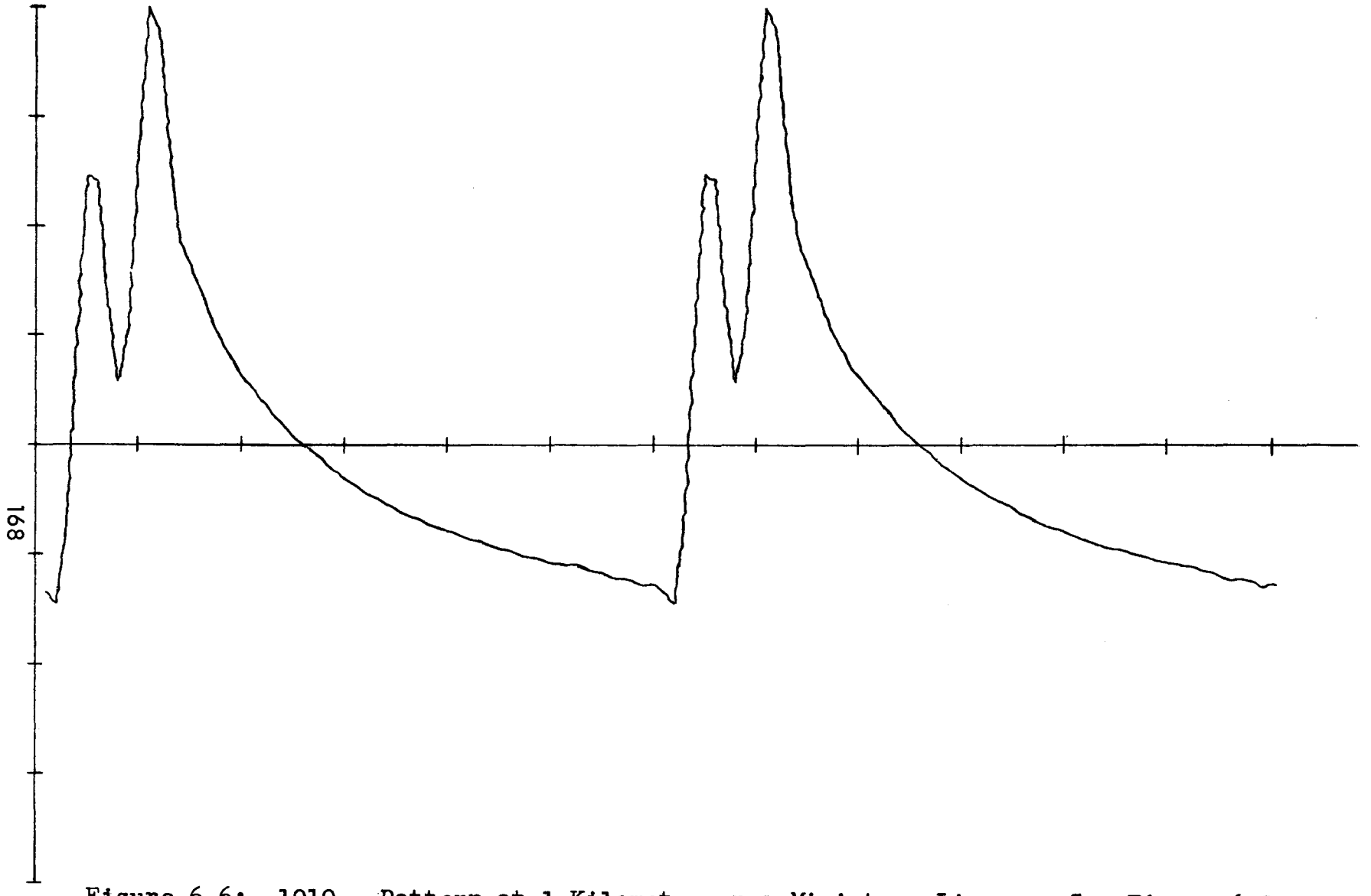

Figure 6-6: 1010_{17} Pattern at 1 Kilometer on a Miniature Line. See Figure 6-1 for an explanation of the plot.

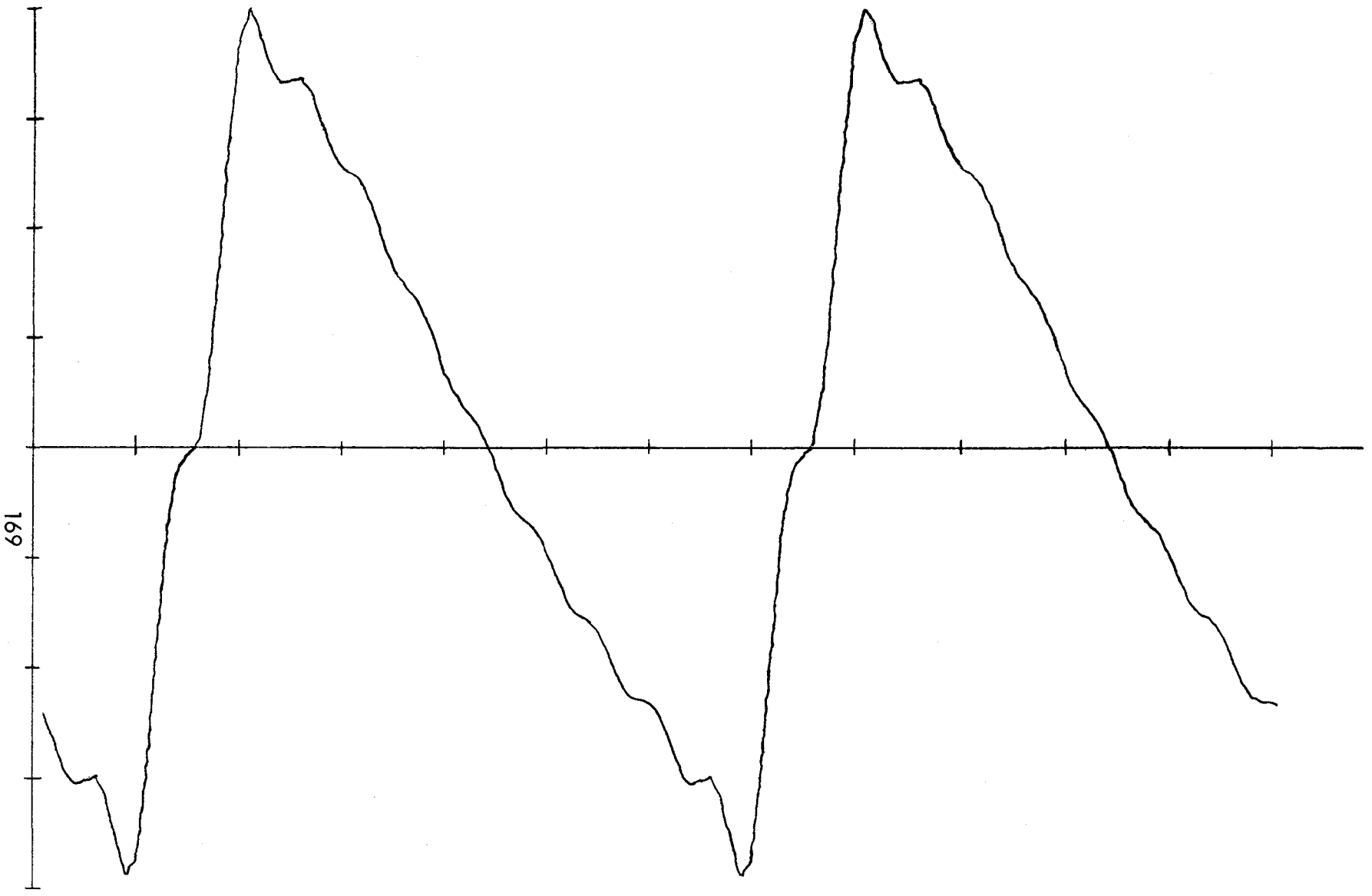

Figure 6-7: 1010_{17} Pattern at 2 Kilometers on a Miniature Line. See Figure 6-1 for an explanation of the plot.

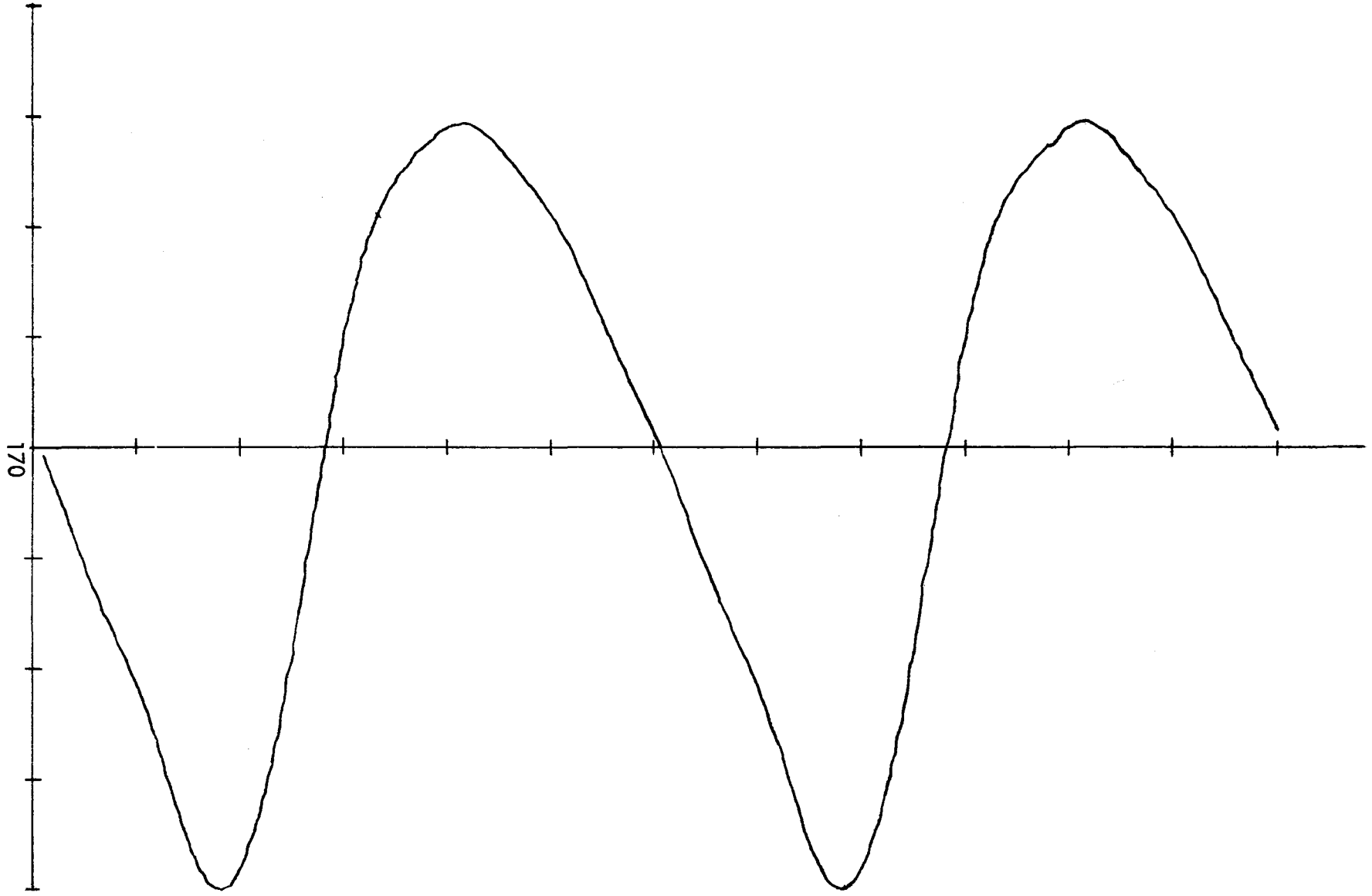

Figure 6-8: 1010_{17} Pattern at 3 Kilometers on a Miniature Line. See Figure 6-1 for an explanation of the plot.

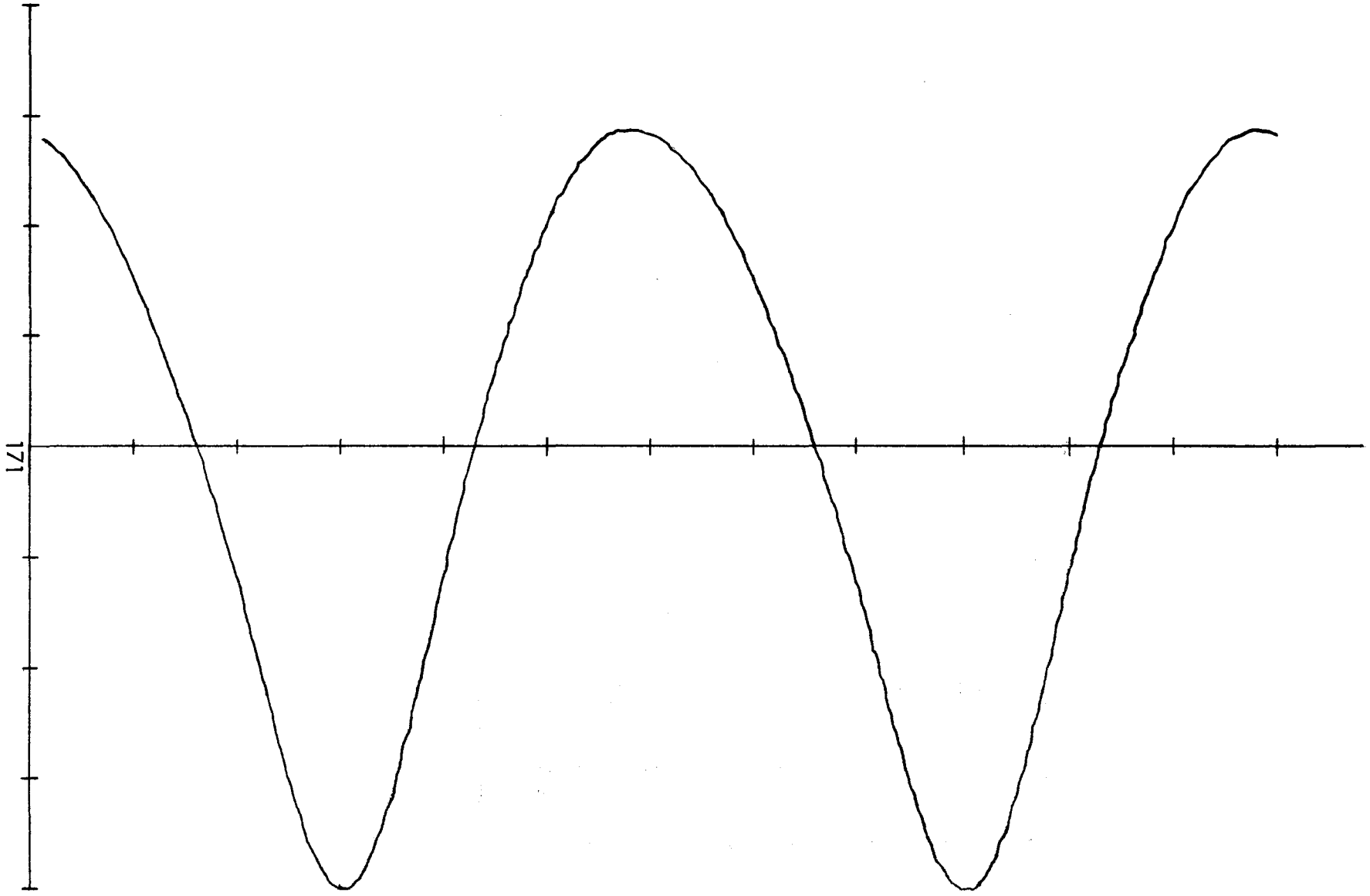

Figure 6-9: 1010_{17} Pattern at 4 Kilometers on a Miniature Line, Unequalized. See Figure 6-1 for an explanation of the plot.

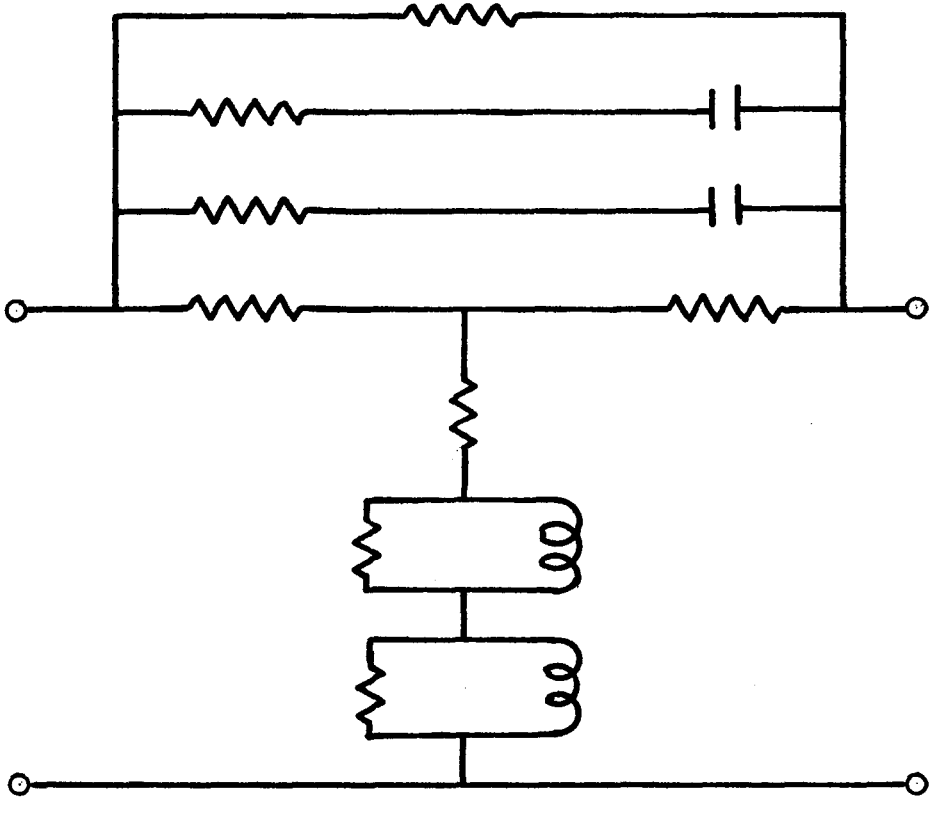

Figure 6-10: Circuit Diagram of a Bridged-Tee Equalizer Section

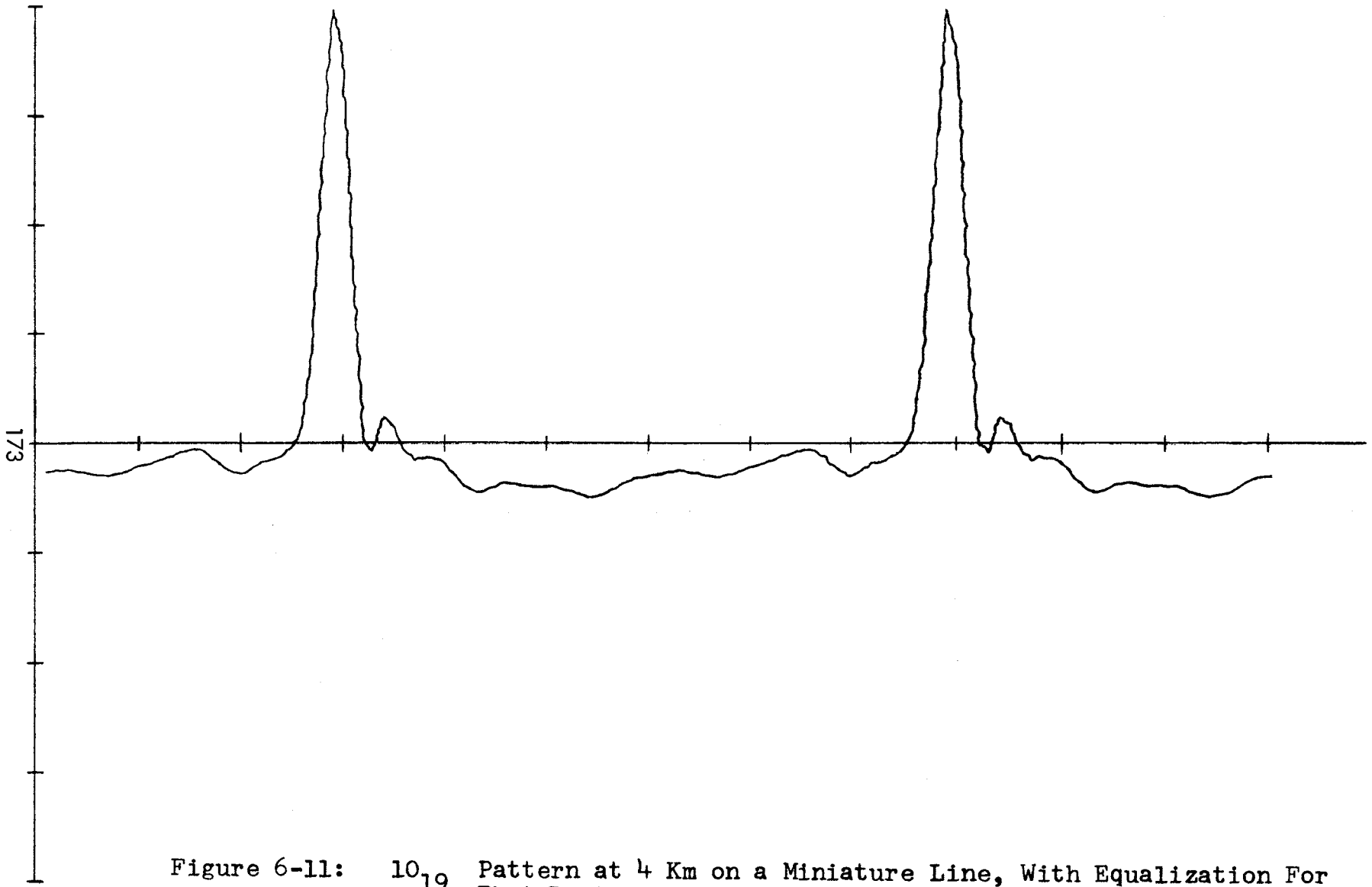

Figure 6-11: 10_{19} Pattern at 4 Km on a Miniature Line, With Equalization For That Distance. See Figure 6-1 for an explanation of the plot.

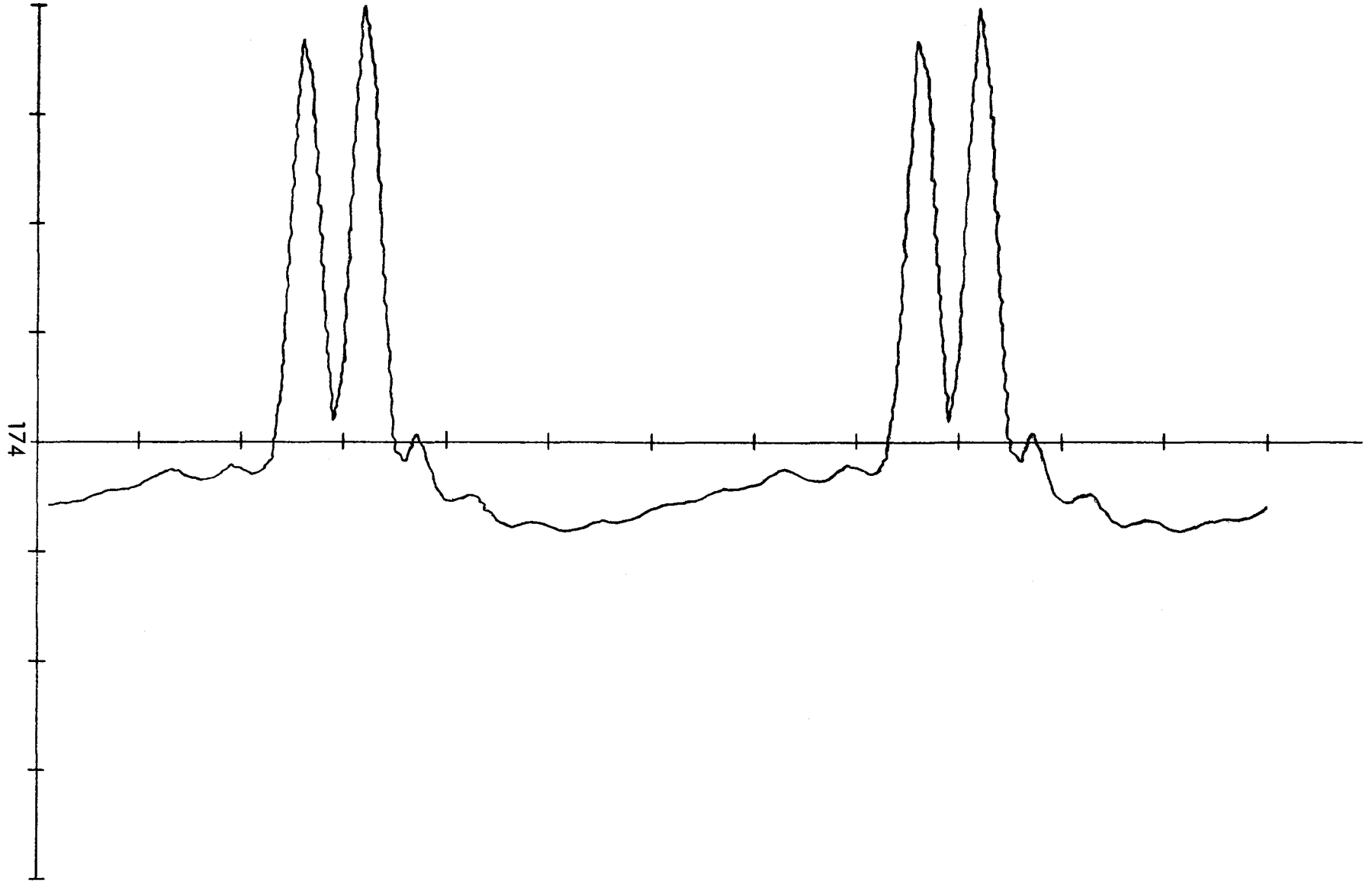

Figure 6-12: 1010_{17} Pattern at 4 Km on a Miniature Line, With Equalization For That Distance. See Figure 6-1 for an explanation of the plot.

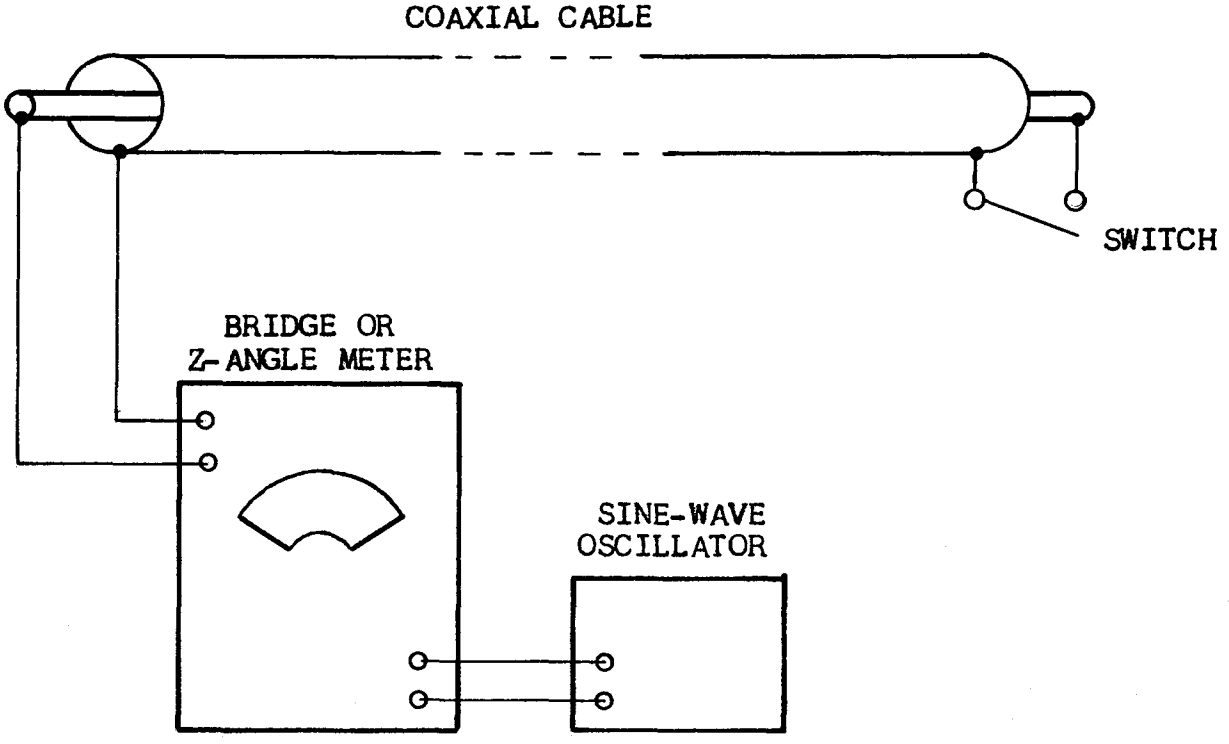

Figure 7-1: Diagram of Method Used to Measure Characteristic Impedance

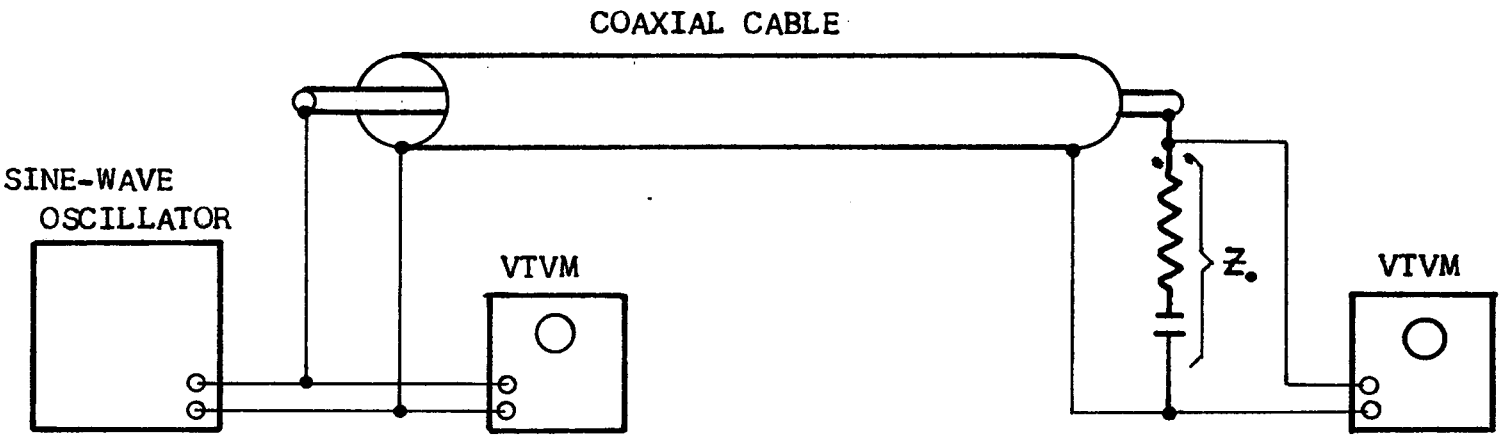

Figure 7-2: Diagram of Method Used to Measure Attenuation

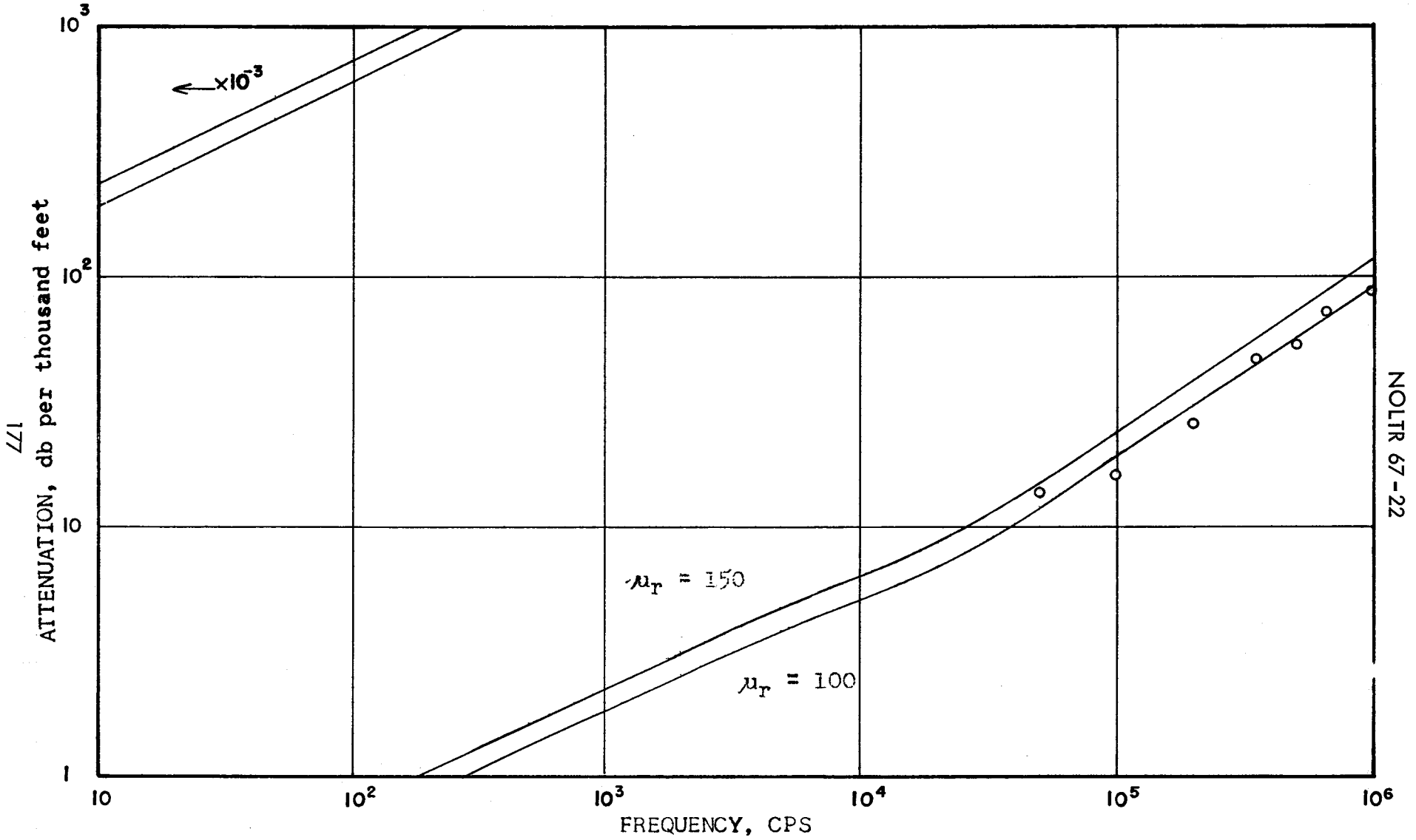

Figure 7-3: Comparison of Experimental and Predicted Attenuation of a Miniature Steel-Cored Cable. Curves based on two estimated values of μ_r .

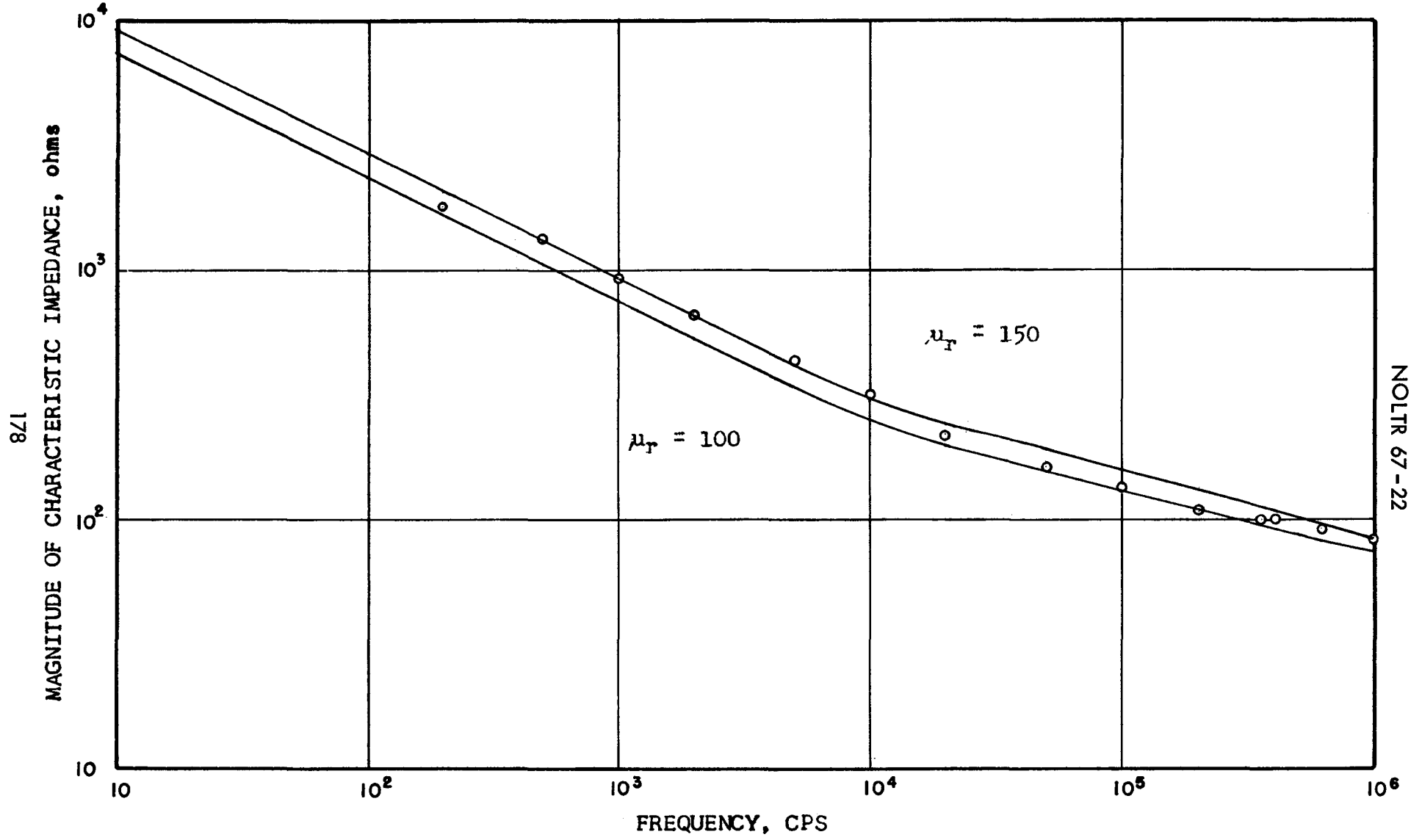

Figure 7-4: Comparison of Experimental and Predicted Characteristic Impedance of a Miniature Steel-Cored Cable. Curves based on two estimated values of μ_r.

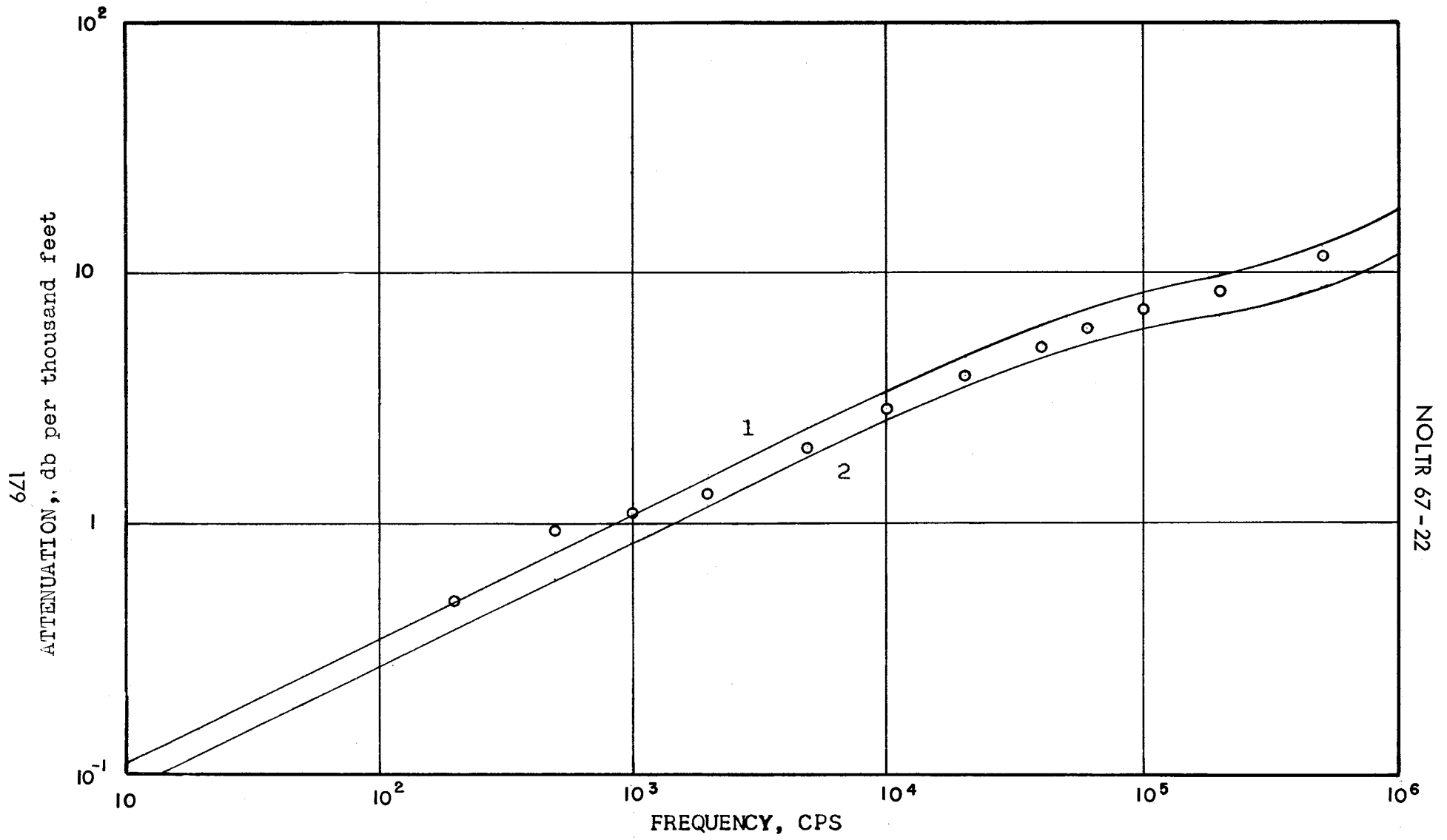

Figure 7-5: Comparison of Experimental and Predicted Attenuation of a Miniature Cable Having a Bimetal Braided Sheath. 1--Bimetal Sheath. 2--Corresponding cable with all-copper sheath.

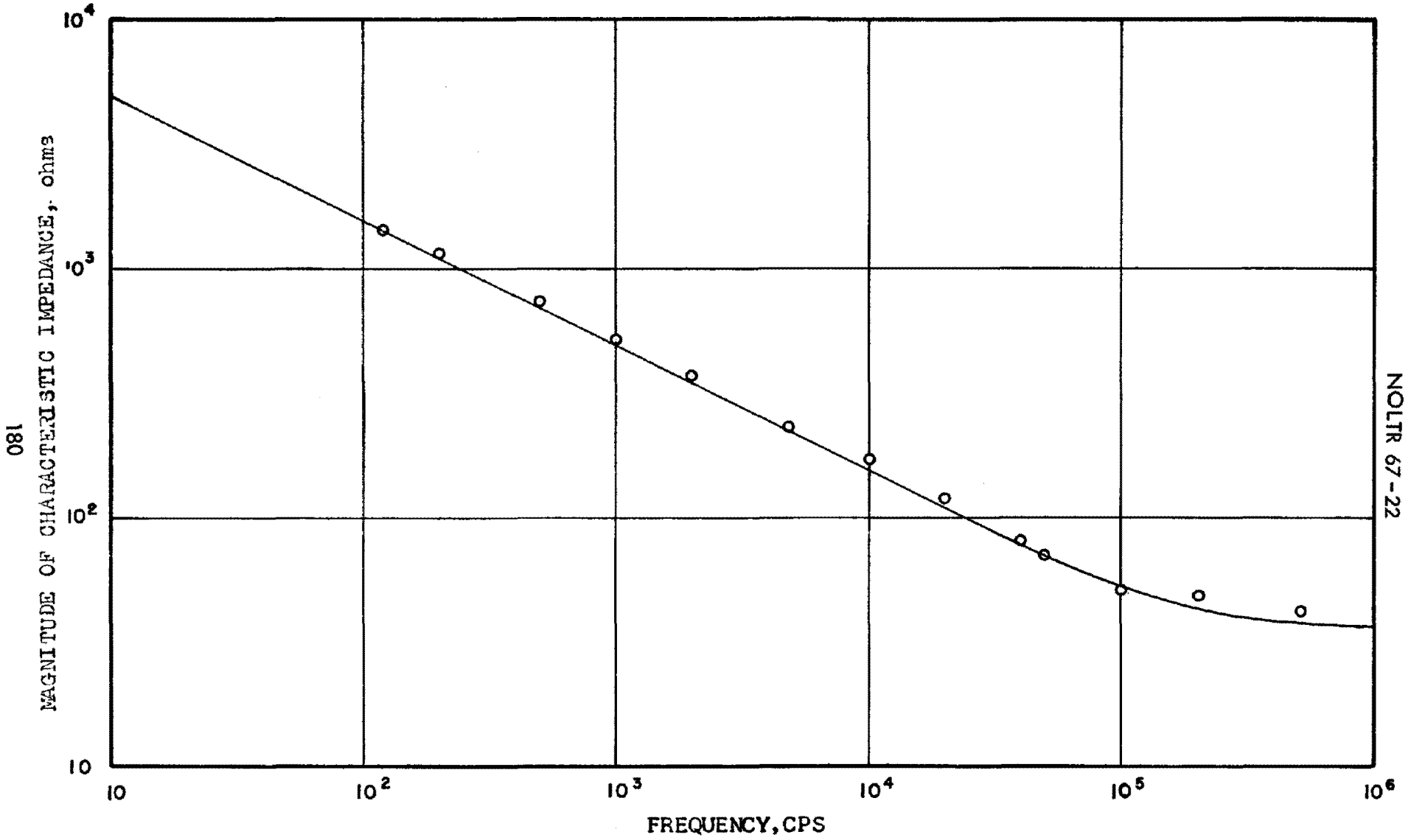

Figure 7-6: Comparison of Experimental and Predicted Characteristic Impedance of a Miniature Cable Having a Bimetal Braided Sheath.

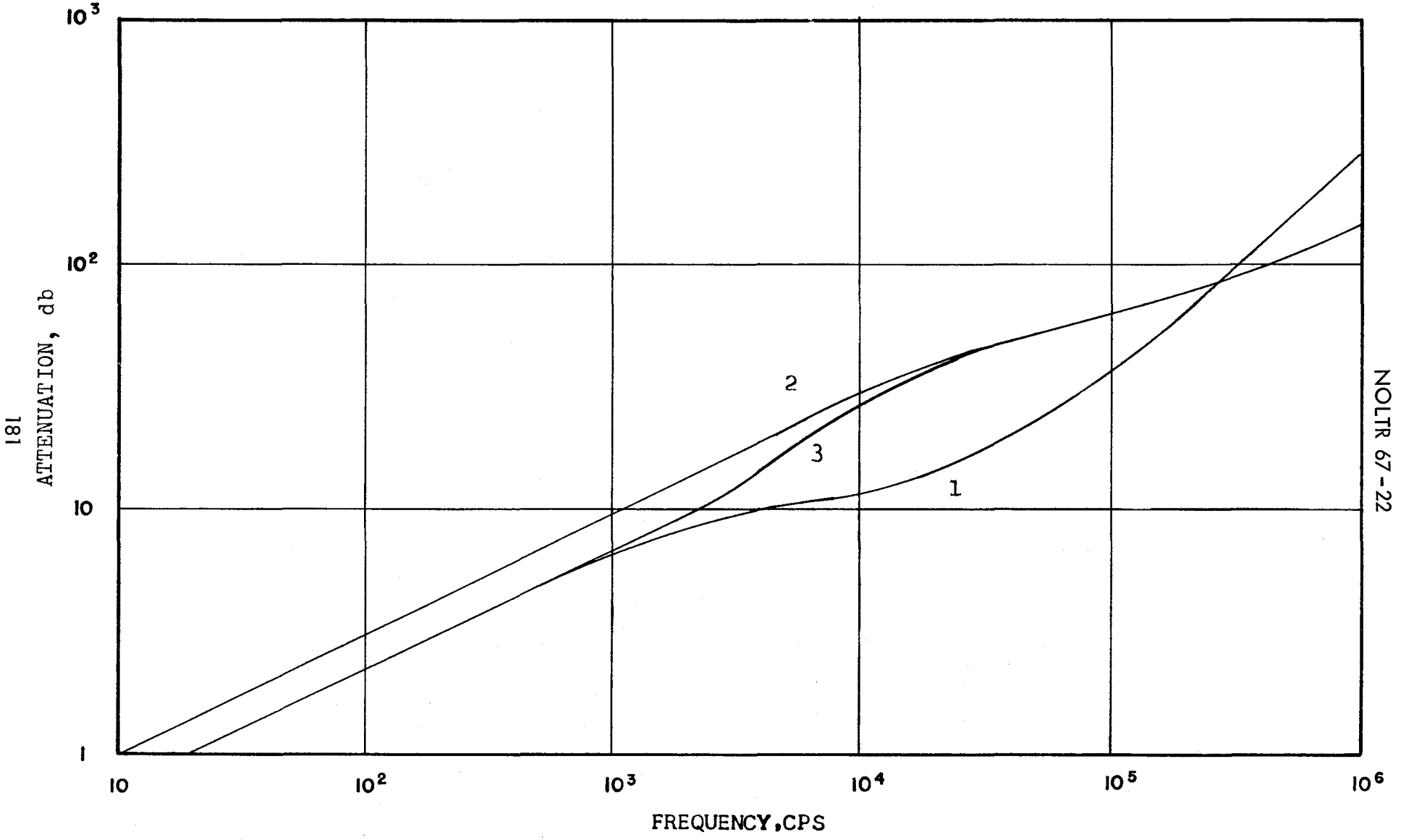

Figure 8-1: Comparison of Insertion Loss of Three Related Miniature Coaxial Cables. 1--Sea-Return Line. 2--Dry Coaxial Cable. 3--Immersed Coaxial Cable.

SELECTED BIBLIOGRAPHY

ARTICLES

1. Carson, J. R. and Gilbert, J. J., "Transmission Characteristics of the Submarine Cable," Bell Syst. Tech. Jour., Vol 1, July 1922, pp 88-115

2. Green, E. I., Leibe, F. A., and Curtis, H. E., "The Proportioning of Shielded Circuits for Minimum High-Frequency Attenuation," Bell Syst. Tech. Jour., Vol 15, April 1936, pp 248-283

3. Espenscheid, L. and Strieby, M. E., "Systems for Wide-Band Transmission over Coaxial Lines," Bell Syst. Tech. Jour., Vol 13, October 1934, pp 654-679

4. Kennelly, A. E. and Affel, H. A., "Skin-Effect Resistance Measurements of Conductors," Proc. IRE, Vol 4, December 1916, pp 523-74; Discussion, pp 575-80

5. Raisbeck, G. and Manley, J. M., "Characteristics of a Three-Conductor Coaxial Transmission Line with Transpositions," Bell Syst. Tech. Jour., Vol 37, July 1958, pp 835-877

6. Rounds, P. W. and Lakin, G. L., "Equalization of Cables for Local Television Transmission," Bell Syst. Tech. Jour., Vol 34, July 1955, pp 713-738

7. Sakurai, T., "'Artificial Matter' for Electromagnetic Wave," Jour. Phys. Soc. Japan, Vol 5, November-December 1950, pp 394-398

8. Schelkunoff, S. A., "The Electromagnetic Theory of Coaxial Transmission Lines and Cylindrical Shields," Bell Syst. Tech. Jour., Vol 13, April 1936, pp 532-579

9. Turin, G. L., "Steady State and Transient Analysis of Lossy Coaxial Cables," Proc. IRE (correspondence), Vol 45, June 1957, pp 878-879

10. Wheeler, H. A., "Transmission Line Impedance Curves," Proc. IRE, Vol 38, December 1950, pp 1400-1403

BOOKS

11. Fuglister, F. C., Atlantic Ocean Atlas of Temperature and Salinity Profiles from International Geophysical Year 1957-58, Vol 1, Woods Hole, Mass.: Woods Hole Oceanographic Institution, 1960

12. Freeman, J. J., Principles of Noise, New York: Wiley, 1958

13. Goldman, S., Transformation Calculus and Electrical Transients, Englewood Cliffs, N. J.: Prentice-Hall, 1949

14. Grover, F. W., Inductance Calculations, New York: D. van Nostrand, 1946

15. Hague, B., Electromagnetic Problems in Electrical Engineering, London: Oxford Univ. Press, 1929

16. Harman, W. W., Principles of the Statistical Theory of Communication, New York: McGraw-Hill, 1963

17. Jahnke, E., and Emde, F., Tables of Functions with Formulae and Curves, New York: Dover Publications, 1943

18. Kimbark, E. W., Electrical Transmission of Power and Signals, New York: Wiley 1949

19. King, R. W. P., Transmission-Line Theory, New York: McGraw-Hill, 1955

20. Kraus, J. D., Electromagnetics, New York: McGraw-Hill, 1953

21. Koehler, G., Circuits and Networks, New York: Macmillan, 1955

22. McLachlan, N. W., Bessel Functions for Engineers, London: Oxford Univ. Press, 1934

23. Pugh, E. M. and Pugh, E. W., Principles of Electricity and Magnetism, Reading, Mass.: Addison-Wesley, 1960

24. Ramo, S. and Whinnery, J. R., Fields and Waves in Modern Radio, New York: Wiley, 1944

25. Ryder, John D., Networks, Lines, and Fields, 2nd ed., Englewood Cliffs, N. J.: Prentice-Hall, 1955

26. Schwarz, M., Information Transmission, Modulation, and Noise, New York: McGraw-Hill, 1959

27. Skilling, H. H., Electric Transmission Lines, New York: McGraw-Hill, 1951

28. Slater, J. C. and Frank, N. H., Electromagnetism, New York: McGraw-Hill, 1947

29. Smythe, W. R., Static and Dynamic Electricity, New York: McGraw-Hill, 1939

30. Stratton, J. A., Electromagnetic Theory, New York: McGraw-Hill, 1941

31. Westman, H. P., ed., Reference Data for Radio Engineers, 4th ed., New York: International Telephone and Telegraph Corp., 1956

32. Wylie, C. R., Advanced Engineering Mathematics, New York: McGraw-Hill, 1951

PUBLICATIONS OF THE GOVERNMENT

33. von Aulock, W., Electrical Characteristics of a Laminated Coaxial Cable with Sea Water Return, Navy Dept., Bureau of Ships, Minesweeping Section, Technical Memo No. 151, September 1950

34. Flath, E. H. and Norgorden, O., Expressions for Input Impedance and Power Dissipation in Lossy Concentric Lines, Naval Research Laboratory Report No. R-3436, March 1949

35. Processing Oceanographic Data, U. S. Naval Oceanographic Office, Publication No. 614, 1951

MISCELLANEOUS

36. Benden, W. J., Investigation into the Electrical Characteristics of a Subminiature Single Conductor Transmission Line in Seawater, Master's Thesis, University of Maryland, August 1963

37. McElroy, N. K., Subroutines KERKEI and BER for IBM-7090 Computer, U. S. Naval Ordnance Laboratory, White Oak, Silver Spring, Md., 1964

38. Peterson, D. A., Final Development Report, Design and Development of a Watertight Low Loss Stable RF Cable, Times Wire and Cable Division of International Silver Co., Wallingford, Conn., February 1963. Available from Office of Technical Services, Washington, D.C., Order AD 299-862

DISTRIBUTION

	Copies
Commander Naval Air Systems Command Washington, D. C. 20360 Code 53302	3
Commander Naval Ships Systems Command Washington, D. C. 20360 Code NAUSEC 6454	1
Chief, Office of Naval Research Washington, D. C. 20360	
Code 466	1
Code 468	1
Chief of Naval Operations Washington, D. C. 20360	
Code OP-03EG	1
Code OP-711	1
NASA Scientific & Technical Information Facility P. O. Box 5700 Bethesda, Maryland 20546	1
Commanding Officer U. S. Naval Ordnance Test Station 3202 E. Foothill Boulevard Pasadena, California 91107	1
Commanding Officer U. S. Naval Underwater Weapons Research and Engineering Station Newport, Rhode Island 02840	1
Commanding Officer & Director U. S. Naval Air Development Center Johnsville, Pennsylvania 18974	1
Commanding Officer & Director U. S. Navy Underwater Sound Laboratory Fort Trumbull New London, Connecticut 06321	1
Commanding Officer & Director Naval Research Laboratory Washington, D. C. 20390	
Code 2021	1
Code 5500	1

	Copies
Defense Documentation Center Cameron Station Alexandria, Virginia 22314	20
Mr. John D. Sherman Department of Electrical Engineering Catholic University of America Washington, D. C. 20017	1

UNCLASSIFIED
Security Classification

DOCUMENT CONTROL DATA - R & D

(Security classification of title, body of abstract and indexing annotation must be entered when the overall report is classified)

1. ORIGINATING ACTIVITY *(Corporate author)*
U. S. Naval Ordnance Laboratory
White Oak, Silver Spring, Maryland 20910

2a. REPORT SECURITY CLASSIFICATION
Unclassified

2b. GROUP

3. REPORT TITLE
Wideband Electrical Characteristics of Small-Diameter Instrumentation Cables in Sea Water

4. DESCRIPTIVE NOTES *(Type of report and inclusive dates)*
Interim Report

5. AUTHOR(S) *(First name, middle initial, last name)*
James E. Cottrell, Jr.

6. REPORT DATE	7a. TOTAL NO. OF PAGES	7b. NO. OF REFS
25 June 1967	185	38

8a. CONTRACT OR GRANT NO.

b. PROJECT NO.
RUDC-3B-000/212-1/S046-00-00

c.

d.

9a. ORIGINATOR'S REPORT NUMBER(S)
NOLTR 67-22

9b. OTHER REPORT NO(S) *(Any other numbers that may be assigned this report)*

10. DISTRIBUTION STATEMENT
Distribution of this document is unlimited

11. SUPPLEMENTARY NOTES

12. SPONSORING MILITARY ACTIVITY

13. ABSTRACT

Certain oceanographic applications exist where it is desired to transmit data over an electrical cable from sea depths of ten to twenty thousand feet. Mechanical handling-packaging and streaming considerations limit cable diameter, yet impose severe strength requirements. In addition, the amount of information to be transmitted dictates a large bandwidth requirement.

The propagation characteristics of several possible cables are analyzed theoretically, considering the effects of seawater. Accurate values of attenuation and characteristic impedance have been determined by IBM-7090 computations and are presented graphically over the frequency range from ten cycles to one megacycle. The inclusion of steel in cables for strength was studied for its effects on electrical character istics.

All cables showed wide parameter variations with frequency, therefore the suitability of a representative cable for transmission of digital signals is briefly investigated. Insofar as receiving amplifier and cable noises allow, a method of countering waveform degradation by proper cable equalization is shown.

DD FORM 1 NOV 65 1473 (PAGE 1)
S/N 0101-807-6801

UNCLASSIFIED
Security Classification

14. KEY WORDS	LINK A		LINK B		LINK C	
	ROLE	WT	ROLE	WT	ROLE	WT
CABLE, COAXIAL						
CABLES, INSTRUMENTATION						
CABLES, UNDERWATER						
PROPAGATION CHARACTERISTICS						
DATA TRANSMISSION						
SEA-RETURN TRANSMISSION LINE						
TRANSMISSION LINES						